NPS ARCHIVE
1959
POTTER, W.

MEASUREMENT OF SEMICONDUCTOR DIODES AT MICROWAVE FREQUENCIES USING A LOW IMPEDANCE SLOTTED LINE

WILLIAM W. POTTER

LIBRARY
U.S. NAVAL POSTGRADUATE SCHOOL
MONTEREY, CALIFORNIA

MEASUREMENT OF SEMICONDUCTOR DIODES AT MICROWAVE FREQUENCIES USING A LOW IMPEDANCE SLOTTED LINE

* * * * *

William W. Potter

MEASUREMENT OF SEMICONDUCTOR DIODES AT MICROWAVE FREQUENCIES USING A LOW IMPEDANCE SLOTTED LINE

by

William W. Potter

Lieutenant, United States Navy

Submitted in partial fulfillment of
the requirements for the degree of

MASTER OF SCIENCE
IN
ENGINEERING ELECTRONICS

United States Naval Postgraduate School
Monterey, California

1959

NPS ARCHIVE
1959
POTTER, W.

Thesis
P749

MEASUREMENT OF SEMICONDUCTOR DIODES AT MICROWAVE FREQUENCIES USING A LOW IMPEDANCE SLOTTED LINE

by

William W. Potter

This work is accepted as fulfilling
the thesis requirements for the degree of
MASTER OF SCIENCE
IN
ENGINEERING ELECTRONICS
from the
United States Naval Postgraduate School

ABSTRACT

A program was started at Varian Associates for the purpose of measuring the resistance and capacitance characteristics of experimental semiconductor p-n junction diodes to be used in low-noise parametric amplifiers. A glass-dielectric slotted line with a characteristic impedance of 8.8 ohms was designed and used for these measurements. Useful results were obtained over a frequency range from 2 to 7.5 kMc. Problems encountered in the calibration of the line and in measurement of the diodes included: determination of the characteristic impedance and the attenuation factors; location of and the method of obtaining a correct reference short position on the slotted line; and determination of the diode capacity versus voltage function. Results for a limited number of diodes indicated that the resistance is essentially constant over the frequency range and that the capacity-voltage function needs further confirmation before reliable figures can be stated. Problems not solved are discussed as well as future prospects for the line.

The writer wished to express his appreciation for the assistance and encouragement given him by the personnel of the Tube Research Division of Varian Associates and, in particular, to Professor Carl E. Menneken of the U. S. Naval Postgraduate School.

TABLE OF CONTENTS

Section	Title	Page
1.	Introduction	1
2.	Parametric Amplifiers	3
3.	Semiconductor Diodes	5
4.	The Low Impedance Slotted Line	10
	4.1 General Background	10
	4.2 Preliminary Calibrations	12
	4.2.1 Characteristic Impedance	12
	4.2.2 Attenuation	14
	4.2.3 Shunt Impedance	17
	4.3 Equipment	19
	4.4 Procedure	20
5.	Results and Interpretation	21
	5.1 Resistance	21
	5.2 Capacity	22
	5.3 Comparison with 50 ohm line Measurements	24
6.	Problems Encountered	25
7.	Conclusions	29
8.	Appendix I (Design of the Low Impedance Slotted Line)	31
9.	Bibliography	96

LIST OF ILLUSTRATIONS

Figure		Page
1.	Equivalent Circuit for a Two-Tank Parametric Amplifier	44
2.	Charge Distribution at Junction between p-type and n-type Semiconductors	44
3.	Election and Hole Concentration in Vicinity of a graded p-n Junction	45
4.	A Charge-Voltage Characteristic of a Non-Linear Capacitor	46
5.	High Frequency Equivalent Circuit of Non-Linear Capacitor	46
6.	P-n Junction "Mesa" Diode	46
7.	Overall View of a Diode	47
8.	Cross-Section of a Diode	47
9.	Diagram for Computing attenuation	48
10.	Attenuation Measurements (Minimum Position vs db)	49
11.	Attenuation Factors vs Frequency	50
12.	Attenuation Curves at 6.5 KMC, 7.0 KMC and 7.5 KMC	51
13.	Impedance Change vs Dummy Diode Distance from Short (5 KMC)	52
14.	Impedance Change vs Dummy Diode Distance from Short (6 KMC)	53
15.	Impedance Change vs Dummy Diode Distance from Short (7.5 KMC)	54
16.	Equivalent Circuit for Diode Plus End Cavity	55
17.	Steps in Reducing Measured Circuit to Diode Circuit	55
18.	Correction of Measured Diode Impedance for Slotted Line Shunt Capacity	56
19.	Complete Laboratory Set-Up	57
20.	Summary of Resistance Readings	58-59
21.	Resistance vs Frequency (at Various Bias Voltages) Diode No. 4	60

LIST OF ILLUSTRATIONS

Figure		Page
22.	Resistance vs Frequency (at Various Bias Voltage) Diode No. 5	61
23.	Summary of Capacitance Readings	62-63
24.	Diode No. 2 (M-17-20) Capacitance vs Voltage Log-Log Plot	64
25.	Diode No. 3 (M-17-19) Capacitance vs Voltage Log-Log Plot	65
26.	Diode No. 4 (M-17-21) Capacitance vs Voltage Log-Log Plot	66
27.	Diode No. 5 (M-17-18) Capacitance vs Voltage Log-Log Plot	67
28.	Diode No. 6 (M-28-10) Capacitance vs Voltage Log-Log Plot	68
29.	Diode No. 7 (M-27-15) Capacitance vs Voltage Log-Log Plot	69
30.	Diode No. 8 (M-21-4) Capacitance vs Voltage Log-Log Plot	70
31.	Diode No. 9 (M-21-4) Capacitance vs Voltage Log-Log Plot	71
32.	Diode No. 10 (M-25-6) Capacitance vs Voltage Log-Log Plot	72
33.	Diode No. 11 (M-22-10) Capacitance vs Voltage Log-Log Plot	73
34.	Diode No. 12 (M-22-23) Capacitance vs Voltage Log-Log Plot	74
35.	Diode No. 1 Smith Chart Plot	75
36.	Diode No. 2 Smith Chart Plot	76
37.	Diode No. 3 Smith Chart Plot	77
38.	Diode No. 4 Smith Chart Plot	78
39.	Diode No. 5 Smith Chart Plot	79
40.	Diode No. 6 Smith Chart Plot	80
41.	Diode No. 7 Smith Chart Plot	81
42.	Diode No. 9 Smith Chart Plot	82
43.	Diode No. 10 Smith Chart Plot	83
44.	Diode No. 11 Smith Chart Plot	84
45.	Diode No. 12 Smith Chart Plot	85

LIST OF ILLUSTRATIONS

Figure		Page
46.	"Inductive" Diode Smith Chart Plot	86
47.	Diode Smith Chart Plot Showing Variable Resistance	87
48.	Smith Chart Plot Showing Diodes in Breakdown	88
I-1	Laboratory Set-up Using 50 ohm Line and Original Diode Holder	89
I-2	Detail of Original Diode Holder	89
I-3	An Equivalent Circuit Representing the Interaction Between the Generator, Probe and the Load Admittances.	89
I-4	Representation of the Probe Circuit and its Equivalent Circuit	89
I-5	Electric Field of some Higher Modes in a Coaxial Line	90
I-6	Detail of the end of the Slotted Line with Plug and Diode in place	90
I-7	Biasing Short	91
I-8	Coaxial Slotted Line	92
I-9	Modification of RG 22/u Connector	93
I-10	Diode Holder and Body	94
I-11	Diode Holder Inner Mechanism	95

1. Introduction.

Improved receiver sensitivity and increased transmitter power have made modern day microwave communication links, such as scatter propagation, feasible. These two factors will become even more important as man reaches out to communicate with satellites and space vehicles. Basically, a receiver endeavors to pick up weak microwave signals and amplify them before taking any intelligence from them. A major problem in the amplification of these weak signals is the noise produced in the process. Anything which can reduce this noise will serve to improve the overall sensitivity of the receiver. Thus, the appeal of the recently developed MASER which obtains its energy from atomic and molecular phenomena rather than from "noisy" electron flow. This device operates near absolute zero temperatures and promises extremely low noise figures.

Another device which shows great promise in noise reduction is the parametric amplifier, which uses semiconductor diodes as active elements. The diodes are used as variable reactances which serve to transfer energy from a high energy pump source to a weak incoming signal and thus amplify it. If these reactances were perfect; i.e., contained no resistance, no noise would be generated in the conversion process. It is not possible to produce pure reactances, but semiconductor diodes are extremely attractive in that their resistance can be made very low - on the order of one ohm or less. Furthermore, since the resistance is already low and the reactance is not a function of temperature, little is gained from operating at lowered temperatures.

Stated briefly - a semiconductor junction diode represents a parallel-plate capacitor whose plates can be moved relative to each other in accordance with a bias voltage applied to the junction. This varying capacitance serves as the varying reactance in the parametric amplifier.

There is a great variety of methods and processes available in the production of semiconductor diodes and it is of extreme importance to be able to determine accurately the resistance and capacitance parameters of these devices so that their performance can be forecast and manufacturing techniques changed with a view toward their improvement. Specifically, measurements are needed to determine what the values of these parameters are over a desired frequency range and what effect varying values of voltage and frequency will have upon them.

It is the intent of this paper to describe a low-impedance slotted line which was designed, built and calibrated for the sole purpose of measuring the resistance and capacitance values of some semiconductor diodes slated for use in parametric amplifiers. The main portion will be devoted to the problems encountered in the calibration of the line and the evaluation of the measurements taken in terms of the variation of the diode parameters with frequency and bias. A section is devoted to the design considerations and to a description of the line itself. A brief description of parametric amplifiers and the mechanism of semiconductor junction diodes is included. In addition, the results of the measurements will be given together with a description of their validity and some suggestions for future endeavor along this line. The results necessarily suffer from the fact that only a small number of diodes were actually measured and no attempt will be made to interpret them in the light of present-day theory.

2. Parametric Amplifiers.[1]

Operation of parametric amplifiers depends primarily upon the fact that under suitable conditions it is possible to extract energy from a source driving an energy storage element and transfer it to the fields of a resonant circuit coupled to the energy storage element. Thus, signals originally present in the resonant circuit can be amplified. In fact, by the transfer of a sufficient amount of energy it is possible to cause the resonant circuit to oscillate. Therefore, the amount of energy transfer is usually adjusted to be that just under the amount necessary for oscillation.

The equivalent circuit for a parametric amplifier can be thought of as two tank circuits coupled by a time varying capacitance -- see Figure 1. Tank 1 is resonant to frequency ω_1, Tank 2 is resonant to frequency ω_2, and the time-varying capacitance is driven sinusoidally; i.e., "pumped", at frequency ω_3, which is the sum of ω_1, and ω_2. If a voltage exists across one of the tanks at its resonant frequency, a corresponding voltage is developed across the second tank at its resonant frequency by the mixing action in the variable capacitance. The phase of the second voltage is automatically adjusted so that net energy flows into the tank circuits from the pumped capacitor.

The process in the capacitor has been likened to the voltage amplification that would take place across the plates of a parallel-plate capacitor if the plates are suddenly pulled apart when the voltage across them is a maximum. Since the capacity is reduced, and the charge remains constant, the voltage must be increased - by the same amount the capacity is decreased. If the plates are pushed together again when the voltage across them is zero, there will be no voltage attenuation and the original amplification will remain.

The process of a voltage in tank 2 produced by a voltage present in tank 1 is completely reversible and the voltage created in tank 2 serves to further amplify the voltage in tank 1. Therefore, if the energy transfer from the pumping source is not too great, an "input" voltage to tank 1 will be amplified.

For amplifier purposes, tank 1 is termed the driving - signal - circuit; tank 2, the idling circuit. Stated generally, what happens is that the idling circuit presents a pure negative conductance to the driving circuit at the signal frequency producing amplification. When the negative conductance becomes equal to the total internal conductance of the signal circuit oscillations commence.

At signal frequencies other than the resonant frequency of the tank, the amount of negative conductance introduced by the second tank is reduced and, in addition, an added susceptance appears. These factors make this device a narrow band amplifier with band widths on the order of .01 percent for a gain of 20 decibels.

Other devices which also use semiconductor diodes are available which do not have this narrow band width limitation. One, with a bandwidth of 25 percent and a gain of ten decibels, uses an array of diodes in a traveling wave amplifier configuration.(2) Another, the so-called reactance amplifier,(3) has a reported gain of ten decibels, a bandwidth of ten percent, an effective input temperature of only 40 degrees Kelvin, and uses semiconductor diodes in a balanced modulator configuration.

3. Semiconductor Diodes.

A semiconductor diode is formed by the junction of two different types of semiconductor material, p-type and n-type. Even the point-contact silicon diode, which was in use as a crystal rectifier long before the advent of modern semiconductor theory, is in reality a semiconductor diode; i.e., a p-n junction.

There are two types of p-n junctions: the graded junction and the abrupt junction - differing mainly in the manner in which the physical junction is made. Their overall properties are similar and therefore the linearly graded junction will be described for ease of explanation. Certain impurities are added to the intrinsic semiconductor; i.e., pure silicon, which make it either a p-type or an n-type semiconductor. An n-type, or donor, semiconductor is created with the addition of an impurity (antimony, phosphorous, or arsenic) which causes (donates) an excess of mobile (conducting) electrons. A p-type, or acceptor, semiconductor is created with the addition of an impurity (gallium, boron, or indium) which causes a dearth of electrons; i.e., an excess of positive charges which accept electrons and thus can be thought of as mobile "holes". When a p-type and an n-type material are brought together to form a junction, there is a charge redistribution, as depicted in Fig. 2, created by the mobile charges diffusing across the junction to annihilate each other until stopped by the potential barrier built up by the ions which are uncovered. At equilibrium the hole and electron concentrations are as shown in Fig. 3,,for three different conditions of bias. Note in particular the depletion layer - the region where there are few holes and electrons. It is the change in width of this layer, as the bias changes, which is of concern.

The junction is forward biased when a positive voltage is applied to the p-type material relative to the n-type. This causes the potential barrier to lower, permits a greater flow of holes and electrons, narrows the depletion layer. Too great a forward bias will cause the holes and electrons to intermingle and the depletion layer will disappear. The junction is reverse biased when a negative voltage is applied to the p-type material relative to the n-type. This raises the potential barrier, causes the holes and electrons to move apart, widens the depletion layer. Too great a reverse bias will cause breakdown due to "avalanche multiplication" and large amounts of current will pass. In the bias range between reverse breakdown and a slight forward bias, the charging and discharging of the junction occurs through the motion of the hole and electron distributions toward and away from each other. This represents a form of capacitance referred to as the "depletion-layer capacitance". If, then, a small time-varying voltage is applied to a semiconductor p-n junction, a non-linear capacitance can be obtained which is a function of the voltage and thus a function of time. The general shape of this charge versus voltage characteristic is shown in Fig. 4. Note the resemblance to the current versus voltage curve of a non-linear resistance. It is this depletion-layer capacitance variation which is thought to be the basis of microwave diode amplifiers.

If the least capacitance obtainable (at reverse bias just short of breakdown), is chosen as C_{min}, the diode can be represented as a variable capacitor shunting C_{min}, and in series with the resistance between the junction and the diode contacts. (See Fig. 5). It is these parameters which are to be measured to determine:

1. What is the value of the capacitance for varying values of bias.

2. What are the non-linear characteristics of the capacitive reactance.

3. What variation, if any, occurs in the series resistance over the desired frequency range, 2 to 7.5 kMc.

A figure of merit which has been advanced is a cutoff frequency, defined as

$$f_c = \frac{1}{2\pi R_s C_{min}} \quad [4]$$

and described as the frequency at which the Q of the device is one. For amplifier work a desired ratio between this cutoff frequency and the working frequency is on the order of ten. Pumping frequencies as high as 10 kMc are proposed for the parametric amplifiers using these diodes and this means cutoff frequencies of 100 kMc. The $R_s C_{min}$ product must then be $1.59\ (10^{-12})$, or a capacitance of 1^{uuf} must carry a resistance of less than 1.6 ohms.

This brings out the principle advantage of the diffused or graded junction: that a low series resistance can easily be obtained. Further, the cutoff frequency is independent of the area of the graded junction since R_s is inversely proportional to the area while the capacitance is directly proportional to the area.

The actual techniques for making p-n junctions are as varied as the manufacturing firms constructing them. In general the alloy, or abrupt, junctions are made by heating a wafer of doped semiconductor in contact with an impurity which forms a liquid alloy at the temperature used. Upon cooling, the semiconductor, heavily doped with the impurity, precipitates out onto the original semiconductor forming the p-n

junction, since the original wafer was doped opposite to that created by the impurity. With silicon the alloying material can be aluminum. For ohmic contact a gold wire can be used.

In one type of diffused junction - the impurity in gaseous form is passed over a suitably doped semiconductor wafer in a heated vacuum furnace so that surface diffusion takes place to a desired depth. Then the process is stopped, a mask is placed over the diffused layer, and the surface is etched until an island of suitably doped material remains. This is the so-called "mesa" type diode - see Fig. 6. Or a different shaped mask can be used such that a hole is etched in the wafer. Suitable contacts can be made by evaporating a film of gold-antimony or bury- a platinum tab on the contact surfaces.

Note that diffusion also takes place in the alloy junction - after the impurity solidifies and as it cools. This means that an absolutely abrupt junction is not obtained, however, the junction gradient is still much sharper than that produced in the diffusion type. Therefore, the difference between the graded and the abrupt junction is a relative one and almost any junction gradient can be and is obtained by a combination of techniques.

The diodes used in these experiments were themselves experimental and were manufactured by the Fairchild Semiconductor Corporation in Palo Alto. The process used varied considerably from diode to diode as to details and actual techniques used. In general, the diodes were diffused, graded-junction silicon diodes mounted on top of a 1/16th inch post. A gold post is joined to the end of the mounting post and machined flat. An n-type silicon wafer - about ten mils thick - is buried in the gold and an oxide coating is allowed to form. In the approximate center of the wafer a small amount of p-type impurity is added, presumably by

diffusion through a small hole etched in the oxide. Then, to establish contact, a gold ball is buried in the p-type impurity. See Figures 7 and 8 for an overall view and a cross-section of a diode.

4. The Low Impedance Slotted Line.

4.1 General Background

In September 1958, Varian Associates began a testing program on the experimental semiconductor diodes manufactured by the Fairchild Corporation expressly for use in parametric amplifiers. It was necessary to measure the parameters, both with a view toward actual diode performance and future improvement.

Initial measurements were made using a 50 ohm slotted line - Hewlett Packard 806-B. A special diode holder was designed and built for use with the 806-B and the results obtained were generally regarded as reliable as far as the value for the diode capacitance were concerned and inconclusive as far as the value for the diode resistance were concerned.

The diode to be measured was placed in an adapter fitted to the end of the slotted line so that the diode pointed outward from the line. A micrometer plunger was advanced until it just contacted the diode; the d-c bias was set, and the positions of minimum electric field along the slotted line were measured. Then the plunger was withdrawn and one with a hollow tip inserted and advanced until the sides of the diode were contacted. This established what was believed to be a reference short at the diode and the new minimum points were measured. The data obtained were entered on a Smith Chart and the results plotted as graphs of resistance and capacitance versus frequency.

Capacitances of around 3 uuf were obtained with the values tending to remain steady. However, standing wave ratios of 30 - 40 db were encountered and this made the resistance readings automatically suspect because of the inherent error in measuring large standing wave ratios.

Therefore, in January 1959, work was begun on the design, construction and testing of a low impedance slotted line in the belief that the lower standing wave ratios would produce reliable diode resistance values as well as consistent capacitance measurements.

The design calculations and procedure, in addition to notes on the actual construction of the slotted line, are given in Appendix I. The following sections are concerned with the calibration, the measurement techniques, and the evaluation and interpretation of the results obtained with the low impedance slotted line.

4.2 Preliminary Calibrations.

The first thing to be done upon the completion of the construction of the slotted line was the determination of its actual characteristic impedance and attenuation factors. Preliminary calculations had indicated a characteristic impedance of 6.2 ohms and an attenuation constant for the entire length varying from about 2 db at 3 kMc to 10 db at 12 kMc (See Appendix I).

4.2.1 Characteristic Impedance.

To measure the characteristic impedance, it was decided to measure the distance between successive voltage minima with the end of the line shorted with a copper strip. This would give a direct measure of the actual wavelength in the dielectric for comparison with the known wavelength in free space. The result is directly proportional to the square-root of the relative dielectric constant, as follows:

The quantity $\lambda\sqrt{\mu\epsilon}$ remains a constant. Therefore

$$\lambda = \frac{\lambda_0\sqrt{\mu_0\epsilon_0}}{\sqrt{\mu\epsilon}}$$

where λ = wavelength of plane TEM wave in the dielectric; λ_0 = wavelength of plane TEM wave in free space; $\epsilon = \epsilon_0\epsilon'$ = the dielectric constant; and $\mu = \mu_0\mu'$ = the permeability. In this case the formula reduces to

$$\sqrt{\epsilon'} = \frac{\lambda_0}{\lambda}$$

Measurements were made between 2 kMc and 7.5 kMc[5] and the dielectric constant was found to vary between 3.62 and 3.82. This variation was attributed mainly to measurement errors since there seemed to be little correlation between the frequencies and the dielectric constant obtained.

This seemingly large variation in dielectric constant did not have nearly as drastic effect on the characteristic impedance as might be suspected since

$$Z_o = \frac{60}{\sqrt{\epsilon'}} \ln \frac{r_o}{r_i}$$

Actually, the characteristic impedance varied between 8.95 ohms and 8.74 ohms with the value 8.8 ohms cropping up so often that it was decided to use this value with a corresponding dispersion of less than 1.7 percent, under any circumstances.(6)

The difference between the calculated value of 6.2 ohms and the actual value of 8.8 ohms is not so surprising when it is realized that the calculated value is for a solid dielectric with no imperfections or parameter variations. It was estimated that parameter variations could produce as much as a 15 percent variation and that the slot could produce an additional eight percent variation in the calculated characteristic impedance. Further, there was no guarantee that the dielectric constant was exactly as specified in the handbook. The important thing was to measure the characteristic impedance and to determine that it could be considered constant with an error of less than two percent. This was more than adequate for the measurements that were to be made.

4.2.2 Attenuation

The determination of the attenuation over the frequency range did not prove as easy. Knowing the attenuation was just as essential as the characteristic impedance because all measurements were made at a minimum distance of 6.5 centimeters from the load. This represented as many as three wavelengths at the higher frequencies and the attenuation in the line for this distance was enough to cause the measured standing wave ratio to differ from the actual standing wave ratio.

The attenuation can be determined by noting the relative difference between successive minima, expressed in decibels, and the standing wave ratio, as follows:

Let V_{m_1} and V_{m_2} represent the voltage at minimum positions 1 and 2 respectively and αl be the attenuation of the dielectric. (See Fig. 9.)

Then

$$\frac{V_{m_1} - V_{m_2}}{V_{m_1}}$$

is the quantity which is measured when the difference between successive minima is found. Breaking V_{m_1} and V_{m_2} up into the difference of their incident and reflected waves,

$$\frac{V_{m_1} - V_{m_2}}{V_{m_1}} = \frac{V_{i_1} - V_{r_1} - V_{i_2} + V_{r_2}}{V_{i_1} - V_{r_1}} = \frac{V_{i_1} - V_{i_1} e^{-\alpha l} - V_{r_1} + V_{r_1} e^{\alpha l}}{V_{i_1} - V_{r_1}}$$

For small αl,

$$e^{\alpha l} = 1 + \alpha l + \cdots \qquad \text{and} \qquad e^{-\alpha l} = 1 - \alpha l + \cdots$$

Then,

$$\frac{V_{m_1} - V_{m_2}}{V_{m_1}} = \frac{V_{i_1} - V_{r_1} - V_{i_1} + V_{i_1}\alpha l + V_{r_1} + V_{r_1}\alpha l}{V_{i_1} - V_{r_1}} = \left(\frac{V_{i_1} + V_{r_1}}{V_{i_1} - V_{r_1}}\right)\alpha l.$$

Now, VSWR is defined as $\frac{V_{m_1}}{V_{m_1}} = \frac{V_{i_1} e^{-\alpha \frac{\ell}{2}} + V_{r_1} e^{\alpha \frac{\ell}{2}}}{V_{i_1} - V_{r_1}} = \sigma$

Again, for small $\alpha \ell$,

$$\sigma = \frac{V_{i_1} - V_{i_1} \alpha \frac{\ell}{2} + V_{r_1} + V_{r_1} \alpha \frac{\ell}{2}}{V_{i_1} - V_{r_1}} = \frac{V_{i_1} + V_{r_1}}{V_{i_1} - V_{r_1}} - \frac{(V_{i_1} - V_{r_1})}{V_{i_1} - V_{r_1}} \alpha \frac{\ell}{2} = \frac{V_{i_1} + V_{r_1}}{V_{i_1} - V_{r_1}} - \alpha \frac{\ell}{2}$$

And then,

$$\frac{V_{m_1} - V_{m_2}}{V_{m_1}} = \left(\frac{V_{i_1} + V_{r_1}}{V_{i_1} - V_{r_1}}\right) \alpha \ell = \left(\sigma + \alpha \frac{\ell}{2}\right) \alpha \ell = \sigma \alpha \ell + \frac{(\alpha \ell)^2}{2}$$

If this equation is solved quadradically, two solutions are obtained

$$\alpha \ell = \left(\frac{V_{m_1} - V_{m_2}}{V_{m_1}}\right) \frac{1}{\sigma} \qquad \text{and} \qquad \alpha \ell = -2\sigma + \left(\frac{V_{m_1} - V_{m_2}}{V_{m_1}}\right) \frac{1}{\sigma}$$

the d**the second one** of which can be discarded.

At least four sets of readings of the difference between adjacent minima were taken for every frequency to be used for measurements and the results plotted. Figure 10 is a representative plot obtained at 5 kMc. Note that there was considerable variation in the results and that it was necessary to find an average for each operating frequency. Incidently, there was also considerable variation between the readings of the Hewlett-Packard 415-A Standing Wave Indicator and the attenuator of the signal generator. It was necessary to use a thermistor mount to calibrate the attenuator before the two showed any signs of agreement.

The results of the attenuation measurements were as follows:

kMc		
1.5	$1.1 (10^{-3}) \frac{\text{nepers}}{\text{cm}}$	$[9.55 (10^{-3})^{db/cm} \times 48.2^{cm} = .46^{db}$ overall$]$
2.0	$1.35 (10^{-3}) \frac{\text{nepers}}{\text{cm}}$	$[1.17 (10^{-2})^{db/cm} \times 48.2^{cm} = .56^{db}$ overall$]$
3.0	$2.70 (10^{-3}) \frac{\text{nepers}}{\text{cm}}$	$[2.34 (10^{-2})^{db/cm} \times 48.2^{cm} = 1.13^{db}$ overall$]$
4.0	$3.05 (10^{-3}) \frac{\text{nepers}}{\text{cm}}$	$[2.65 (10^{-2})^{db/cm} \times 48.2^{cm} = 1.28^{db}$ overall$]$
5.0	$3.30 (10^{-3}) \frac{\text{nepers}}{\text{cm}}$	$[2.87 (10^{-2})^{db/cm} \times 48.2^{cm} = 1.38^{db}$ overall$]$
6.0	$3.85 (10^{-3}) \frac{\text{nepers}}{\text{cm}}$	$[3.34 (10^{-2})^{db/cm} \times 48.2^{cm} = 1.61^{db}$ overall$]$
7.5	$6.20 (10^{-3}) \frac{\text{nepers}}{\text{cm}}$	$[5.38 (10^{-2})^{db/cm} \times 48.2^{cm} = 2.6^{db}$ overall$]$

Fig. 11 is a plot of these results and shows that the curve is not linear. It was indeed far more jagged than shown at frequencies above 6.4 kMc where the minima actually decreased as the distance from the load increased - a negative attenuation. A sample set of readings is plotted in Fig. 12 showing these negative attenuation dips at 6.5 kMc and 7.0 kMc. These dips were deemed to be locally excited modes of higher order since the overall attenuation still tended to be positive and because the attenuation smoothed out at 7.5 kMc. It would seem that it does not matter what the attenuation factor is as long as it could be experimentally determined. However, an erratic attenuation curve would tend to cause misgivings as far as the basic assumption that the attenuation remains constant for the 6.5 centimeters between the last measuring point and the load is concerned. Note further that these attenuation factors compare favorably with the calculated values.

Once the attenuation factors had been determined it was necessary to use them. The formula[7]

$$\rho = \coth\left[\tanh^{-1}\left(\frac{1}{\rho_m}\right) - \alpha\ell\right] \quad \text{where} \begin{cases} \rho = \text{actual VSWR} \\ \rho_m = \text{measured VSWR} \end{cases}$$

supplies the answer but it can be further simplified, using the first two terms of the series expansions, into

$$\rho = \frac{1}{\frac{1}{\rho_m} - \alpha\ell} + \frac{\frac{1}{\rho_m} - \alpha\ell}{3\rho_m}$$

And, finally, the second term can be neglected for standing wave ratios greater than about seven as its effect could not even be noticed on a Smith Chart. As it turned out, the formula that was used, for ease of calculation, was,

$$\frac{1}{\rho} = \frac{1}{\rho_m} - \alpha\ell$$

4.2.3 Shunt Impedance

The final step before the diode measurements could begin was the determination of the shunt impedance representing the cavity at the end of the line. Attempts to calculate it had only resulted in a different answer for every method attempted. There were admittedly many factors which were inexplicable. (See Appendix I). Therefore, it was decided that the value of this shunt impedance would be measured at each pertinent frequency and the results plotted on a Smith Chart to determine the resistive and reactive components.

The procedure was to use a "dummy diode", which was in reality a diode mounting post, silver-plated to reduce the resistance. This "diode" was brought up until firm contact was made with the inner conductor. The "short min" and VSWR were noted and then the diode was withdrawn one-half mil at a time and the "min" position and VSWR noted until the movement no longer had any effect on the minimum position (at about 6 mils). Measurements were obtained at 5, 6, and 7.5 kMc and calculations showed that the shunt capacity was .386 uuf, .484 uuf and .580 uuf respectively. (See Figs. 13, 14, 15). There are several interesting things to note in these Smith Charts. First, for the first half mil the short was still in contact, the only change being in an increased "short" resistance (although in the 7.5 kMc case it also appeared to go slightly capacitive). The fact that contact was still maintained indicated a slight spring to the system while the increased resistance was the cause of much confusion in the readings and the probable loss of many diodes. More about this later.

Second, the cavity actually became inductive at the one mil point. This, of course, is not surprising since the post actually does represent an inductance which was apparently great enough to overcome the cavity capacity at these frequencies.

Finally, note that the final impedance occurs at the same point on each diagram, that is, the capacitive reactance was constant. This fact was utilized in the calculations for the shunt capacity at 2, 3, and 4 kMc. The resultant values were 1.45 uuf, .968 uuf and .725 uuf respectfully.

In each case the shunt resistance was so great that its effect was considered negligible. Thus, the equivalent circuit represented by the load together with the shunt capacity could be represented as shown in Figure 16. Measurements would provide an overall capacity, an overall resistance and a value for the cavity shunting capacitance. It was necessary, therefore, to find the relationships between the diode parameters and these measured values.

Consider Figure 17. The measured values could be represented as a series impedance. This impedance can be transformed into a parallel admittance from which the value of cavity shunt susceptance could be subtracted. This "corrected" admittance can again be transformed to an equivalent impedance to give the diode circuit representation desired (Fig. 5).

Computations using this procedure proved to be complicated, extremely laborious, and fortunately, not necessary. The Smith Chart impedance diagram proved to be admirably suited for this type of circuit reduction - particularly since the slotted line measurements had already been plotted as impedances. Furthermore, accuracy could be maintained. Using normalized values, a simple 180 degree rotation provided the desired admittance. The constant value of the cavity shunt susceptance (.16 mhos) was then subtracted by moving the required distance along a constant conductance line. This new admittance was again rotated 180 degrees to obtain the series impedance of the diode circuit.

Figure 18 is a Smith Chart showing the transformation of a sample impedance measurement. Note that the value of the resistance is changed as well as the value of capacitance.

4.3 Equipment

Now that all the preliminary measurements have been detailed it would be in order to describe the complete set-up in the laboratory before outlining the general procedure - see Figure 19. Refer to Appendix I for a complete description of the slotted line.

It was necessary to provide a "d-c isolator" between the r-f signal generator and the stub tuners since the generator represented a virtual d-c short and the stub tuners were used to apply the bias voltages. The stub tuners were themselves "isolated" so that a bias voltage could be applied between the inner and outer conductor. See Appendix I. The d-c isolator was constructed by removing the center conductor of a standard double female fitting, cutting it in half, and in reassembling it with a thin piece of mica inserted between the two conductor halves. When so constructed the insertion loss was practically negligible.

The purpose of the a-c power supply and the oscilloscope was to display the diode characteristics as it was brought into contact with the inner conductor of the slotted line. A small a-c voltage was applied to the line as the diode was brought into contact with the inner conductor. The same voltage was also applied to the plates of a cathode ray oscilloscope - the actual voltage, E, to the vertical plates and a voltage proportional to the current, I, to the horizontal plates. By observing the scope, the instant of contact could be determined by the appearance of the so-called diode picture. An idea as to the quality of the diode could also be gained from the slope of the voltage versus current picture. A switch

was manufactured enabling the d-c bias voltage to be interchanged with the a-c monitoring voltage so that the status of the diode could be quickly ascertained at any time during the measurements.

4.4 Procedure

The procedure was to:

1. Determine the reference short position by the use of a "dummy diode" for all the desired frequencies.

2. Measure the minimum positions and the voltage standing wave ratios for the diodes at various bias voltages and frequencies.

3. Correct the VSWR readings for attenuation and plot the results on Smith Charts.

4. Correct these plotted impedances for the cavity shunt capacity.

5. Tabulate the separate values of resistance and capacitive reactance, - see Figures 20 and 23, for summaries of the resistance and capacitive readings.

5. Results and Interpretation.

The purpose of these measurements was twofold:

1. To determine whether the value of resistance was a function of the frequency.

2. To determine the behavior of the junction capacity as a function of the bias voltage.

5.1 Resistance

In the summary the results are given to three significant figures. This accuracy is of course not warranted from the plots on the impedance diagram. It is possible, however, to read the plotted values for the normalized resistance accurate to within one-tenth. Then, all recorded resistance readings are correct to within an extreme of ten percent and most to within five percent, which means to within four numbers in the second significant figure.

This does not take into account the random errors in taking the measurements but these would tend to balance out over the series of measurements at any one frequency. Any gross errors should be apparent from the plots of the readings.

With the above in mind the following observations are pertinent:

1: In every case but one the resistance at 7.5 kMc was lower than that at 6 kMc.

2. At all other frequencies for fixed bias there is no established trend evident. (Figures 21 and 22 are offered in evidence of this).

3. For fixed bias, the greatest divergence is less than one-half ohm over the frequency range.

4. At each frequency, over the bias range -.5 volts to -5 volts, the resistance increased, on the order of 1-2 percent.

Therefore, as a general conclusion, it can be stated that the resistance remains constant for a constant bias voltage over the frequency range 2 - 7.5 kMc and that the resistance increases slightly as the reverse bias increases at a fixed frequency.

It would be more correct to make the negative statement that the resistance is not inversely proportional to the frequency.

5.2 Capacity

The fulfillment of the second purpose - the behavior of the junction capacity - was a little more involved. According to theory[8], the junction, or depletion layer, capacitance can be considered a function of the bias voltage, V_j and may be represented as

$$C = C_o V^{-m}$$

where m varies between .33 in the case of the diffused junction and .5 in the case of the abrupt junction.

To this end it was necessary to construct a plot of capacitance versus voltage on log-log paper at each frequency for each diode. Then to determine a straight line approximation, if this was feasible, and from this determine the value for C_o and the exponent m. Figure 23 is a "Summary of Capacitance Reading" obtained including the exponents. Figures 24 through 34 are the log-log plots for determining the value of m.

Again, the three significant figure accuracy is not warranted because the impedance plots could not be read closer than one-tenth. However, a one-tenth error produced no greater than a four percent error or a three number error in the second decimal place. The cumulative effect of errors could at times have been large because of the Smith Chart maneuvering to correct for the effect of the cavity shunt capacity.

Further, a great deal of accuracy was sacrificed in some cases with the straight line approximation to obtain the exponent - so much so that the validity of the second decimal place is doubtful.

With the above in mind, the following observations are pertinent:

1. The capacitance at 7.5 kMc was always the highest, as was the exponent in all but one case.

2. The capacitance always decreased as the bias increased at any fixed frequency.

3. Except for one diode, the exponents ranged between .437 and .613 with the greatest spread for one diode from .613 to .417, or some 30 percent variation and the least from .244 to .220, or ten percent.

4. The capacity decreased with frequency at constant bias except between 5 kMc and 4 kMc where the capacity actually increased.

5. When a low frequency C_o, at 15 kcs, was given by the manufacturer, the value of capacity corresponding most closely to it occurred at either 4 kMc or 5 kMc.

Accordingly, nothing can be stated relative to the actual values of capacity but it is felt that the exponents are valid because of their consistency. Therefore, as a general conclusion, it can be stated that the junction capacity can be assumed to be a function of the bias voltage; i.e., $C = C_o V^{-m}$ and that the values of m varied between .4 and .6.

Figures 35 through 44 are the Smith Chart plots of Diodes 1 through 11 less 9.

5.3 Comparison with 50 ohm line measurements.

By way of comparison, a few measurements were made on a 50 ohm line. Figure 45 is the Smith Chart plot while "Diode Number 12" is a tabulation of the results. Note that the resistances obtained are as much as twice as great while the general trends appear to be the same.

The important advantage of the low-impedance slotted line is its ability to measure more accurately the diode resistances and the diode capacitance changes under varying bias conditions. For the same diode the low-impedance line will have a smaller voltage standing wave ratio. Because the voltage minimum is not so deep, the standing wave ratio, and ultimately the diode resistance, can be measured with a greater degree of accuracy.

Because the wavelength is reduced; i.e., the apparent frequency is increased, in the low-impedance slotted line an equal change in capacitance with a change in bias will produce a greater change in the capacitive reactance and thus a greater rotation, or spreading, on the Smith Chart. Then, the distance between the capacity values or the relative capacity can be measured with a smaller percentage error. Compare Figures 44 and 45.

6. Problems Encountered

As the measurements were being made and the results plotted, it became more and more apparent that the constant reference short position obtained with the dummy diode was not valid. This fact became readily apparent when some of the diodes plotted inductive. That is to say, the zero bias point would be inductive and the succeeding bias points would swing in a capacitive direction but not enough to cross the zero resistance - short - line. Figure 46 is an example of this. Diode Number 7, in fact, has an entire frequency range of measurements - from 7.5 kMc to 1.5 kMc - but only the lower two were useful because all the others were inductive.

Discussion subsequent to the completion of this experiment suggested that each diode be measured in a forward biased condition where the capacitance is greater and the capacitative reactance smaller. The reference position might then be chosen as the zero bias condition including the contact potential; i.e., about .6 volts forward bias. However, it is not clear that this would supply the correct absolute value of the capacitance unless it could be assumed that the same forward bias produced the same conditions in all diodes.

One reason that has been advanced for the apparent inductive diodes is the effect of the diode post. This post has been shown to cause the shunt impedance to appear inductive when the post is approximately a mil away from the inner conductor. The thickness of the gold ball and the silicon wafer is such that when the diode is in place the post may be as little as 1 or 2 mils from the inner conductor. Particularly, is this true when the gold ball is flattened by the pressure of contact. But, this distance will vary from diode to diode merely through the variations

Drill & Ream to .0625-.15 min deep then taper to .120

.25 threads/in

1/4-28 tap .25 deep

.300 ±.10

.450

.125

.250

.600

.040

.050 mils

.120

50 mils/in

Drill hole 1/16 dia. 1/4 deep

.030

50 threads/in

Cut 4-10 mil slots 1/4 deep

Drill hole to hole #3 drilled

.25 threads/in

Drill & Ream to .50 to fit plunger

.300

.100

.005

PLUG

COLLET (Make 4 collets)

COLLET SLIDE CYLINDER

PLUNGER

END

REVISIONS		TITLE	ENG.	DATE
		VARIAN associates ENGINEERING SKETCH	MAT'L.	MODEL
			FINISH	J. O. NO
			SCALE	SK. NO

FORM 449-9 1 1 November 52

of the manufacturing process and the shunt impedance at that distance is extremely sensitive to the post position. No statement can be made regarding a constant distance nor an equivalent shunt impedance.

It was noted in subsequent measurements that forward bias conditions did indeed produce different reference points for different diodes under the same forward bias conditions. In any event, however, more consistent results would almost certainly be obtained using the forward bias reference positions rather than the constant reference position obtained with the dummy diode.

This reference short confusion is the main reason the measurements of the capacitance are not considered as reliable as the resistive results. A glance at the Smith Chart plot of the inductive diode shows that the resistance circles are virtually the same as the standing wave ratio circles in the region of confusion, on either side of a short position. Therefore, any shift of reference value that would eliminate the inductive portion would not alter any of the resistance values appreciably; nor would the new correction for the cavity shunt capacitance. The same is not true for the absolute values of capacitance. Any shift would have a very decided effect on their values. However, the amount of change, or the relative capacity, would remain virtually the same. Therefore, it can be said that the values obtained for the diode resistance, the relative capacity changes and the exponents are valid.

This brings up another problem - the exponents greater than .5. Diodes have been manufactured with exponents even greater than this value but not without special processing. As far as can be determined, these higher exponents were not expected, but the possibility of their occurrance is not ruled out. Certainly, more measurements need to be

taken using a procedure that inspires more confidence before these exponents can be confirmed or denied.

Another problem which assumed major proportions was the extremely high mortality rate among the diodes during the measurements. The total number of diodes tested was 15 and of these only 5 remained intact for all frequencies (and one of these proved inductive).

There were at least two major causes for this short life span: increased pressure to maintain constant resistance and inner conductor movement when tuning. Note that the low frequency resistance readings, R_s (taken at 15 kcs and measured by the manufacturer), when given in the resistance summary, are considerably greater than those given in the table. It was discovered early in the measurement process that considerable pressure was required on the diode after the initial contact was made in order to maintain consistent readings. If this pressure was not applied the resistance readings were erratic. Figure 47, a Smith Chart plot of M-25-13 at 6 kMc, is given as an example of the change occasioned by increased pressure.

It is believed that the answer to this lies in the contact resistance encountered when just touching the top of the gold ball. This contact resistance is pressure sensitive. Increasing the pressure effectively eliminated this contact resistance by flattening the gold ball and increasing the area of contact. An interesting sidelight to this is the fact that the gold ball apparently flowed when under pressure. This was evidenced by the fact that it was continually necessary to readjust the pressure during the measurements - so much so that the gold ball was eventually flattened flush with the silicon wafer and the effectiveness of the diode was destroyed.

The second cause of diode mortality is related to the first in that the gold ball was crushed. It was discovered that when either of the single stub tuners was adjusted by moving the plunger the inner conductor of the line was bowed or flexed enough to move and change significantly the pressure on the diode. In some cases the pressure was increased enough to destroy the diode. Even though the diode was not crushed it may have been the cause of the continual readjustment mentioned above. The remedy was found to be increased support under the stub tuners.

Figure 48 is included because it shows a diode going into reverse (Zener) breakdown. Note how the resistance increased with reverse current and how the capacity tended to remain constant.

7. Conclusions

An overall survey of the results obtained using the low-impedance slotted line shows three facts, for the small number of diodes measured: That reliable values for the diode resistance can be obtained. That an accurate indication of the relative diode capacitance change with a change in the bias voltage can be determined. And that the exponent of the voltage function of the capacitance can be found with a reasonable degree of accuracy.

Conclusions were further drawn that the resistance was not a function of frequency in the range from 2 to 7.5 kMc and that the diode contact resistance could be a major factor in the resistance value. It was also gratifying to achieve actual values for the line parameters that, in some cases, approached the calculated values, considering the large number of variables and unaccountable factors involved.

Future endeavor with this low-impedance line should be centered around efforts to determine a reliable position for the reference short. It seems likely that this position will have to be determined individually for each diode at each frequency to be used for measurements. This is because the variabilities in the manufacturing process are enough to cause each diode to modify the shunt cavity to a different degree. It may be that the best solution will be to return to the diode holder originally used on the 50 ohm line where the diode became an actual extension of the inner conductor. The most objectional feature of this holder, the wiping action of the plunger as it advanced on the diode, could be eliminated in much the same way the rotary motion was eliminated in the diode holder now in use on the low impedance line. This procedure would also

eliminate the step now required to compensate for the cavity shunt capacitance. However, there are also problems here regarding the actual position of the reference short.

Another factor which needs further investigation is the maintenance of uniform contact pressure. It was noted that while a great deal of pressure was required to stabilize the resistances, once this value was reached, further pressure did not appreciably alter the resistance values. The elimination of inner conductor movement when the stub tuners were used should reduce the diode mortality considerably. It should be possible now to determine a more or less constant, or uniform, pressure to exert on the diode for use both in measurements and in parametric amplifiers. In the amplifiers, if the contacting pressure were less than this minimum, the diode resistance would be increased, with a consequent increase in the noise generated, and a reduction in one of the principle advantages of the parametric amplifier.

Finally, it may be that the low-impedance line would best be used to measure just the resistance of the diode. There may be better methods available for the capacitance measurements; e.g., substitution in a resonant circuit.

APPENDIX I

DESIGN OF THE LOW IMPEDANCE SLOTTED LINE

The first decision was to pattern the line after the coaxial slotted section of the HP 806B, for the emminently practical reason that it was already available, and thus the carriage and probe assembly could be used directly. Secondly, a search turned up about a three foot piece of Corning 0120 glass with a dielectric constant near six. Hurried measurements and rapid calculations showed the characteristic impedance would be about six.

The dielectric rod - Corning 0120 - was measured carefully. The The outer diameter was .227 inches, the inner diameter was .175 inches and the dielectric constant listed as 6.64 at 3 kMc.(9)
Using the formula for the characteristic impedance of a coaxial line:

$$Z_o = 60/\sqrt{\epsilon'} \quad \ln \frac{(r_o)}{(r_i)}$$

where $60 = n/2\pi : \frac{\sqrt{\mu/\epsilon}}{2\pi}$ for air dielectric, ϵ' = relative dielectric constant and r_o and r_i are the outer and inner radii respectively. The characteristic impedance of the glass-dielectric slotted line calculates as:

$$Z_o = \frac{60}{\sqrt{6.64}} \ln \frac{.227}{.175} = 23.4 \ln 1.298 = 23.4 (.261) = 6.12$$

If the value of diode capacitance remains at 3uuf, as already indicated, the capacitive reactance will be 53.2/f kMc ohms and will vary from 17.7 to 4.4 ohms. This means that the normalized capacitive reactance will lie between 2.9 and .72 ohms - comfortable values to fit on the Smith Chart. If, however, the diode capacity proves to be 1 uuf, as is desired, the normalized values will range from 8.7 to 2.2 ohms and the

low frequency values will fall on an unhappy portion of the Smith Chart. Thus, it may turn out that the best value for Zo will lie around 20.

Since the characteristic impedance is a function of the dielectric constant and the inner and outer radii, the effect of small parameter variations can be found by taking the total differential. Thus,

$$dZ_o = \frac{\partial Z_o}{\partial \epsilon'} d\epsilon' + \frac{\partial Z_o}{\partial r_o} dr_o + \frac{\partial Z_o}{\partial r_i} dr_i$$

Now, the final result is not necessarily cumulative and, while the effect of each parameter can be calculated separately for small changes, the overall change is Zo is not always additive.

For a small change is dielectric constant - $d\epsilon'$

$$\frac{\partial Z_o}{\partial \epsilon'} = 60 \ln \frac{r_o}{r_i} \frac{\partial}{\partial \epsilon'} \left(\frac{1}{\sqrt{\epsilon'}} \right) = 60 \ln \frac{r_o}{r_i} \left(-\frac{1}{2} \epsilon'^{-\frac{3}{2}} \right) = -\frac{.455}{6.12} = -6.85\%$$

Therefore, for small changes in the dielectric constant, the change in characteristic impedance is approximately 7% per unit change in dielectric constant, in the opposite direction.

For a small change in the outer radius - dr_o

$$\frac{\partial Z_o}{\partial \epsilon} = \frac{60}{\sqrt{\epsilon'}} \frac{\partial}{\partial r_o} \ln \frac{r_o}{r_i} = \frac{60}{\sqrt{\epsilon'}} \frac{1}{r_o} = .206 \frac{\text{ohms}}{\text{mil}} = 3.36\%/\text{mil}$$

Therefore, the change in characteristic impedance is some 3.7% per mil change in the outer radius, in the same direction.

For a small change in the inner radius - dr_i

$$\frac{\partial Z_o}{\partial r_i} = \frac{60}{\sqrt{\epsilon'}} \frac{\partial}{\partial r_i} \ln \frac{r_o}{r_i} = -\frac{60}{\sqrt{\epsilon'}} \frac{1}{r_i} = -.268 \frac{\text{ohms}}{\text{mil}} = -4.38\%/\text{mil}$$

Therefore, the change in characteristic impedance is some 4.4% per mil change in inner radius, in the opposite direction.

This means that the most undesirable condition would be a change of the two radii in opposite directions where their overall effect would be additive. If it is assumed that the outer and inner diameters are maintained to within an accuracy of 1 mil, the largest change in Zo could be .206 .268 = .474 ohms or .474/6.12 = 7.75%. This would mean a difference of some 2 uuf for the final diode capacitance at the lower end of the frequency scale (assuming a normalized reactance of 3 ohms).

The presence of the slot produces a change in Zo, a field variation, a wave velocity change and possible additional modes.[10] First, the slot changes Zo in the coaxial cable according to the formula:

$$\frac{\Delta Z_o}{Z_o} = \frac{1}{4\pi^2} \frac{\omega^2}{r_2^2 - r_1^2}$$

where w = width of the slot. The probe on the HP 806B is approximately 35 mils in diameter and if a slot width of 50 mils is used the change in the characteristic impedance would only be 1.2%. But a slot width of 120 mils must be used, as will be explained later, and the change in Zo is 8.3%.

Second, abrupt slot terminations mean that the fields in the slotted and unslotted lines are somewhat different. This can be compensated by changing some other dimensions in the slotted line, changing conductor radii, or providing a small ramp attached to the inner conductor. Or, the effect can be reduced somewhat by extending the slot to the end of the line - in the vicinity of the load - where probe measurements would seldom be made. Lowering the Zo of the line had aided this cause since the reflections from the small load will be greater relatively than in the 50 ohm line.

Third, the slot changes the wave velocity. This shift is seldom important and it is usually sufficient to measure the distance between successive minima with the slotted line shorted. If the correction is desired, it can be computed by using the nodal-shift method to obtain the ideal transformer representation.(11)

Finally, it is possible to excite "slot resonant" modes which can completely alter the true standing wave picture. These modes can be suppressed by maintaining symmetry in the slotted line construction; "damping the slot mode" by placing powdered iron absorbing material at each end of the slot and by tapering the severity of the slot termination.

Next of concern is the probe, even though the one already mounted in the HP 806B was used. This is because the probe does extract power from the line and the fact that the wide slot, low probe-slot capacity requirement is directly in conflict with the narrow slot low characteristic impedance change requirement. The power absorbed by the probe is generally explained in terms of the probe impedance which can be considered to be in shunt with the load, as shown in Figure 13. The effect of the probe impedance depends upon the relative values of the generator, probe and load impedances and upon the position of the probe with respect to the load. Note that the probe susceptance can be cancelled out by tuning the probe for maximum output with a reactive tuner in shunt. The greater the probe penetration the greater the power absorbed and the greater the effect on the impedance measurements. It is therefore necessary to reduce the probe penetration to as small a value as possible consistent with a useful detector response. The situation is a complicated one and let it suffice to say that the best results obtain when both the power from the generator and the detector sensitivity are high.

The probe and its detection circuit can be represented, as shown in Figure I-4, relative to the transmission line. Here C_1 represents the capacity of the probe to the opposite side of the line and C_2 represents the capacity of the probe to the shot. C_2 is clearly much greater than C_1 and the narrower the slot the greater the ratio. This condition is not serious in itself however, it imposes a rather severe mechanical restriction inasmuch as a constant value of C_2 becomes exceedingly difficult to maintain as the probe moves in a very narrow slot.

Two methods are suggested for reducing the effect of changes in the probe-to-slot capacity. One is to detune the probe tuning mechanism by a significant factor, such as 10. However, this is wasteful of power and power is not likely to be overabundant in the first place due to the large Zo change between the generator and the slotted line.

The other method is to reduce C_2 by the insertion of a "skirt" into the slot to shield the probe. But this, of necessity, enlarges the size of the slot. The latter method was the one chosen in the case of the HP 806B and the size of the slot must therefore be some 120 mils.

One very good way to gain an idea of the overall effect of the probe on the line is to place a second "standing wave detector" ahead of the probe and note the voltage distribution when the probe is moved or the depth of the penetration is varied.(12)

Next, the effect of dielectric inhomogeneities; i.e., large, sudden changes in the dielectric constant must be considered. The worst situation that can be thought of is an air bubble in the dielectric material. Now, obviously a large air bubble would cause considerable reflections and seriously impair the accuracy of the results. Therefore, only small bubbles are of concern - that is those that are barely visible.

Assume the air bubble is a wedge-shaped piece, one degree in width, extending from the inner to the outer radius. Then the change in Zo would be:

$$1 - \frac{1}{\sqrt{\epsilon' - (1-\epsilon')\,\theta/360}} = 1 - .993 = .007$$

which is completely negligible in the light of the other factors.

All of the discussion relative to coaxial lines has assumed that the only mode propagated by the waveguide has been the principle or TEM mode. But higher order modes can exist. For these higher modes, the coaxial line acts like a high-pass filter, and a given line will carry energy in one of the higher modes only if excited at a frequency above the critical or cutoff frequency for that mode. The higher modes may be excited at lower frequencies in the vicinity of discontinuities in the line, in order to fulfill the boundary conditions they must exist, but they are attenuated rapidly and draw no real power.

Now the critical wavelength for the lowest order higher mode is approximately equal to the mean circumference of the coaxial line inner and outer conductors. That is:

$$\lambda_c = \pi (r_o + r_i) = \pi (.1135 + .0875)\, 2.54 = \pi (.2015)\, 2.54 = 1.6 \text{ cm}$$

In a coaxial line with air dielectric this would correspond to a frequency of 18.75 kMc, well above the desired frequency range. However, in a waveguide filled with a dielectric other than air the frequency of propagation is directly proportional to $1/\sqrt{\epsilon'}$. Therefore, the frequency corresponding to a cutoff wavelength of 1.6 cm is 7.28 kMc and this may very well indeed cause spurious reading at frequencies much above 9 kMc.

This cutoff frequency is for the $TE_{1,1}$ mode. The cutoff frequency for the next higher mode, $TE_{2,1}$ occurs at twice the cutoff frequency for the $TE_{1,1}$ mode, or 14.56 kMc. The first TM mode does not enter the picture until about 80 kMc. It may seem surprising at first thought that the first higher-order mode is not the $TE_{0,1}$ mode but a glance at Figure 5 will show that the $TE_{1,1}$ mode is the most readily formed.

Finally, the attenuation of the dielectric must be considered. The attenuation can be divided into two losses: conductor and dielectric. The attenuation resulting from conductor losses in a coaxial line is given by

$$\alpha_c = 13.6 \frac{\delta \mu}{\lambda} \frac{1}{r_o} \left(1 + \frac{r_o}{r_i}\right) \frac{\sqrt{\epsilon'}}{\ln \frac{r_o}{r_i}} \quad \frac{db}{\text{unit length}}$$

where δ = skin depth and λ is the free-space wavelength. Skin depth is considered as the depth at which the current density has fallen to $1/\epsilon$ of its surface value - it amounts to considering that the total current is of uniform density to a depth δ. It is a function of frequency and conductor material and is given by

$$\delta = \frac{1}{2\pi} \sqrt{\frac{\lambda \rho}{30 \omega}} \text{ cm}$$

where ρ is the resistivity in ohm-cm; λ is the free-space wavelength and μ is the permeability. If the conductor walls are silver-plated then the skin depth varies from .047 mils at 3 kMc to .03 mils at 12 kMc. Thus, the attenuation resulting from conductor losses amounts to 2730 δ/λ db/in. and is .03 db/in. at 3 kMc and .08 db/in. at 12 kMc.

The dielectric loss however is apt to be considerably higher. The attenuation in a coaxial line resulting from dielectric losses is

$$\alpha_d = 27.3 \frac{\sqrt{\epsilon'}}{\lambda} \tan \delta \quad \frac{db}{\text{unit length}}$$

where $\tan \delta$ = the loss tangent of the dielectric. For the two frequencies of concern, $\tan \delta$ = .0041 at 3 kMc and .0063 at 10 kMc. Thus, α_d = 179 $\tan \delta / \lambda_{cm}$ dg/in. and calculates to .073 db/in. for 3 kMc and .38 db/in for 10 kMc. This means that the total loss for a line ten inches long will vary between 2.06 db and 9.2 db and offers convincing evidence in support of the statement that "solid dielectric lines are not widely used at microwave frequencies when low attenuation is important."(13)

Undoubtedly, the attenuation will have to be taken into account in the standing wave measurements. In fact, such measurements can be used to determine what the effective dielectric constant actually is and then compared with the dielectric constant obtained by measuring the distance between electric field minima. This comparison could then be used to determine the effective loss tangent or dissipation factor.

One other point, a slab line(14) would reduce the mechanical tolerances necessary, the effect of the probe and the radiation from the slot but these benefits would be accompanied by the problem of obtaining a block of dielectric some ten cm long and placing an inner conductor in the center of it. Time and the facilities available simply would not permit entertaining the thought of using the slab line.

In summary, then, parameter variations can produce a change in the characteristic impedance of as much as 15%; the slot changes the impedance by about 8% and can introduce undesired fields; the probe extracts power from the line and places a shunt impedance across the load; dielectric inhomogeneities are not serious as long as they are small; a higher order mode, $TE_{1,1}$ will probably interfere around 9 kMc; and, finally, the attenuation will be considerable and must be taken into account. All of these factors lead to the conclusion that a very complete investigation and calibration of the line, as built, will have to be made before any hope of obtaining significant measurements of the diode are concerned.

Design of the Diode Holder. (See Figures 1-7 through 1-10)

After the design of the slotted line section, the next problem was the design of the diode holder - the device to fit on the end of the slotted line - which would move the diode to make contact, establish the short for calibration purposes, and allow a dc bias to be maintained.

In the first diode holder, the diode was placed in an extension of the coaxial inner conductor - see Figure I-2 - and the micrometer plunger was advanced until contact was made. One objectionable feature of this diode holder was that the plunger was advanced by rotating the micrometer head and the possibility existed that the gold ball on the diode could be wiped off by the plunger as contact was made. Therefore, what was needed was a differential which would convert the rotary motion of the plunger to translational motion. This was accomplished by a slide cylinder which would fit into a longitudinal hole in the holder body and would carry the diode at one end and slide in the hole a distance directly proportional to the advance of the micrometer plunger.

The micrometer barrel is threaded for 40 threads per inch and has a distance of travel of .5 inches. Now, if the micrometer plunger and a hole in the slide cylinder are threaded for 80 threads per inch in the same sense as the micrometer barrel threads, then the plunger will advance .250 inches into the slide cylinder while the micrometer is advancing .5 inches into the body and the overall travel of the diode will be .25 inches in the same direction as the micrometer head. To insure that no rotary motion will be translated to the diode, the slide cylinder was keyed to a keyway in the diode holder body.

Because a dc bias must be maintained on the diode it is important that the inner conductor be connected to the outer conductor only through the diode. This means that a cavity must exist between the diode and the dielectric of the slotted line - but it must be as small as possible. Therefore, a threaded plug was designed to fit into the end of the diode holder and to contact the end of the slotted line. The plug has a hole tapered to 1/16 inch for the diode and a cylindrical hole about 5 mils deep with a diameter equal to the outer diameter of the slotted line dielectric. See Figure I-6 for details. The depth of the hole is nominally that of the height of the diode with the idea of eliminating the diode post as part of the circuit but this height may vary - see the details of diode construction. Now then, if any effects introduced by the diode post are ignored, a simple parallel-plate capacitor shunts the diode. The magnitude of the capacitance can be calculated using the formula:

$$C = \epsilon A/d$$

where ϵ = absolute dielectric constant i.e., $\epsilon_0 \epsilon'$, A = area of one plate and d = the separation. Then C calculates to 1.82 uuf.

The reactance is 87.5/f and varies from 29.8 ohms to 7.3 ohms and this value can be deducted from the measured diode reactance if it is not accounted for by the short.

The third function of the diode holder is to provide a short. There are two ways envisaged for accomplishing this. One is to manufacture a metal diode of the same shape as a regular diode and to make a series of measurements using this "dummy diode". The second method is to actually short the end of the line with a piece of metal. If the inductance of the "dummy diode" post can be ignored, the difference between the readings of these two shorts should be negligible.

Design of the Coaxial Connector and the Tuning Stubs.

Now the other end of the line must be considered - the actual electrical and physical connection to a coaxial cable of 50 ohms impedance.

To go from a 50 ohm line to a 6 ohm line is a tremendous change - it is not too far away from a short on the 50 ohm line. The reflection coefficient is $\frac{50-6}{50+6} = .786$, which means that over 60% of the incident power is reflected. Therefore, means of matching these lines must be considered.

The match must exist over a frequency range of some five to one and this rules out any stationary quarter-wave devices such as sleeves or beads. Tapers or multiple quarter-wave matching sections are feasible but not practical because of their length. A substantial reduction in the Standing Wave Ratio does not occur until the section is greater than two wavelengths long, and a 20 cm tapered section is too long to be practical. This leaves the shunt susceptance, or tuning stub, as the only feasible method and this is the one employed.

Then, the shape of the actual connection between the coaxial line and low impedance slotted line is not too important as long as the connection is positive and "clean". Therefore, it was decided to modify an existing N-type Amphenol UG-22B/U connector. See Figure I-9 for details. The inner conductor of the slotted line will be tapered to fit the inner conductor of the connector. This amounts to a taper of .175 to .120 in a distance of .438 inches or about .4 degrees. At the same time the outer ring of the connector is tapered in the opposite direction to meet the outer conductor of the slotted line.

This amounts to a change from .227 to .280 in a distance of .288 inches or about .5 degrees. Thus, the inner conductor will be continuous until after the taper and the outer conductor will join the connector before the taper - assuring a positive contact.

Tuning stubs for coaxial lines are common. There is only the problem of maintaining a dc bias while providing an rf short. This problem had already been adroitly handled in the original diode tester used with the 50 ohm line by constructing a "Biasing Short" - see Figure I-7. Very thin sheets of dielectric were placed at every metal-to-metal contact between the inner and outer conductors of the tuner allowing the rf to pass but still allowing a dc bias.

One of these shorts had already been constructed and it was merely necessary to build another. By building them on different sections the distance between the tuners can be varied thus permitting a little wider range of tuning should the double stub tuner prove inadequate.

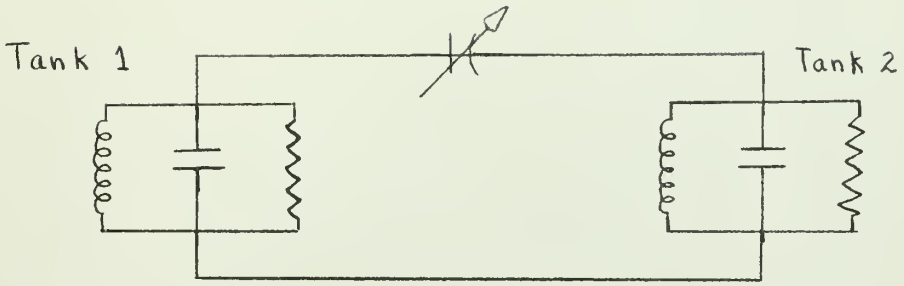

Fig. 1 Equivalent circuit for a two-tank parametric amplifier.

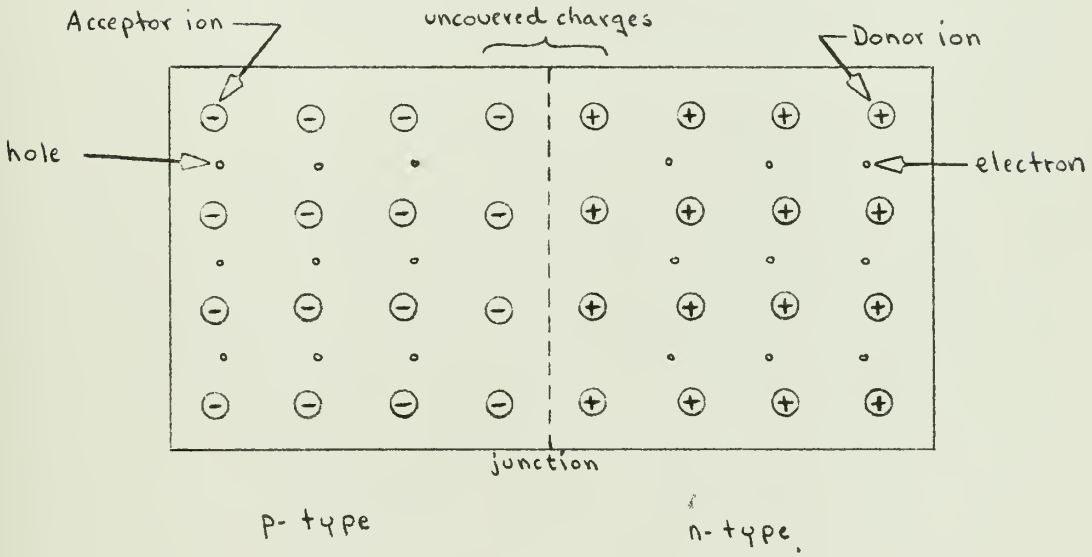

Fig. 2 Charge distribution at junction between p-type and n-type semiconductors

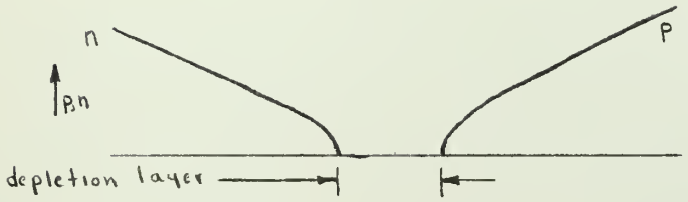

(a) Zero Bias

(b) Small Forward Bias

(c) Reverse Bias

n = concentration of electrons

p = concentration of holes

Fig 3 Electron and hole concentration in vicinity of a graded p-n junction.

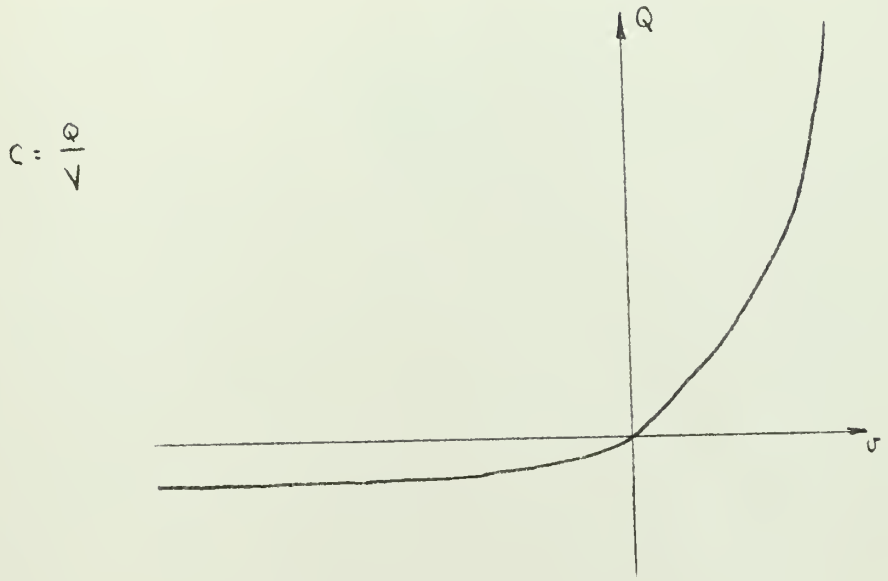

Fig 4 A charge-voltage characteristic of a non-linear capacitor

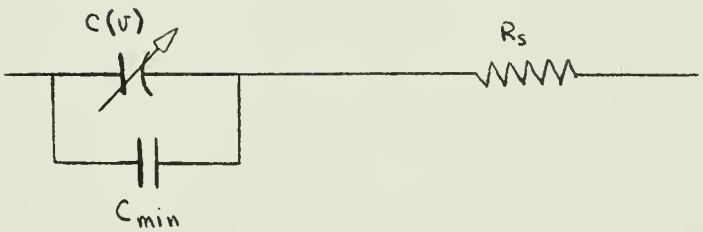

Fig 5 High-frequency equivalent circuit of non-linear capacitor

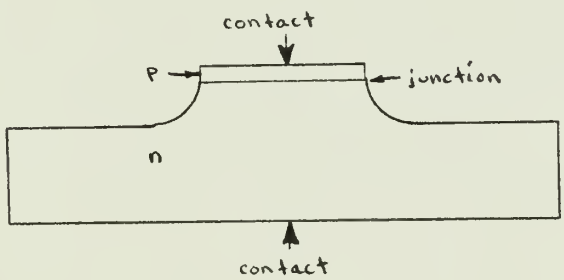

Fig 6 P-n junction "mesa" diode

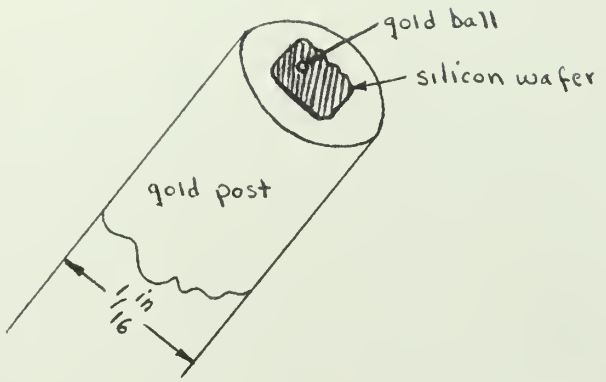

Fig 7 Overall view of a diode

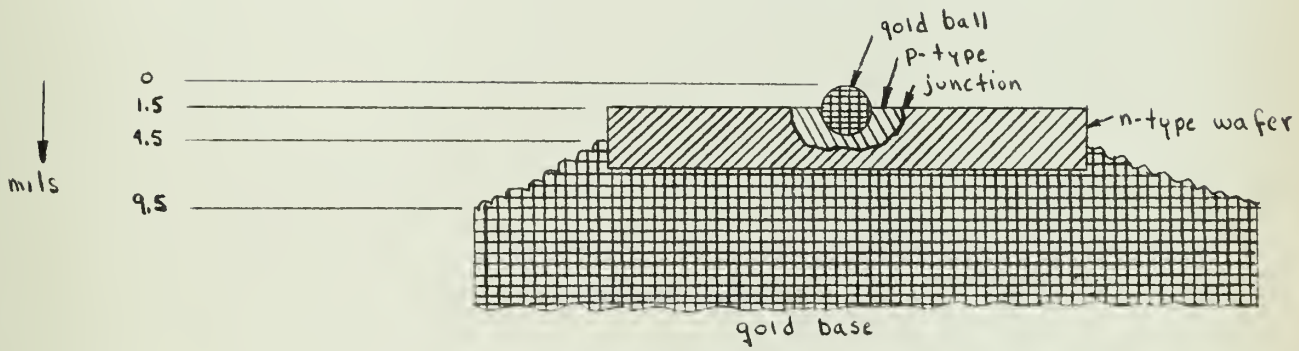

Fig 8 Cross-section of a diode

$$V_{m_1} = V_{i_1} - V_{r_1}$$

$$V_{m_2} = V_{i_2} - V_{r_2}$$

$$V_{i_2} = V_{i_1} e^{-\alpha l}$$

$$V_{r_2} = V_{r_1} e^{\alpha l}$$

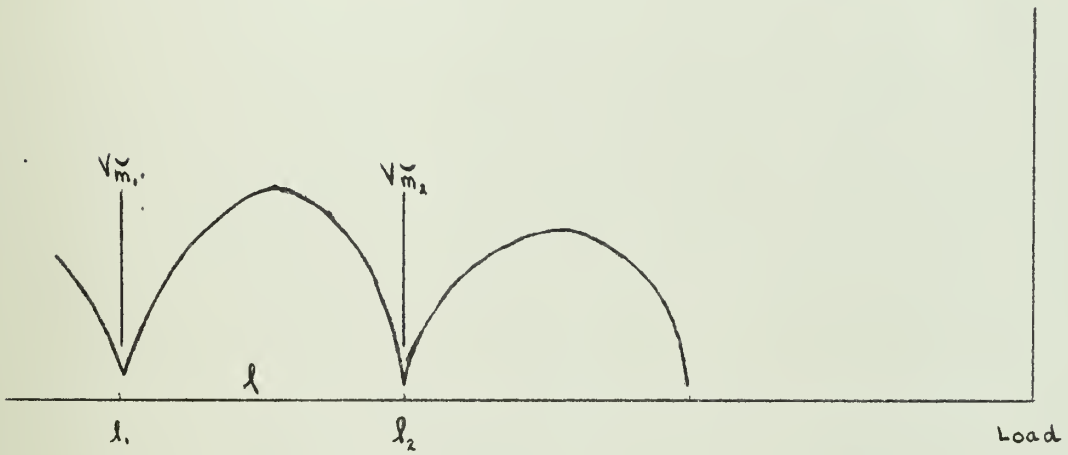

Fig 9 Diagram for computing attenuation

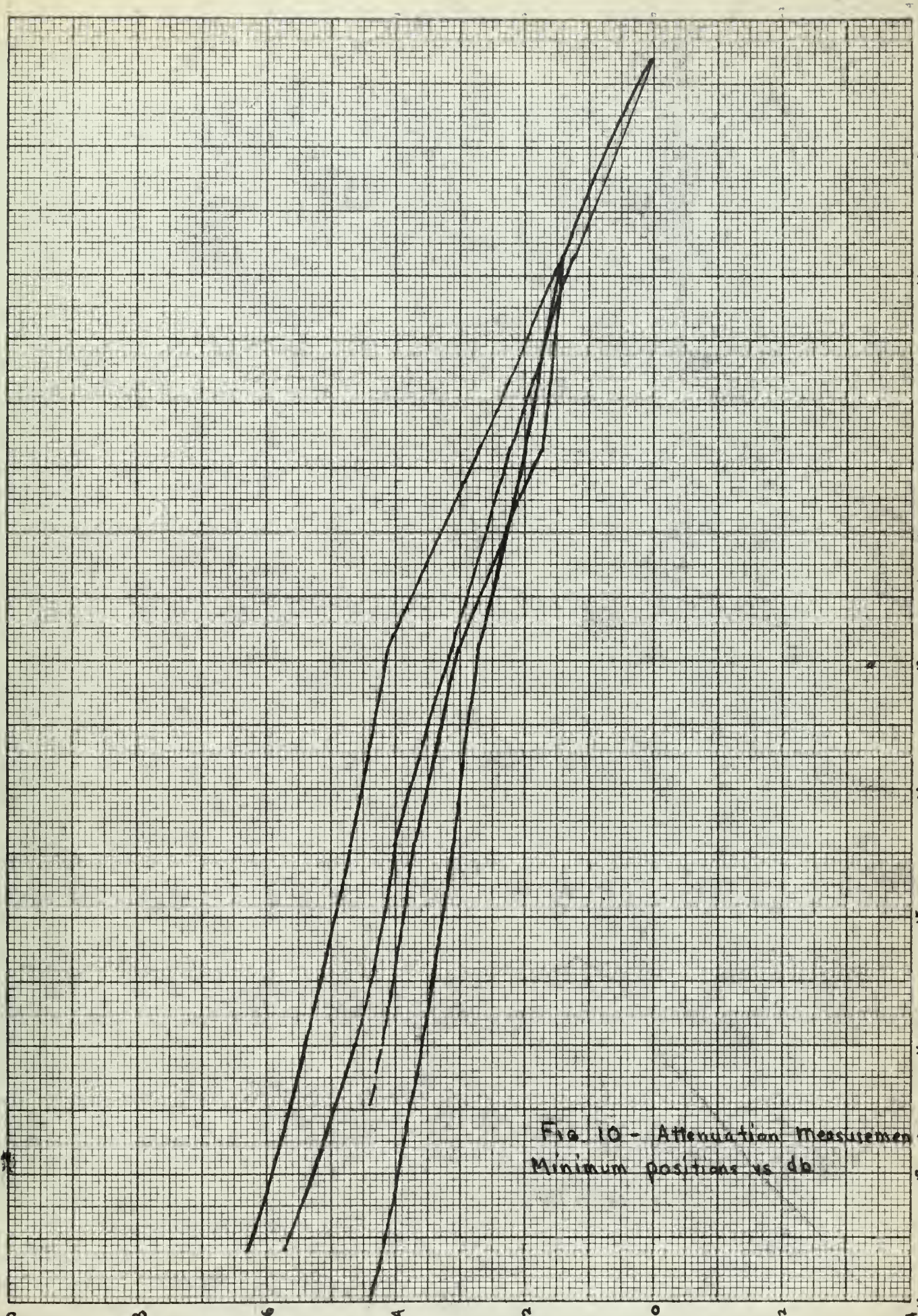

Fig. 10 - Attenuation Measurements
Minimum positions vs db

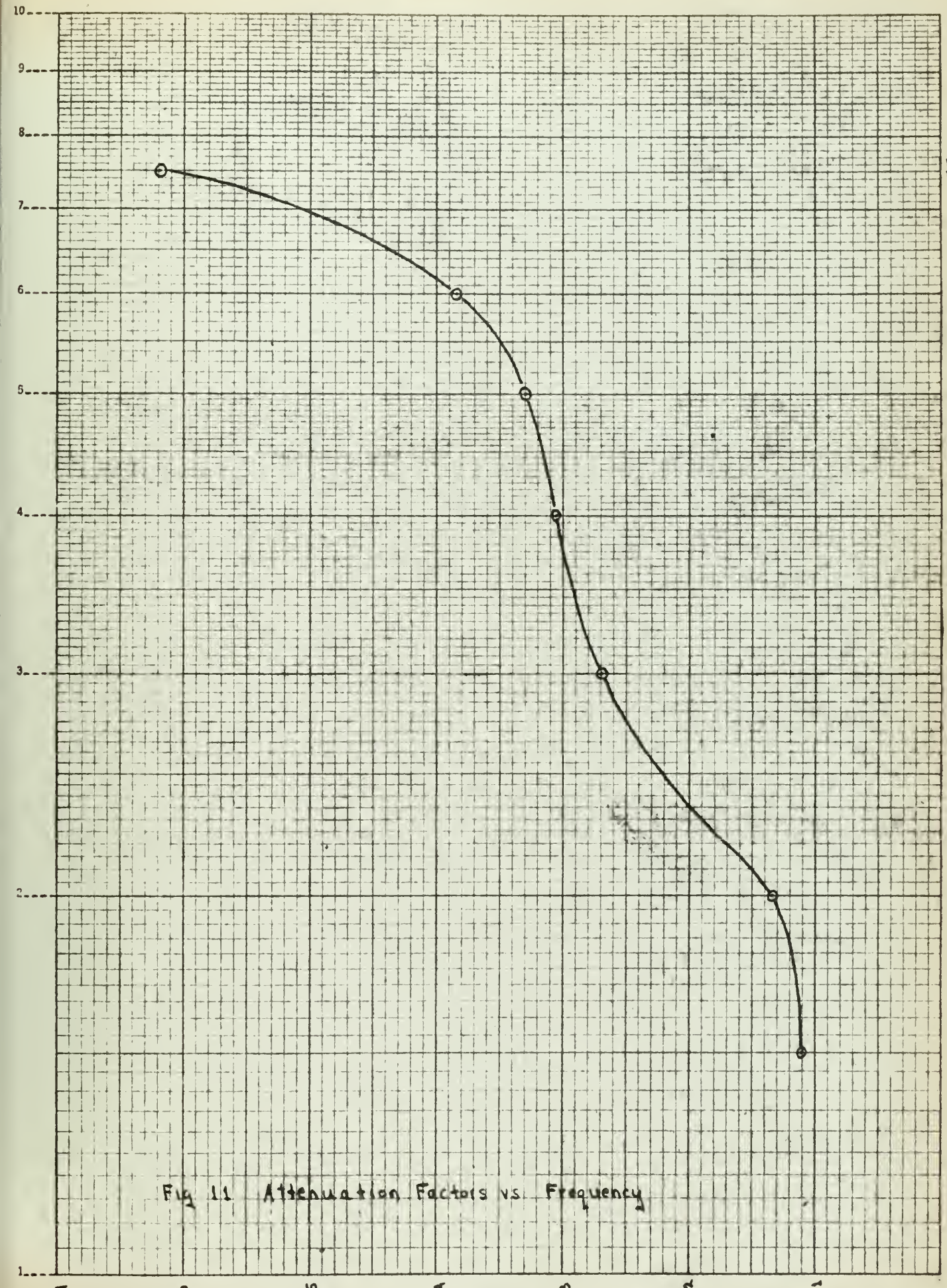

Fig 11 Attenuation Factors vs. Frequency

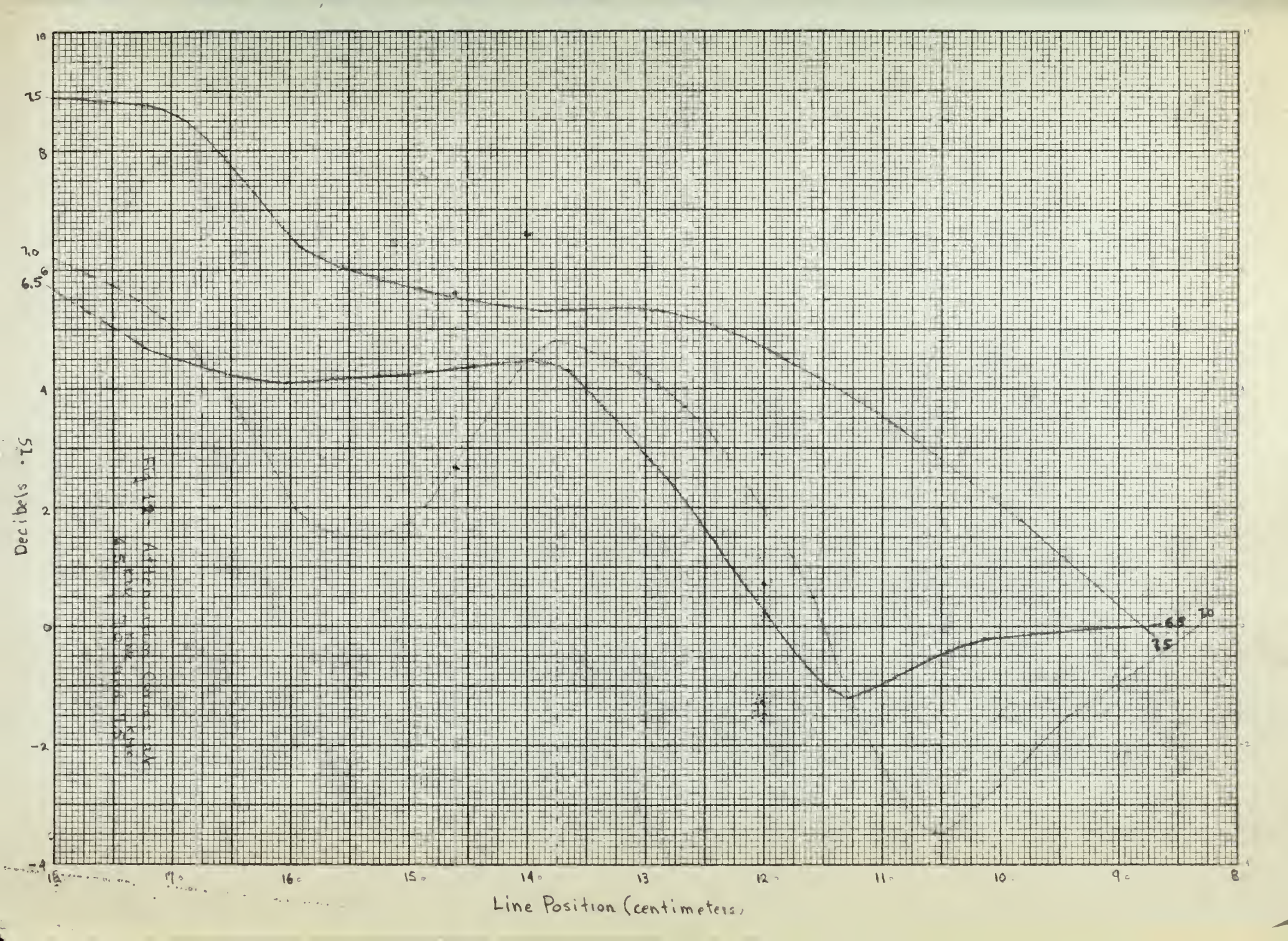
Decibels · SL
Line Position (centimeters)
6.5
7.0
6.8
7.0
7.5

NAME	TITLE	DWG. NO.
Fig 13	Impedance Change vs Dummy Diode Distance from Short	
SMITH CHART FORM 82BSPR (2-49)	KAY ELECTRIC COMPANY, PINE BROOK, N.J. ©1949 PRINTED IN U.S.A.	DATE

IMPEDANCE OR ADMITTANCE COORDINATES

Frequency - 5 kMc

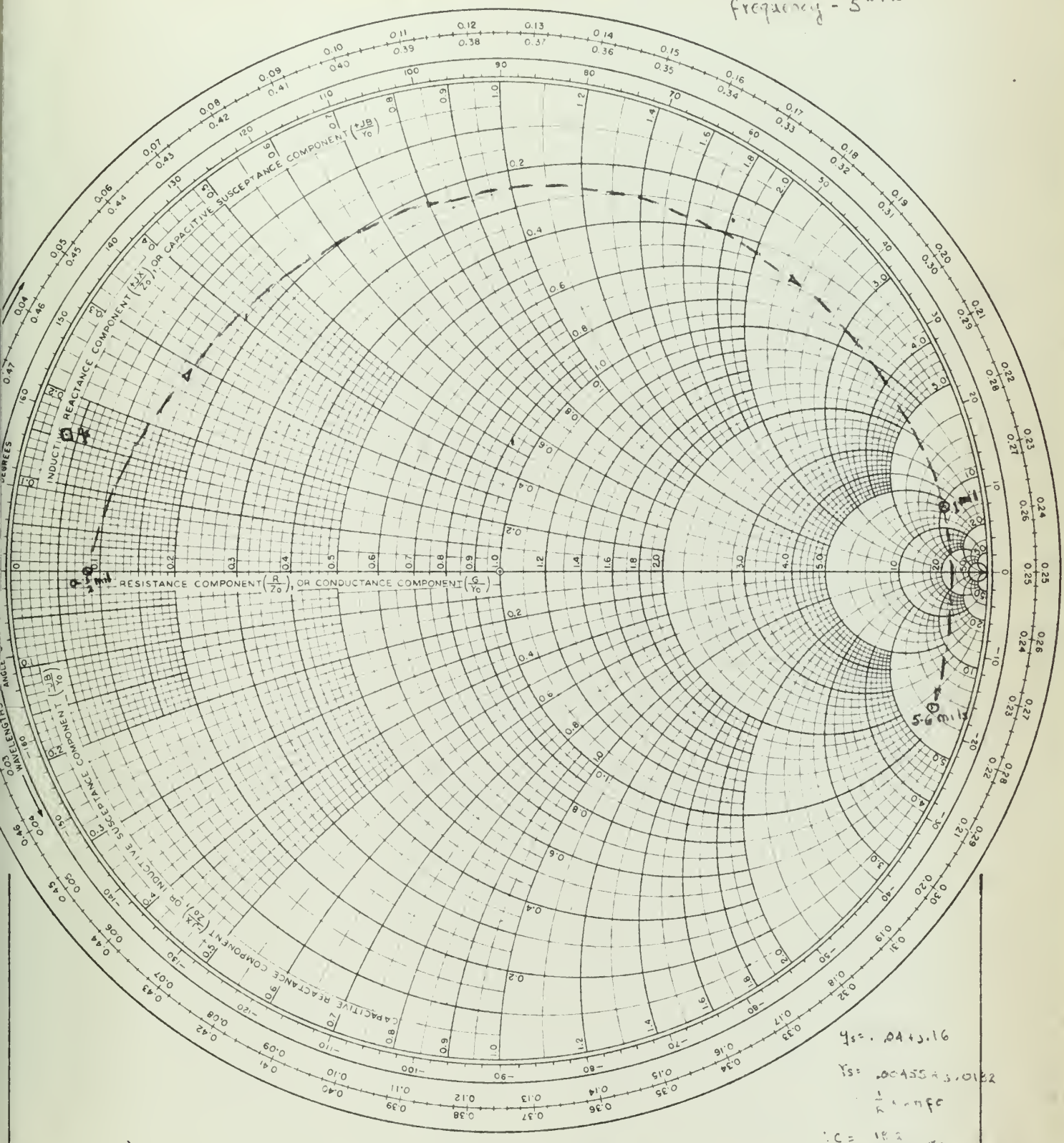
RESISTANCE COMPONENT $\left(\frac{R}{Z_0}\right)$, OR CONDUCTANCE COMPONENT $\left(\frac{G}{Y_0}\right)$
INDUCTIVE REACTANCE COMPONENT $\left(\frac{+jX}{Z_0}\right)$, OR CAPACITIVE SUSCEPTANCE COMPONENT $\left(\frac{+jB}{Y_0}\right)$
CAPACITIVE REACTANCE COMPONENT $\left(\frac{-jX}{Z_0}\right)$, OR INDUCTIVE SUSCEPTANCE COMPONENT $\left(\frac{-jB}{Y_0}\right)$
WAVELENGTHS TOWARD GENERATOR
DEGREES
0 mils
2 mils
5-6 mils

$Y_s = .04 + j.16$

$Y_s = .0645 + j.0182$

$\frac{1}{Y_s} = \text{complex}$

$Y_C = \frac{1}{10K} = .1580$

RADIALLY SCALED PARAMETERS

TOWARD GENERATOR → ← TOWARD LOAD

REFLECTION COEFF. | VOLT. REFL. COEFF. | POWER REFL. COEFF. | LOSS IN DB

CENTER 52.

Electronics - VOL. 17, NO. 1, PP 130-133, 318-325, JAN 1944

A MEGA-CHART

NAME	TITLE	DWG. NO.
Fig 14	Impedance Change vs Dummy Diode Distance	4
SMITH CHART FORM 828SPR (2-49)	KAY ELECTRIC COMPANY, PINE BROOK, N.J. ©1949 PRINTED IN U.S.A.	DATE

IMPEDANCE OR ADMITTANCE COORDINATES Frequency - 6 kMc

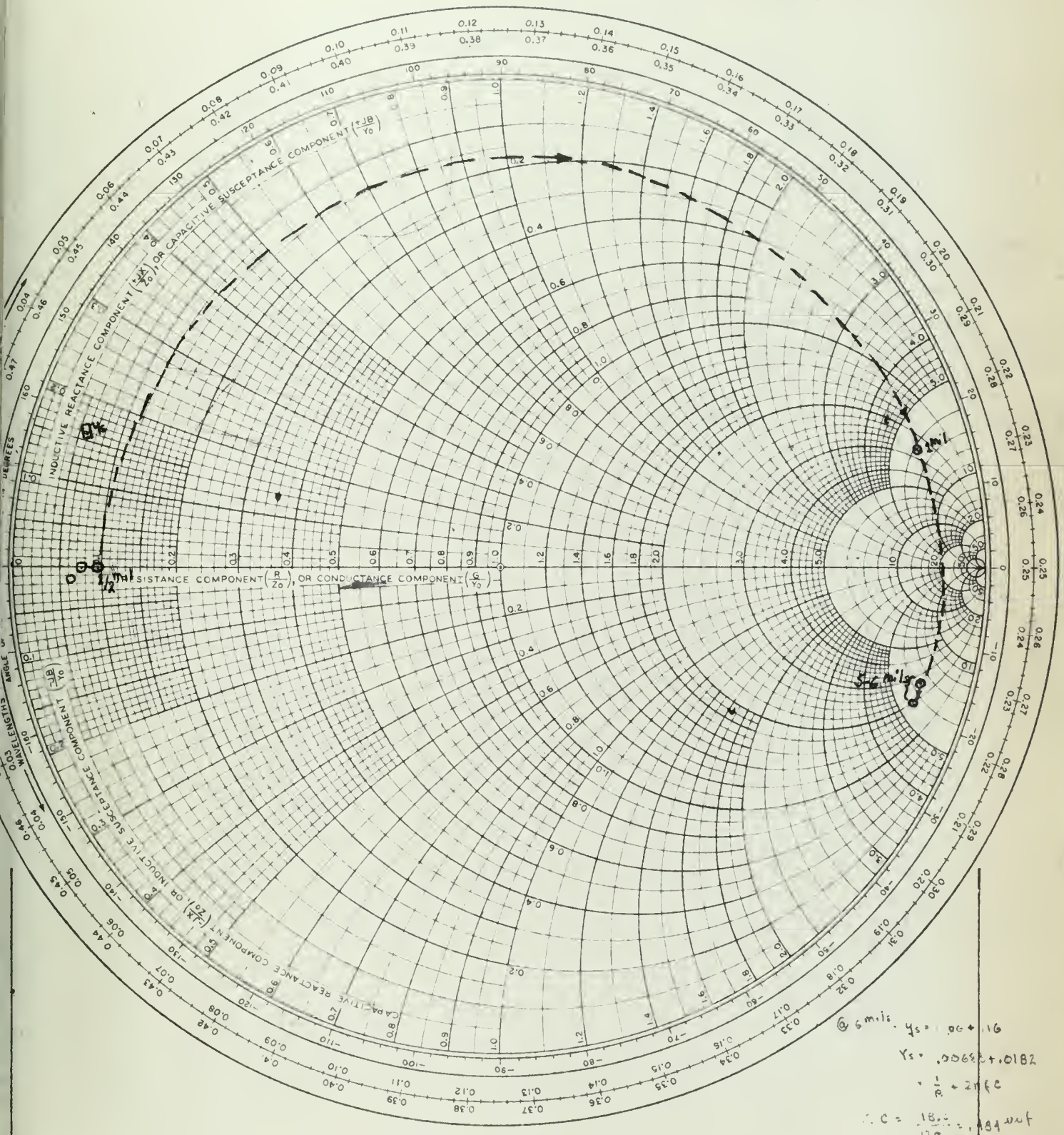
INDUCTIVE REACTANCE COMPONENT $\left(\frac{+jX}{Z_0}\right)$ OR CAPACITIVE SUSCEPTANCE COMPONENT $\left(\frac{+jB}{Y_0}\right)$
RESISTANCE COMPONENT $\left(\frac{R}{Z_0}\right)$, OR CONDUCTANCE COMPONENT $\left(\frac{G}{Y_0}\right)$
CAPACITIVE REACTANCE COMPONENT $\left(\frac{-jX}{Z_0}\right)$ OR INDUCTIVE SUSCEPTANCE COMPONENT $\left(\frac{-jB}{Y_0}\right)$
WAVELENGTHS TOWARD GENERATOR
ANGLE OF REFLECTION COEFFICIENT IN DEGREES
0 mils
1/2 mil
6 mils
52 mils

@ 6 mils. $Y_s = .96 + .16$

$Y_s = .0566 + .0182$

$= \frac{1}{17.6} + 2\pi fC$

$\therefore C = \frac{18.2}{12\pi} = 1.484\ \mu\mu f$

RADIALLY SCALED PARAMETERS

TOWARD GENERATOR → ← TOWARD LOAD

REFLECTION COEFF. | VOLTAGE REFLECTION COEFF. | POWER REFLECTION | LOSS IN DB

CENTER

Electronics - VOL 17, NO.1, PP 130-133, 318-325, JAN 1944

A MEGA-CHART

ME	TITLE	DWG. NO.
Fig 15	Impedance Change vs Dummy Diode Distance	
ITH CHART FORM 82BSPR (2-49)	KAY ELECTRIC COMPANY, PINE BROOK, N.J. ©1949 PRINTED IN U.S.A.	DATE

IMPEDANCE OR ADMITTANCE COORDINATES

frequency - 7.5 KMc

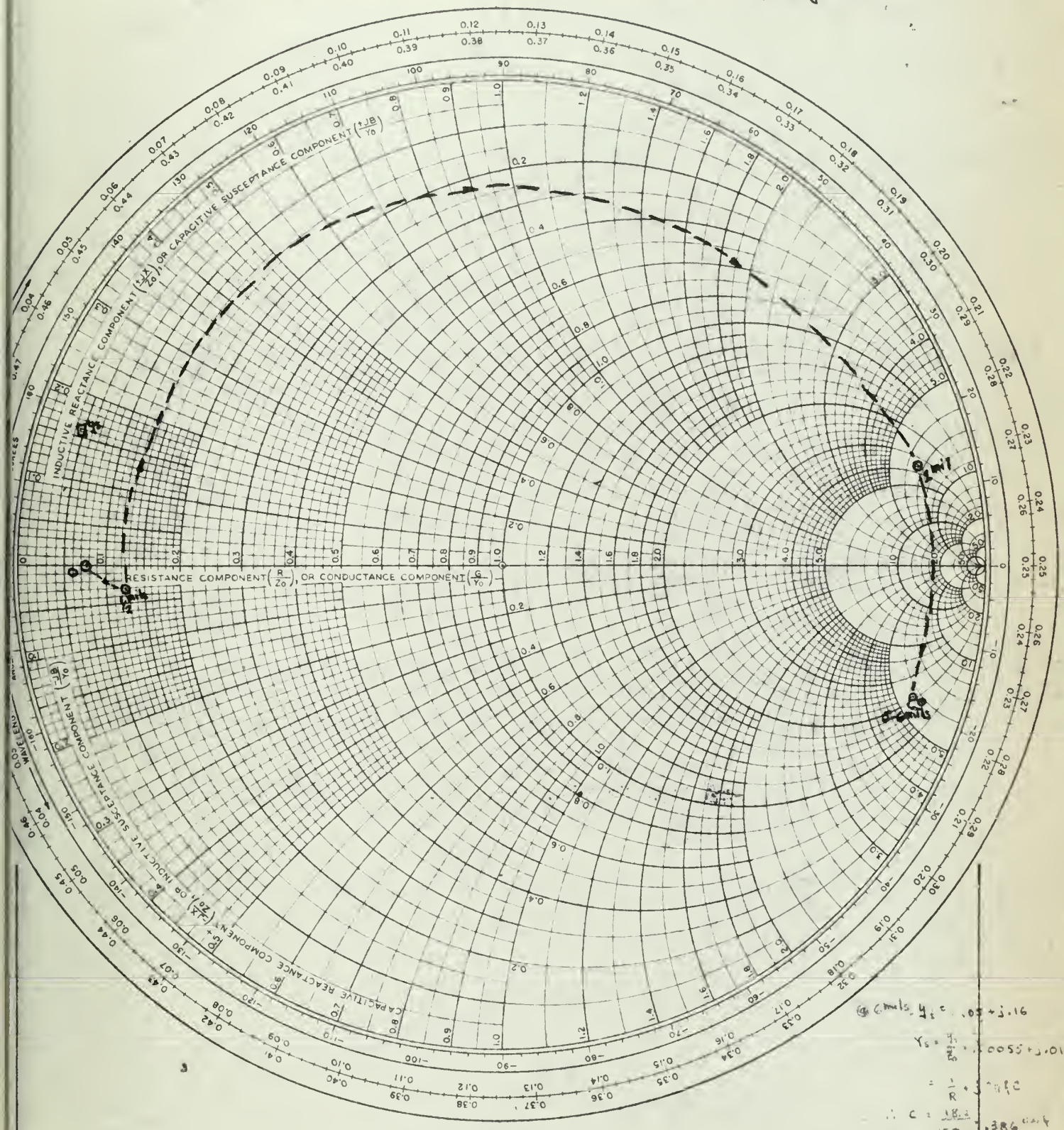

@ 6 mils $Y_L = .05 + j.16$

$Y_S = \frac{Y_L}{Z_0} = .0055 + j.0182$

$= \frac{1}{R} + j\omega C$

$\therefore C = \frac{.182}{15\pi} = .386$ mmf

RADIALLY SCALED PARAMETERS

TOWARD GENERATOR → ← TOWARD LOAD

REFLECTION COEFF | LOSS IN DB | VOL. PWR. RETN REFL

CENTER

Electronics - VOL 17, NO.1, PP 130-133, 318-325, JAN. 1944

A MEGACHART

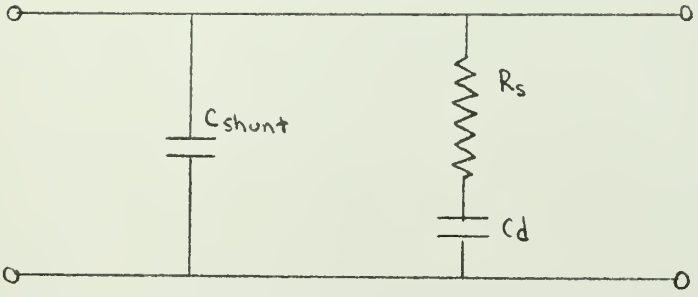

C_{shunt} = effect of end cavity

C_d = diode capacity at back bias - C_{min} + $C(v)$

R_s = spreading resistance

Fig 16 Equivalent circuit for diode plus end cavity

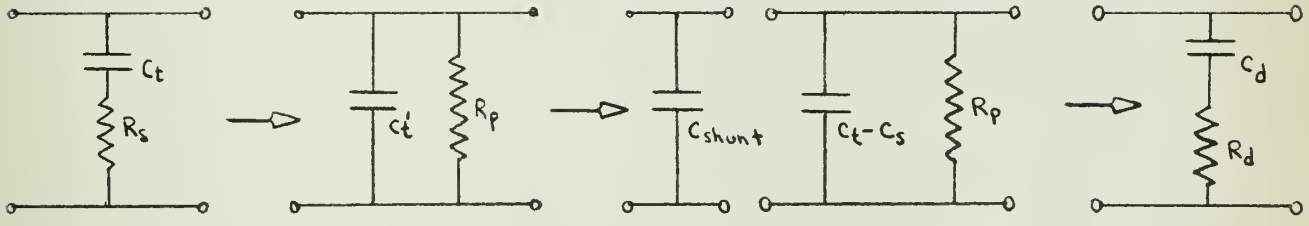

Fig 17 Steps in reducing measured circuit to diode circuit

NE	TITLE	DWG. NO.
TH CHART FORM 82BSPR (2-49)	KAY ELECTRIC COMPANY, PINE BROOK, N.J. ©1949 PRINTED IN U.S.A.	DATE

IMPEDANCE OR ADMITTANCE COORDINATES

Fig 18- Correction of measured diode impedance for slotted line shunt capacity.

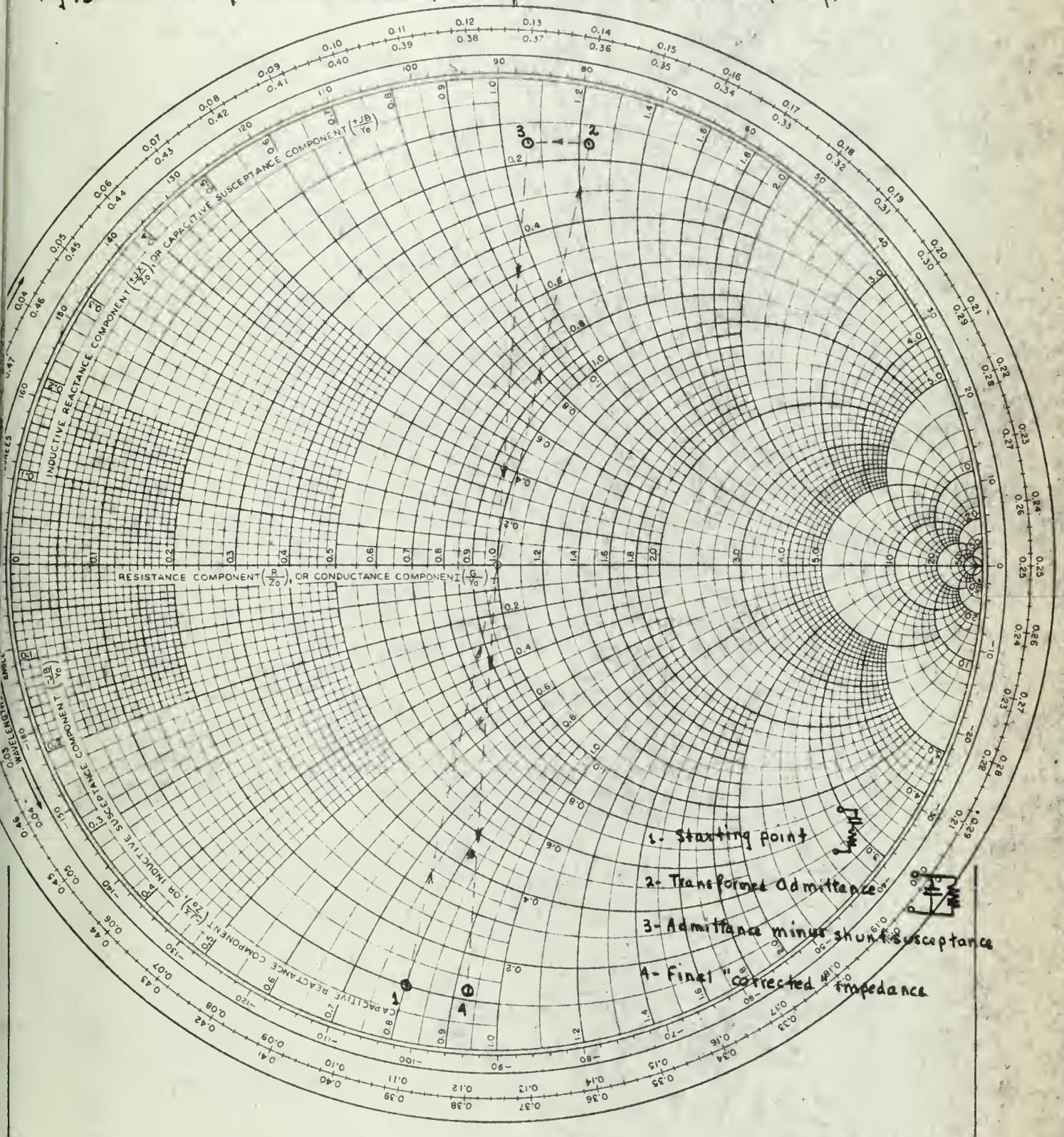
INDUCTIVE REACTANCE COMPONENT $\left(\frac{+jX}{Z_0}\right)$, OR CAPACITIVE SUSCEPTANCE COMPONENT $\left(\frac{+jB}{Y_0}\right)$
RESISTANCE COMPONENT $\left(\frac{R}{Z_0}\right)$, OR CONDUCTANCE COMPONENT $\left(\frac{G}{Y_0}\right)$
CAPACITIVE REACTANCE COMPONENT $\left(\frac{-jX}{Z_0}\right)$, OR INDUCTIVE SUSCEPTANCE COMPONENT $\left(\frac{-jB}{Y_0}\right)$
WAVELENGTHS TOWARD GENERATOR
1
2
3
4

1- Starting point

2- Transformed Admittance

3- Admittance minus shunt susceptance

4- Final "corrected" impedance

RADIALLY SCALED PARAMETERS

TOWARD GENERATOR → ← TOWARD LOAD

REFLECTION COEFF. | VOL. PWR. RETN | REFL. LOSS IN DB

CENTER

Electronics - VOL. 17, NO.1, PP 130-133, 318-325, JAN. 1944

A MEGA-CHART

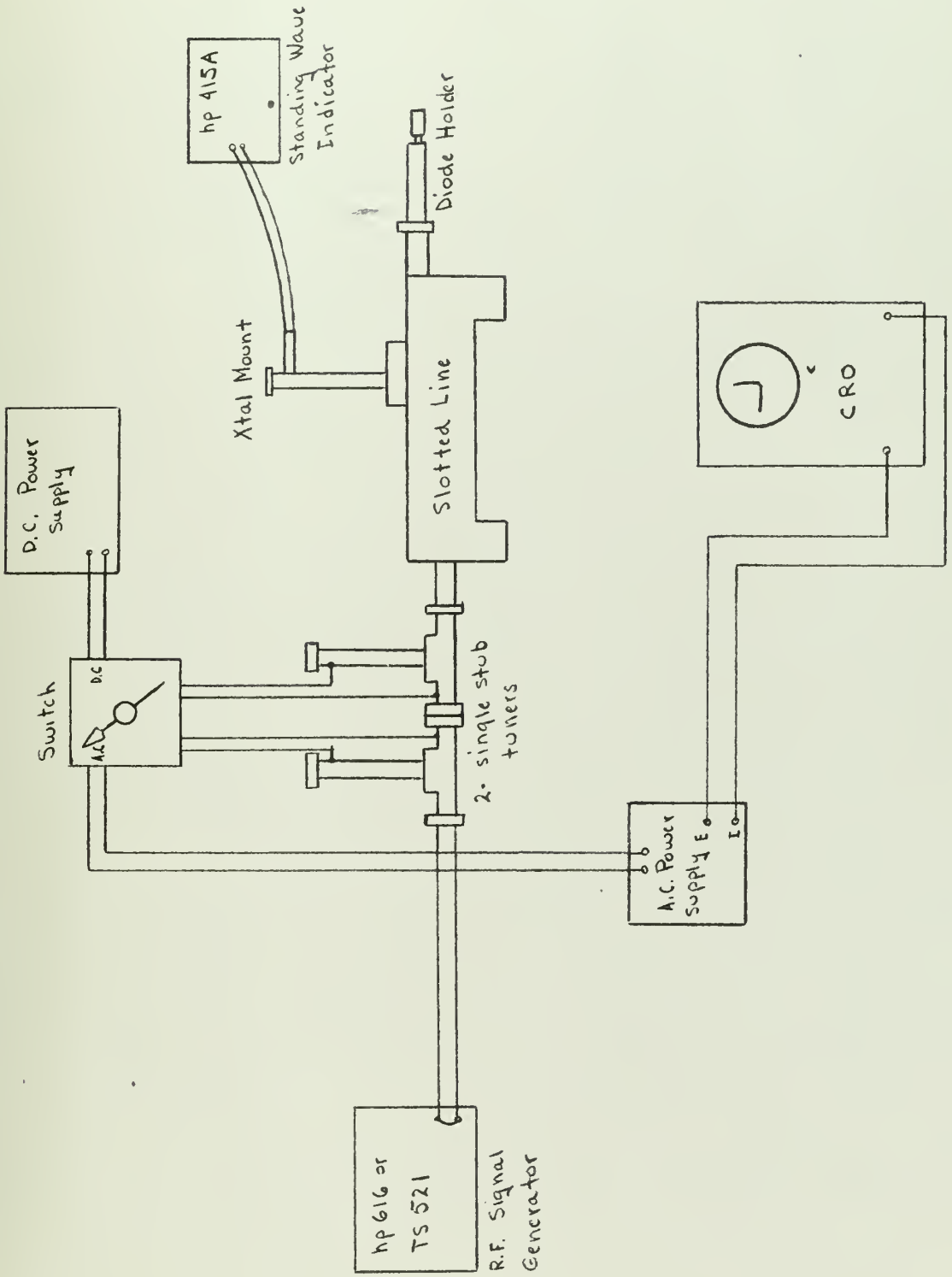

Fig 19 Complete Laboratory Set-up

Summary of Resistance Readings - 1

	Diode	Frequency	Bias Voltages												
			0	-.5	-1.0	-1.5	-2.0	-2.5	-3.0	-3.5	-4.0	-4.5	-5.0		
1.	M-27-21	7.5	.721	.792	.792		.792		.792		.792		.836		
	p⁺n	6.0	.924	.924	.967		.967		1.01		1.10		1.10		
	[R_s = 2.2Ω	5.0	.792	.836	.88		.88		.967		1.06		1.10		
	C_o = 8.9 pf]	4.0	.616	.792	.704		.88								
2.	M-17-20	7.5	.862	.924	.897		.967		1.06		1.06		1.14		
	n⁺p	6.0	1.14	1.1	1.14		1.23		1.14		1.28		1.41		
	[R_s = 2.5Ω	5.0	.924	1.1	1.14		1.19		1.23		1.41		1.49		
	C_o = 6.8 pf]	4.0	.924	1.06	1.06		1.32		1.23		1.49		1.67		
3.	M-17-19	7.5	1.06	1.09	1.01		1.1		1.14		1.16		1.23		
	n⁺p	6.0	1.1	1.01	1.14		1.32		1.49		1.54		1.58		
	[R_s = 4.5Ω	5.0	.88	1.14	1.14		1.23		1.49		1.41		1.32		
	C_o = 6.7 pf]	4.0	.967	1.14	1.41		1.32		1.32		1.58		1.58		
		3.0	1.23	1.06	.967		1.14		1.41		1.58		1.76		
		2.0	1.49	1.49	2.02		1.93		1.93		3.2		3.2		
4.	M-17-21	7.5	.634	.616	.616		.704		.704		.669		.748		
	n⁺p	6.0	.722	.792	.836		.836		.88		.88		.905		
		5.0	.572	.572	.642		.66		.704		.748		.88		
		4.0	.616	.572	.704		.704		.66		.66		.66		
		3.0	.484	.616	.616		.704		.704		.88		.967		
		2.0	.616	.616	.616		.616		.616		.616		.792		
5.	M-17-18	7.5	1.04	1.1	1.19		1.28		1.32		1.19		1.19		
	n⁺p	6.0	1.06	1.06	1.1		1.14		1.28		1.23		1.32		
	[R_s = 3Ω	5.0	.81	.88	.88		1.06		1.06		.88		1.14		
	C_o = 9.4]	4.0	.748	.792	.792		.836		.88		.89		1.14		
		3.0	.572	.616	.704		.792		.88		.88		.88		
		2.0	.88	.968	.88		1.14		1.41		1.06		1.41		
6.	N-28-10	7.5	1.34	1.41	1.63		1.23		1.58				1.425		
	n⁺p	6.0	1.32	1.41	1.49		1.49		1.76				1.94		
		5.0	1.58	1.56	1.49		1.58		1.94				2.28		
		4.0	1.23	1.41	1.49		1.49		1.76				2.02		
		3.0	1.49	1.49	1.49		1.76		1.94				1.94		
		2.0	1.76	2.02	2.2		3.08		3.52				11.4		
7.	M-27-15	2.0	.396	.396	.44		.44		.44		.44		.503		
	p⁺n	1.5	.308	.352	.352		.352		.352		.352		.396		
8.	M-21-4	7.5	.484	.484	.484	.484									
	n⁺p	6.0	.617	.555	.555	.555	.555	.555							
		5.0	.528	.484	.44	.528	.458	.44							
		4.0	.528	.528	.484	.528	.457	.457							
		3.0	.44	.44	.44	.484	.528	.44							
		2.0	.528	.616	.616	.66	.616	1.06							

Summary of Resistance Readings - 2

	Diode	Frequency	0	-.5	-1.0	-1.5	-2.0	-2.5	-3.0	-3.5	-4.0	-4.5	-5.0
9.	M-21-1	6.0	.924	.924	1.32	.967	.967	.924	.967	.967	.88		
	p+n												
	C_o = 11pf												
10.	M-25-6	5.0	.704	.704	.792	.748	.792	.792	.704	.792	.792	.792	
	p+n												
	C_o = 18pf												
11.	M-22-10	7.5	1.06	.967	1.06	1.01	1.06	1.06	.967	1.06	1.1	1.06	
	p+n	6.0	1.23	1.23	1.32	1.41	1.49	1.49	1.49	1.49	1.58	1.58	
	C_o = 6pf	5.0	1.06	.88	1.14	1.14	1.14	1.23	1.23	1.32	1.32	1.41	
12.	M-22-23	5.0	1.95	1.75	2.1	2.0	2.0	1.9	1.75				
	(with 50^ line)												
	(another run)	7.5	1.55	1.55	1.49		1.66						
		6.0	2.55	2.6	2.5		2.8						
		5.0	3.1	2.5	2.45		2.65						
		4.0	6.22	4.38	3.79		3.46						

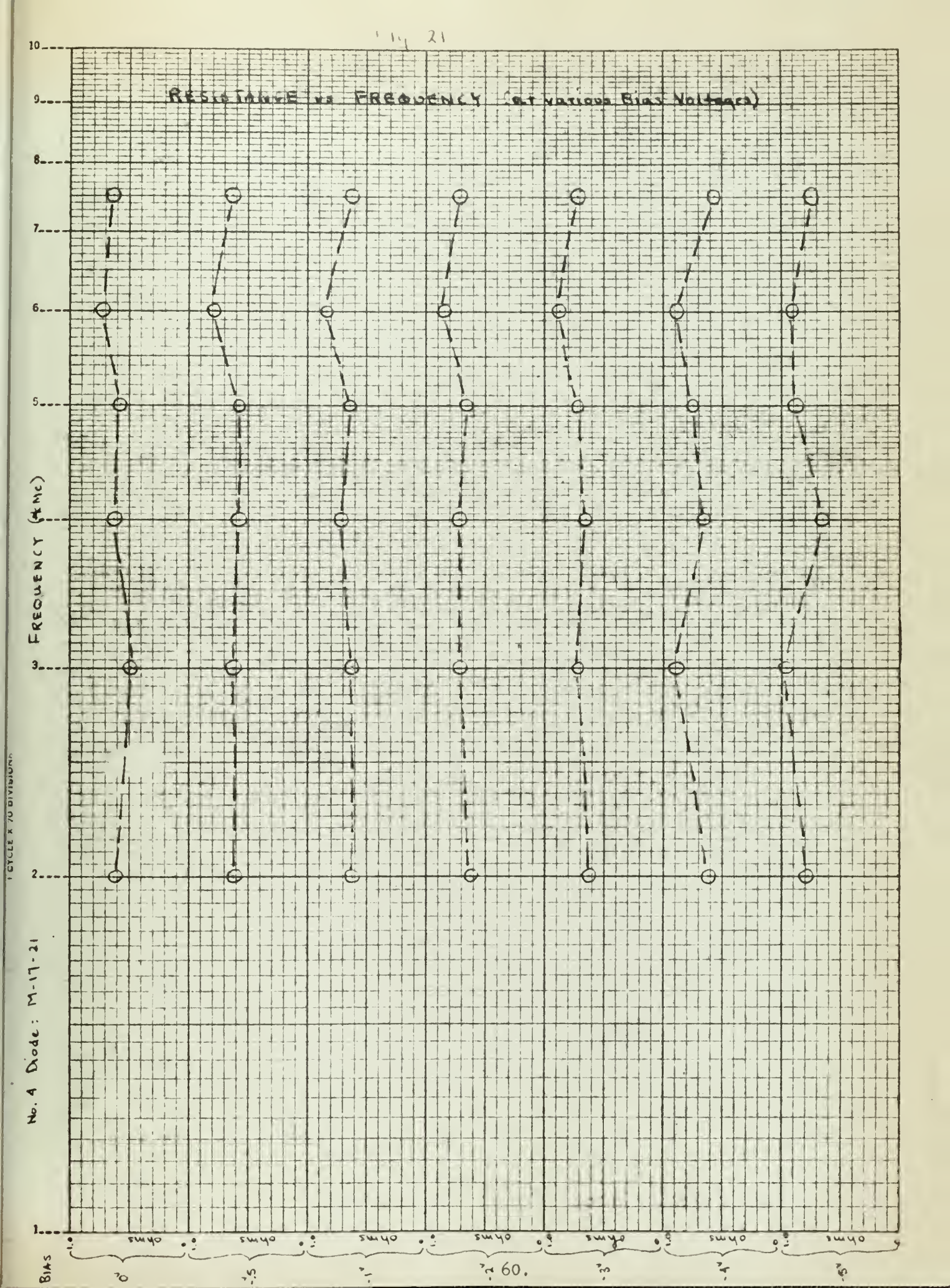

No. 4 Diode: M-17-21

1 CYCLE X 70 DIVISIONS

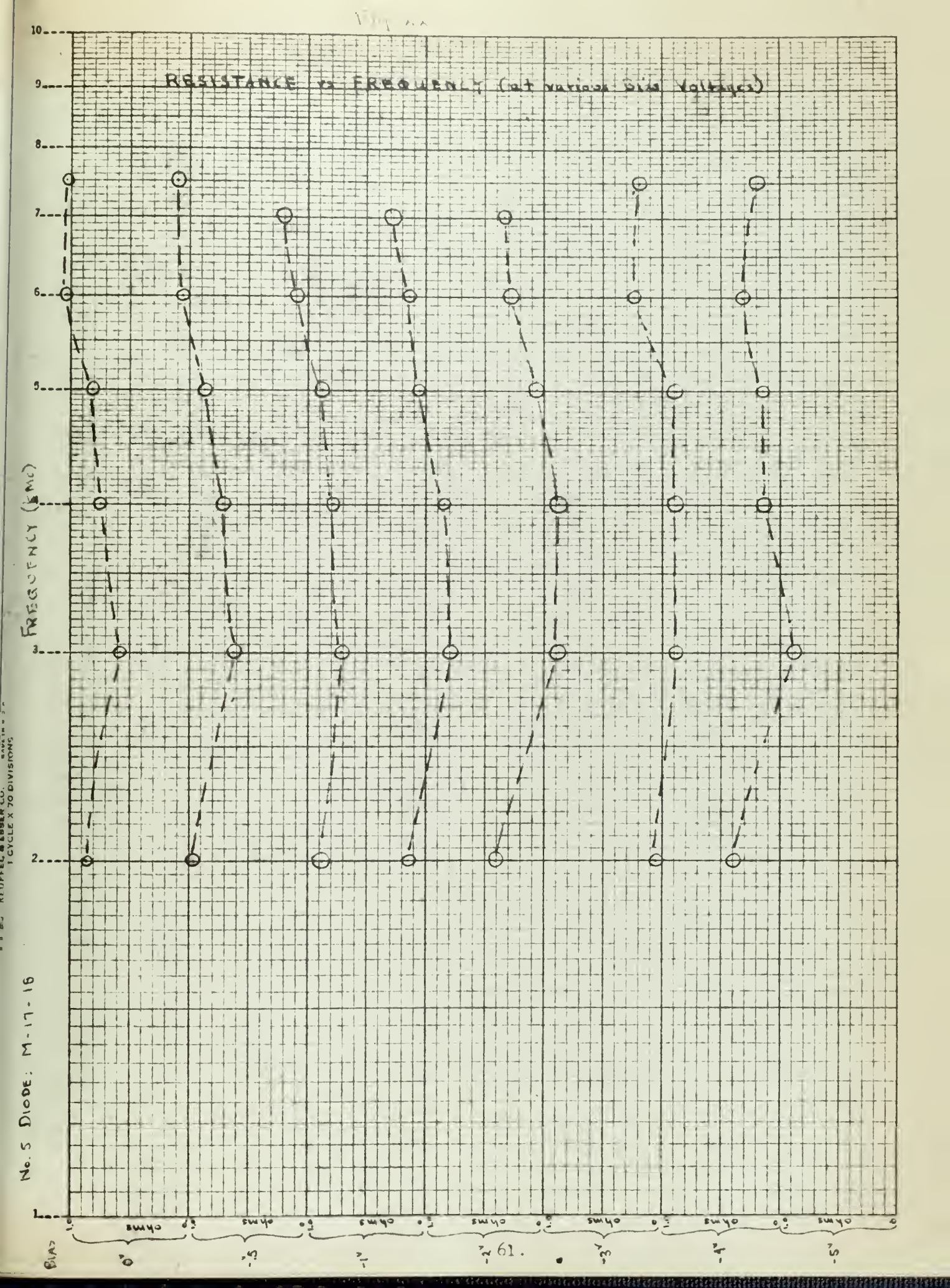
RESISTANCE vs FREQUENCY (at various bias voltages)
FREQUENCY (KMC)
10
9
8
7
6
5
4
3
2
1
ohms
0
No. 5 DIODE: M-17-16
BIAS

Summary of Capacitance Readings - 1

	Diode	Frequency	Bias Voltages										m	C_o
			(.6) 0	(1.1) $-\frac{1}{2}$	(1.6) -1	(2.1) -1.5	(2.6) -2	(3.1) -2.5	(3.6) -3	(4.1) -3.5	(4.6) -4	(5.1) -4.5	(5.6) -5		
1.	M-27-21	7.5	105	34.5	22		14.6		11.5		9.3		8.3		
	p^+n	6.0	23.2	14.4	11.4		8.63		7.2		6.43		5.75	-.557	14.8
	$[R_s = 2.2\Omega$	5.0	12.5	8.94	7.78		6.24		5.4		4.7		4.37	-.449	9.5
	$C_o = 8.9^{pf}]$	4.0	11.9	9.05	7.8		6.12								
2.	M-17-20	7.5	201	36	19		11.2		8.26		6.8		5.96	-.740	22.5
	n^+p	6.0	23.2	11.97	8.9		6.42		5.3		4.65		4.03	-.610	11.8
	$[R_s = 2.5\Omega$	5.0	10.97	7.24	5.89		4.52		3.74		3.45		2.92	-.560	7.8
	$C_o = 6.8^{pf}]$	4.0	9.83	6.85	5.8		4.27		3.62		3.28		2.83	-.553	7.5
3.	M-17-19	7.5	44	23	14.2		8.8		6.9		6.05		5.5	-.548	14.2
	n^+p	6.0	15.9	10.9	7.74		5.48		4.64		4.18		3.59	-.580	10
	$[R_s = 4.5\Omega$	5.0	10.1	6.96	5.75		4.42		3.7		3.15		3.02	-.532	7.1
	$C_o = 6.7^{pf}]$	4.0	9.05	6.28	5.14		4.18		3.48		3.02		2.79	-.535	6.9
		3.0	7.83	5.58	4.68		3.7		3.08		2.9		2.52	-.502	6.0
		2.0	6.51	4.64	3.80		2.84		2.38		2.06		1.81	-.570	4.9
4.	M-17-21	7.5	302	60.5	39.0		21.9		16.8		14.2		11.5	-.770	46
	n^+p	6.0	48.2	25.2	17.8		13.7		11.2		9.73		8.62	-.613	25
		5.0	21.3	14.5	11.7		9.53		8.23		7.38		6.7	-.460	15
		4.0	21.5	15.1	12.6		9.42		8.22		7.3		6.75	-.496	15.8
		3.0	18.5	13.1	11.2		8.62		7.27		6.7		6.1	-.471	13.8
		2.0	15.1	11.0	9.4		7.6		6.45		5.87		5.45	-.474	11.5
5.	M-17-18	7.5	105	28.8	20.1		13.05		10.3		8.47		7.54	-.749	29
	n^+p	6.0	21.6	13.7	10.8		8.37		6.85		6.42		5.69	-.503	13.7
	$[R_s = 3^{\Omega}$	5.0	12.1	8.83	7.47		5.4		5.17		4.47		4.12	-.464	9.17
	$C_o = 9.4^{pf}]$	4.0	12.9	9.62	7.8		6.12		4.92		4.48		4.15	-.506	9.9
		3.0	12.85	8.32	6.85		5.39		4.68		4.22		3.78	-.471	8.7
		2.0	9.28	7.37	5.84		4.72		3.84		3.42		3.18	-.510	7.6
6.	M-28-10	7.5	30.2	15.1	12.1		7.78		6.53				5.03		
	n^+p	6.0	12.1	8.15	7.02		5.48		4.78				3.82	-.446	8.6
		5.0	8.62	6.47	5.48		4.37		3.74				3.02	-.461	6.84
		4.0	9.42	6.76	5.8		4.67		3.94				3.24	-.464	7.22
		3.0	8.75	6.42	5.28		4.34		3.68				2.74	-.518	7.0
		2.0	7.55	5.17	3.98		3.35		2.58				2.06	-.518	5.2
7.	M-27-15	2.0	201	116	86.2		62.4		56.5		50.2		43.1	-.437	113
	p^+n	1.5	124.3	80.4	65.2		52.5		44.7		40.2		36.6	-.468	83
8.	M-21-4	7.5	37.2	33.1	29.5	27.8									
	n^+p	6.0	36.8	30.8	27.4	26.9	25.2	24.2						-.224	31.2
		5.0	22.6	19.6	18.1	17.25	16.5	15.75						-.221	20.4
		4.0	29.2	24.5	21.6	20.6	19.7	18.9						-.231	24.6
		3.0	28.1	24.2	20.8	20.2	18.9	17.75						-.244	24.0
		2.0	23.2	18.9	17.25	15.9	15.6	14.85						-.220	19.2

Summary of Capacitance Readings - 1

	Diode	Frequency	Bias Voltages (.6) 0	(1.1) $-\frac{1}{2}$	(1.6) -1	(2.1) -1.5	(2.6) -2	(3.1) -2.5	(3.6) -3	(4.1) -3.5	(4.6) -4	(5.1) -4.5	(5.6) -5	m	C_o
1.	M-27-21	7.5	105	34.5	22		14.6		11.5		9.3		8.3		
	p+n	6.0	23.2	14.4	11.4		8.63		7.2		6.43		5.75	-.557	14.8
	$[R_s = 2.2\Omega$	5.0	12.5	8.94	7.78		6.24		5.4		4.7		4.37	-.449	9.5
	$C_o = 8.9^{pf}]$	4.0	11.9	9.05	7.8		6.12								
2.	M-17-20	7.5	201	36	19		11.2		8.26		6.8		5.96	-.740	22.5
	n+p	6.0	23.2	11.97	8.9		6.42		5.3		4.65		4.03	-.610	11.8
	$[R_s = 2.5\Omega$	5.0	10.97	7.24	5.84		4.52		3.74		3.45		2.92	-.560	7.8
	$C_o = 6.8^{pf}]$	4.0	9.83	6.85	5.8		4.27		3.62		3.28		2.83	-.553	7.5
3.	M-17-19	7.5	44	23	14.2		8.8		6.9		6.05		5.5	-.548	14.2
	n+p	6.0	15.9	10.9	7.74		5.48		4.64		4.18		3.59	-.580	10
	$[R_s = 4.3\Omega$	5.0	10.1	6.96	5.75		4.42		3.7		3.15		3.02	-.532	7.1
	$C_o = 6.7^{pf}]$	4.0	9.05	6.28	5.14		4.18		3.48		3.02		2.79	-.535	6.9
		3.0	7.83	5.58	4.68		3.7		3.08		2.9		2.52	-.502	6.0
		2.0	6.51	4.64	3.80		2.84		2.38		2.06		1.81	-.570	4.9
4.	M-17-21	7.5	302	60.5	39.0		21.9		16.8		14.2		11.5	-.770	46
	n+p	6.0	43.2	25.2	17.8		13.7		11.2		9.73		8.62	-.613	25
		5.0	21.3	14.5	11.7		9.53		8.23		7.38		6.7	-.460	15
		4.0	21.5	15.1	12.6		9.42		8.22		7.3		6.75	-.496	15.8
		3.0	18.5	13.1	11.2		8.62		7.27		6.9		6.1	-.471	13.8
		2.0	15.1	11.0	9.4		7.6		6.45		5.87		5.45	-.474	11.5
5.	M-17-18	7.5	105	28.8	20.1		13.05		10.3		8.47		7.54	-.749	29
	n+p	6.0	21.6	13.7	10.8		8.37		6.85		6.42		5.69	-.503	13.7
	$[R_s = 3\Omega$	5.0	12.1	8.83	7.47		5.4		5.17		4.47		4.12	-.464	9.17
	$C_o = 9.4^{pf}]$	4.0	12.9	9.62	7.8		6.12		4.92		4.48		4.15	-.506	9.9
		3.0	12.85	8.32	6.85		5.39		4.68		4.22		3.78	-.471	8.7
		2.0	9.28	7.37	5.84		4.72		3.84		3.42		3.18	-.510	7.6
6.	M-28-10	7.5	30.2	15.1	12.1		7.78		6.53				5.03		
	n+p	6.0	12.1	8.15	7.02		5.48		4.78				3.82	-.446	8.6
		5.0	8.62	6.47	5.48		4.37		3.74				3.02	-.461	6.84
		4.0	9.42	6.76	5.8		4.67		3.94				3.24	-.464	7.22
		3.0	8.75	6.42	5.28		4.34		3.68				2.74	-.518	7.0
		2.0	7.55	5.17	3.48		3.35		2.58				2.06	-.518	5.2
7.	M-27-15	2.0	201	116	86.2		62.4		56.5		50.2		43.1	-.437	113
	p+n	1.5	124.3	80.4	65.2		52.5		44.7		40.2		36.6	-.468	83
8.	M-21-4	7.5	37.2	33.1	29.5	27.8									
	n+p	6.0	36.8	30.8	27.4	26.9	25.2	24.2						-.224	31.2
		5.0	22.6	19.6	18.1	17.25	16.5	15.75						-.221	20.4
		4.0	24.2	24.5	21.6	20.6	19.7	18.9						-.231	24.6
		3.0	28.1	24.2	20.8	20.2	18.9	17.75						-.244	24.0
		2.0	23.2	18.9	17.25	15.9	15.6	14.85						-.220	19.2

SUMMARY of CAPACITANCE READINGS - 2

	DIODE	FREQUENCY	BIAS VOLTAGES (.6) 0	(1.1) -½	(1.6) -1	(2.1) -1.5	(2.6) -2	(3.1) -2.5	(3.6) -3	(4.1) -3.5	(4.6) -4	(5.1) -4.5	(5.6) -5	m	C_o
9	M-21-4 p⁺n C_o = 11 pf	6.0	27.4	18.9	14.4	12.6	10.8	10.1	9.42	9.14	8.62			-.480	17.6
10.	M-25-6 p⁺n C_o = 18 pf	5.0	24.2	12.95	10.35	9.8	7.96	7.24	6.9	6.3	6.04	5.75		-.493	12.9
11.	M-22-10 p⁺n C_o = 6 pf	7.5	12.1	7.54	6.04	5.14	4.56	4.2	3.9	3.66	3.45	3.33		-.487	7.3
		6.0	7.18	5.2	4.37	3.86	3.47	3.21	3.05	2.79	2.69	2.65		-.442	5.4
		5.0	6.35	4.17	3.77	3.45	3.15	2.97	2.83	2.64	2.57			-.442	5.25
12.	M-22-23 (with 50Å line)	5.0	7.96	6.06	4.9	4.92	4.19	3.84	3.71					-.27	5.1
	(another run)	7.5	14.1	8.48	6.52		5.3								
		6.0	6.65	5.32	4.08		3.54								
		5.0	6.84	4.9	4.54		3.98								
		4.0	6.22	4.38	3.79		3.46								

Note: the voltage figures in parenthesis refer to the actual bias voltages plotted and take into account an assumed -.6 volt for contact potential.

DIODE No. 2 - M-17-20

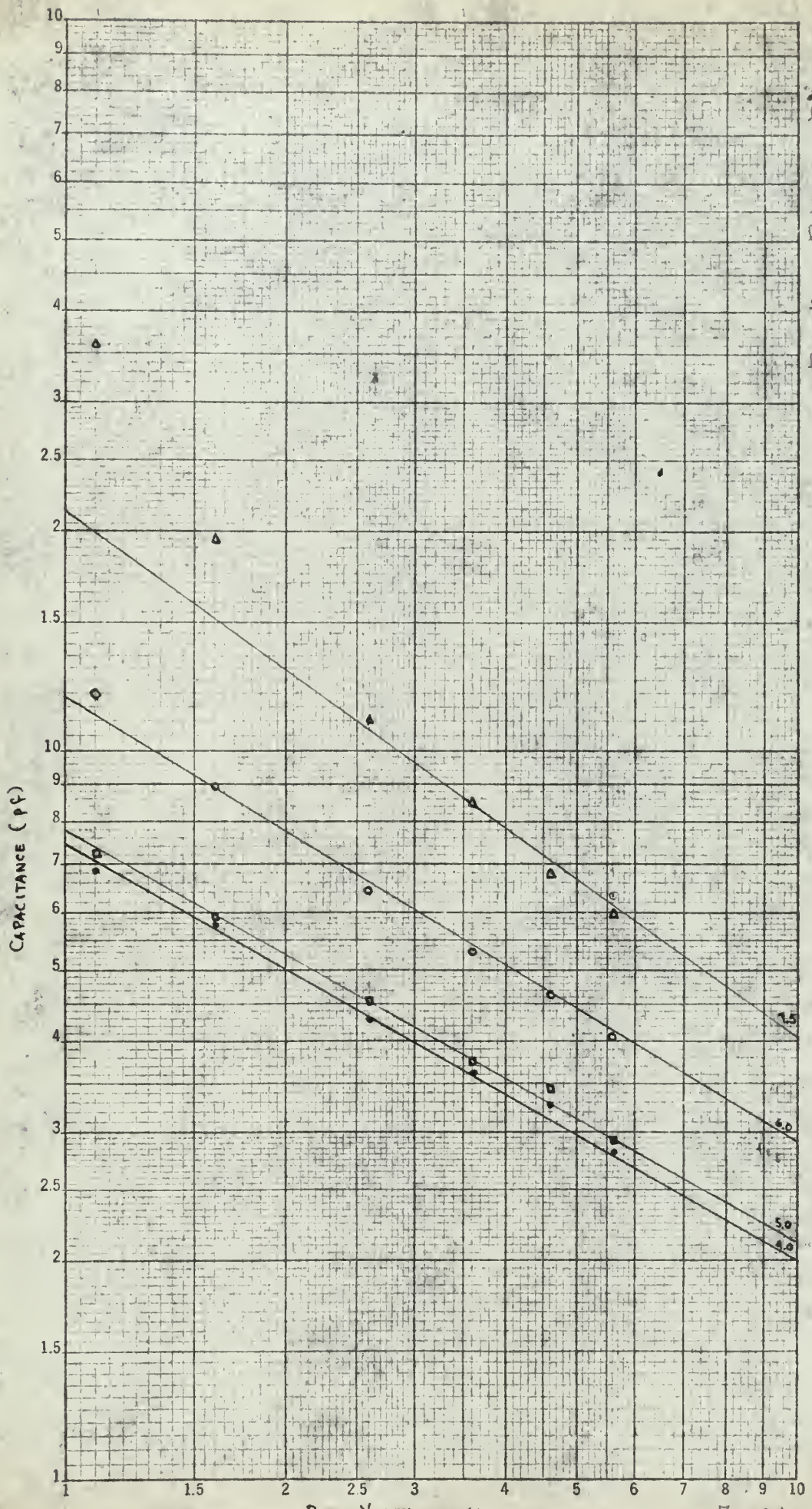

Fig 24

DIODE No. 3 - M-17-19

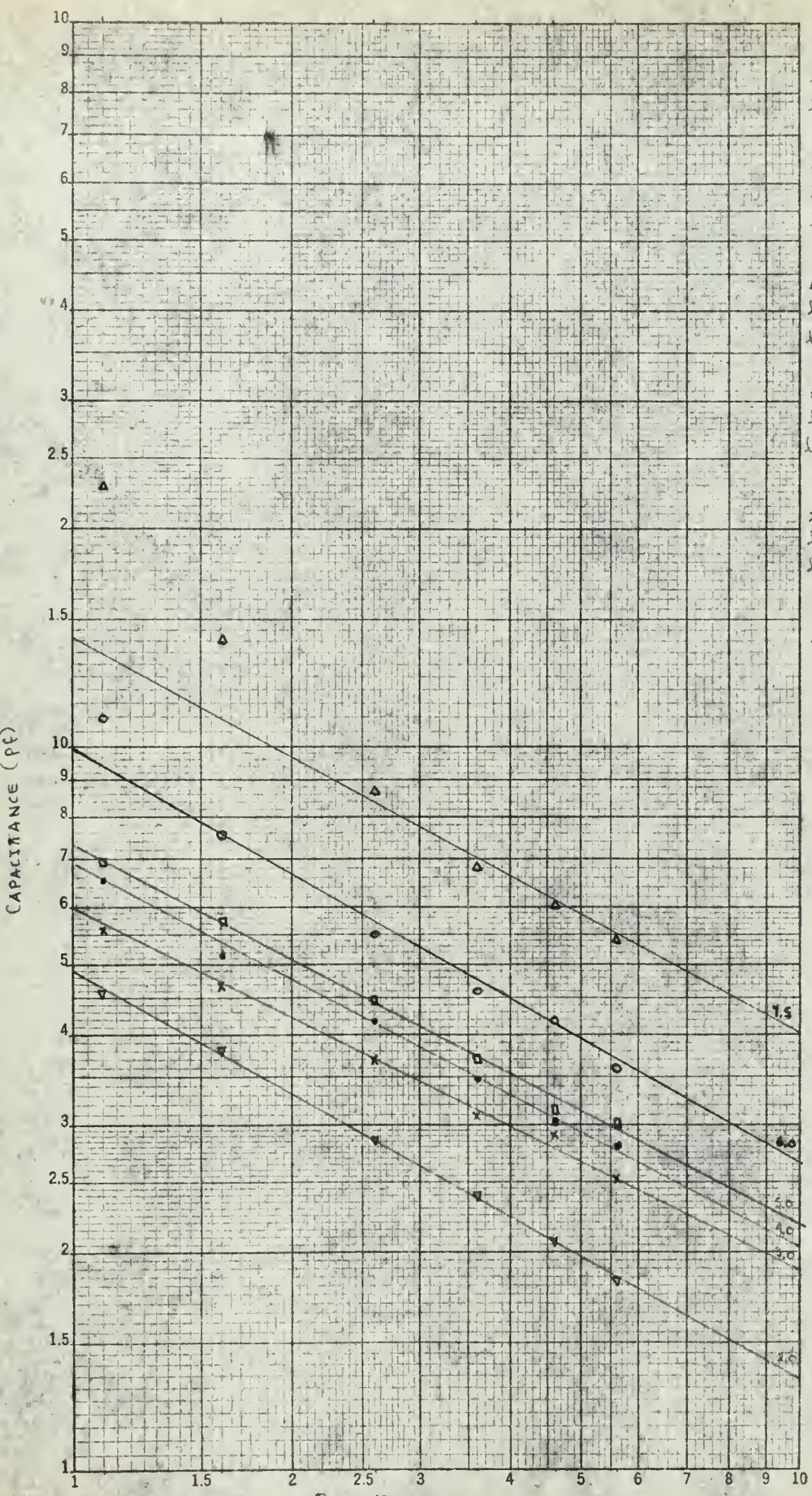

	6.0 kMc		
log C_0 =	1.029	1.009	
log C_0 - m =	.471	.420	
- m =	.558	.589	
	5.0 kMc		
log C_0 =	.897	.868	
log C_0 + m =	.412	.330	
- m =	.485	.538	
	4.0 kMc		
log C_0 =	.869	.859	
log C_0 + m =	.437	.324	
- m =	.432	.535	
	3.0 kMc		
log C_0 =	.858	.778	
log C_0 + m =	.459	.278	
- m =	.399	.502	
	2.0 kMc		
log C_0 =	.796	.698	
log C_0 + m =	.414	.120	
- m =	.382	.578	
1.5		1.152	
		.604	
		.548	

Fig 25

DIODE No 4 - M-17-21

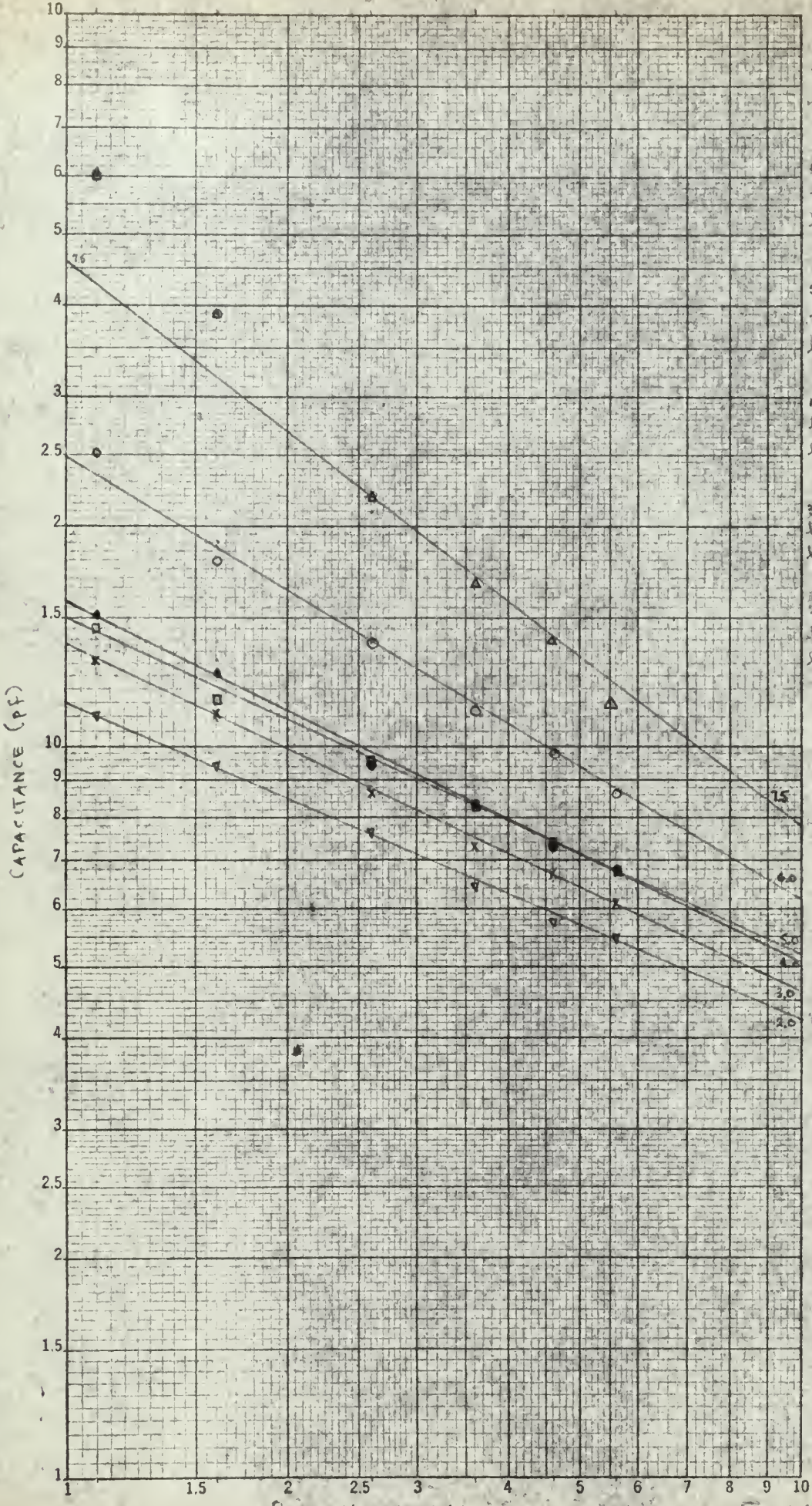

7.5		
log C_0 =	1.662	
log $C_0 + mv$ =	.892	
$-m$ =	.770	
6.0		
log C_0 =	1.408	1.398
log $C_0 + mv$ =	.819	.785
$-m$ =	.589	.613
5.0		
log C_0 =	1.196	1.176
log $C_0 + mv$ =	.748	.716
$-m$ =	.448	.460
4.0		
log C_0 =	1.203	1.198
log $C_0 + mv$ =	.740	.702
$-m$ =	.463	.496
3.0		
log C_0 =	1.161	1.190
log $C_0 + mv$ =	.732	.669
$-m$ =	.429	.471
2.0		
log C_0 =	1.124	1.088
log $C_0 + mv$ =	.740	.614
$-m$ =	.384	.474

Fig 26

DIODE No. 5 - M 17-18

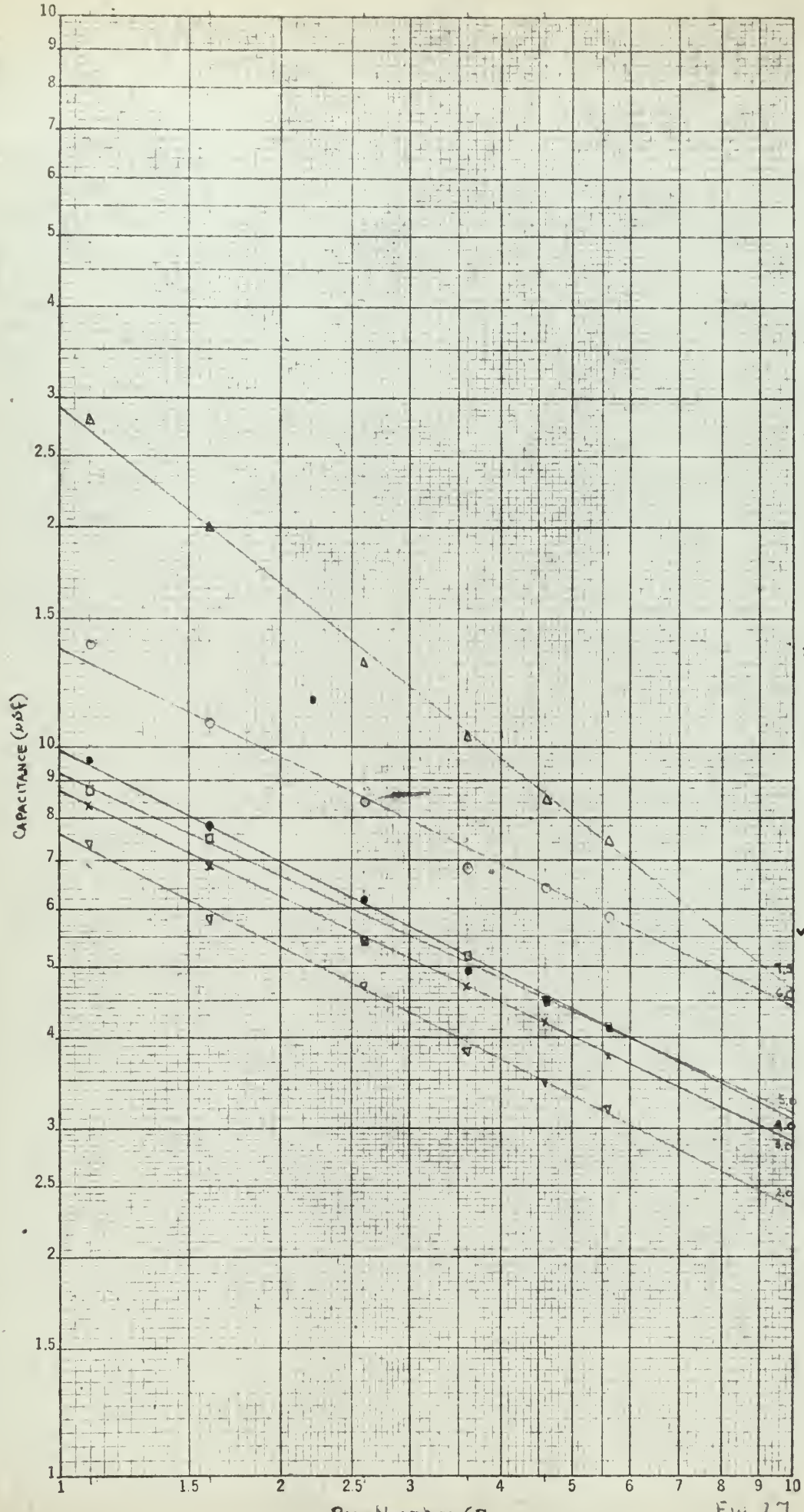

7.5
log C_o = 1.413
log C_o + m = .664
- m = .749

6.0
log C_o = 1.155 1.176
log C_o + m = .664 .633
- m = .491 .503

5.0
log C_o = .982 .962
log C_o + m = .563 .493
- m = .419 .469

4.0
log C_o = 1.021 .795
log C_o + m = .562 .466
- m = .453 .502

3.0
log C_o = .968 .739
log C_o + m = .579 .466
m = .389 .477

2.0
log C_o = .942 .
log C_o + m = .568
- m = .377

Fig 27

No 6. DIODE 1N-2810

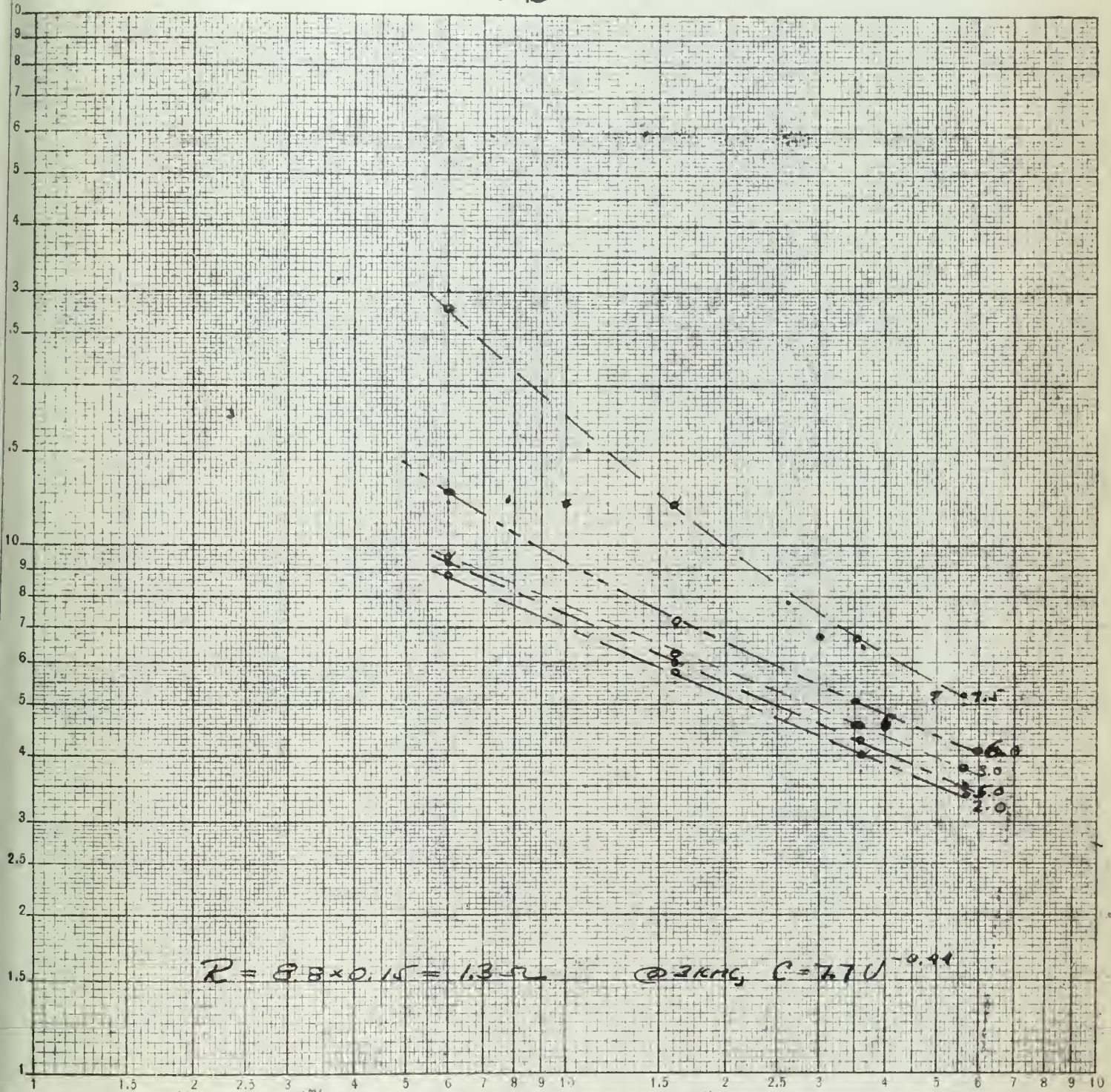

$\log C_o$: $\log C_{10}$ =	.949	.869		.472	.845	
$\log C_{10}$: $\log C_0 + m$ =	.512	.481		-.414	-.418	-.427
m =	.437	.388				
(corrected)	.934	.835	.858	.845	.716	
	.486	.374	.394	.327	.198	
m =	.446	.461	.464	.518	.518	

Fig 23

DIODE No. 7 - M-27-15

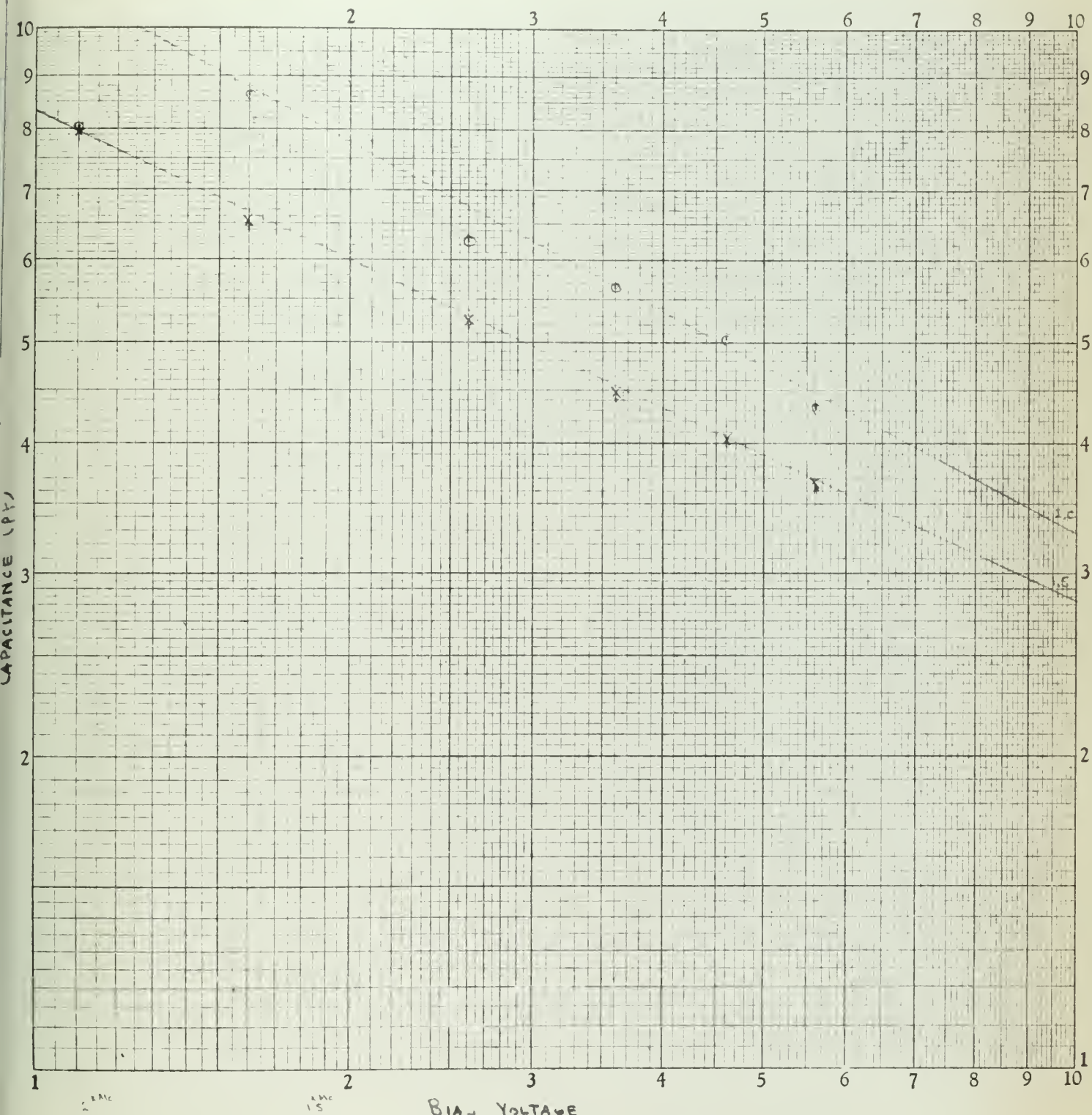

DIODE No. 8 - M-21-4

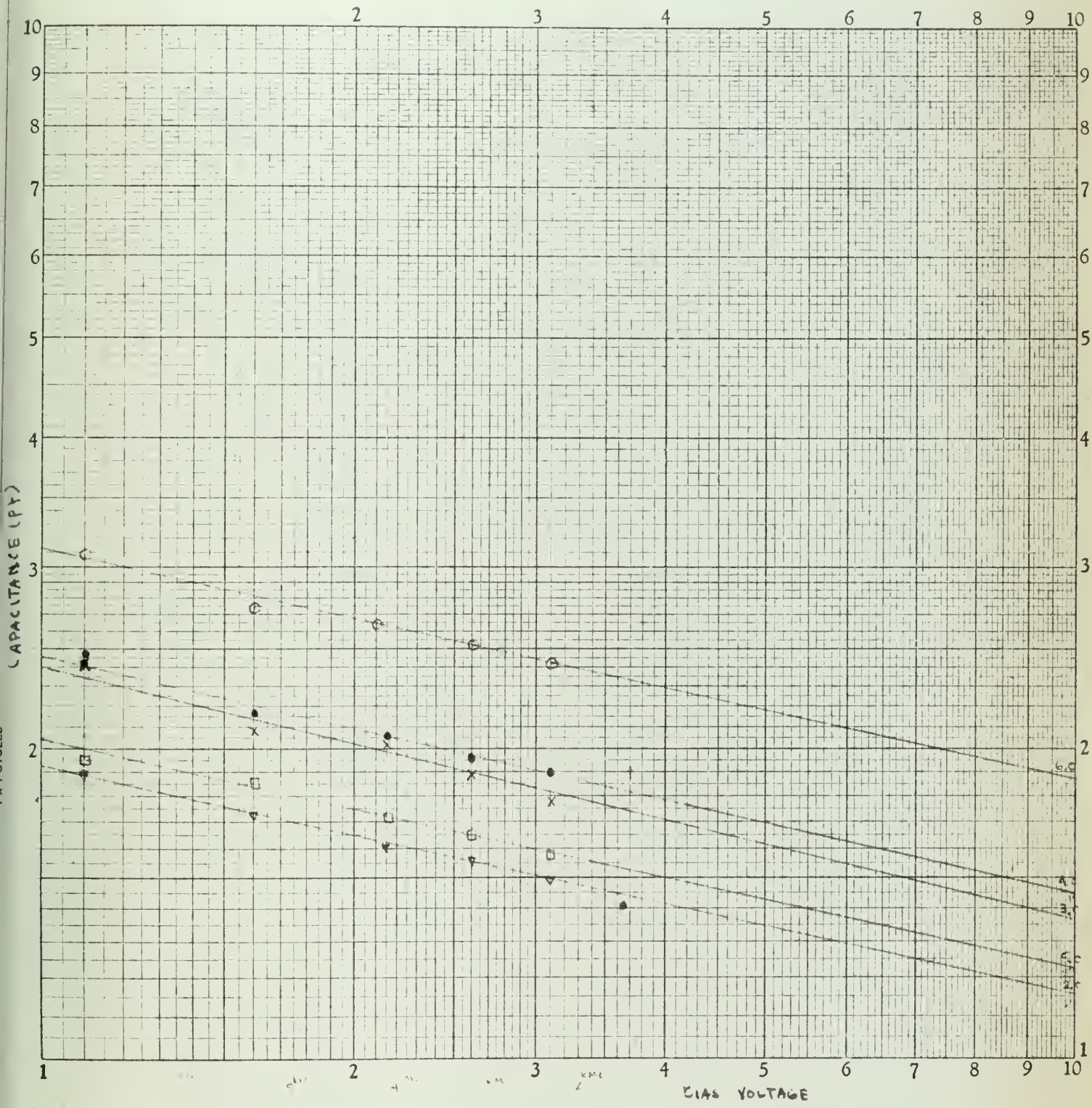

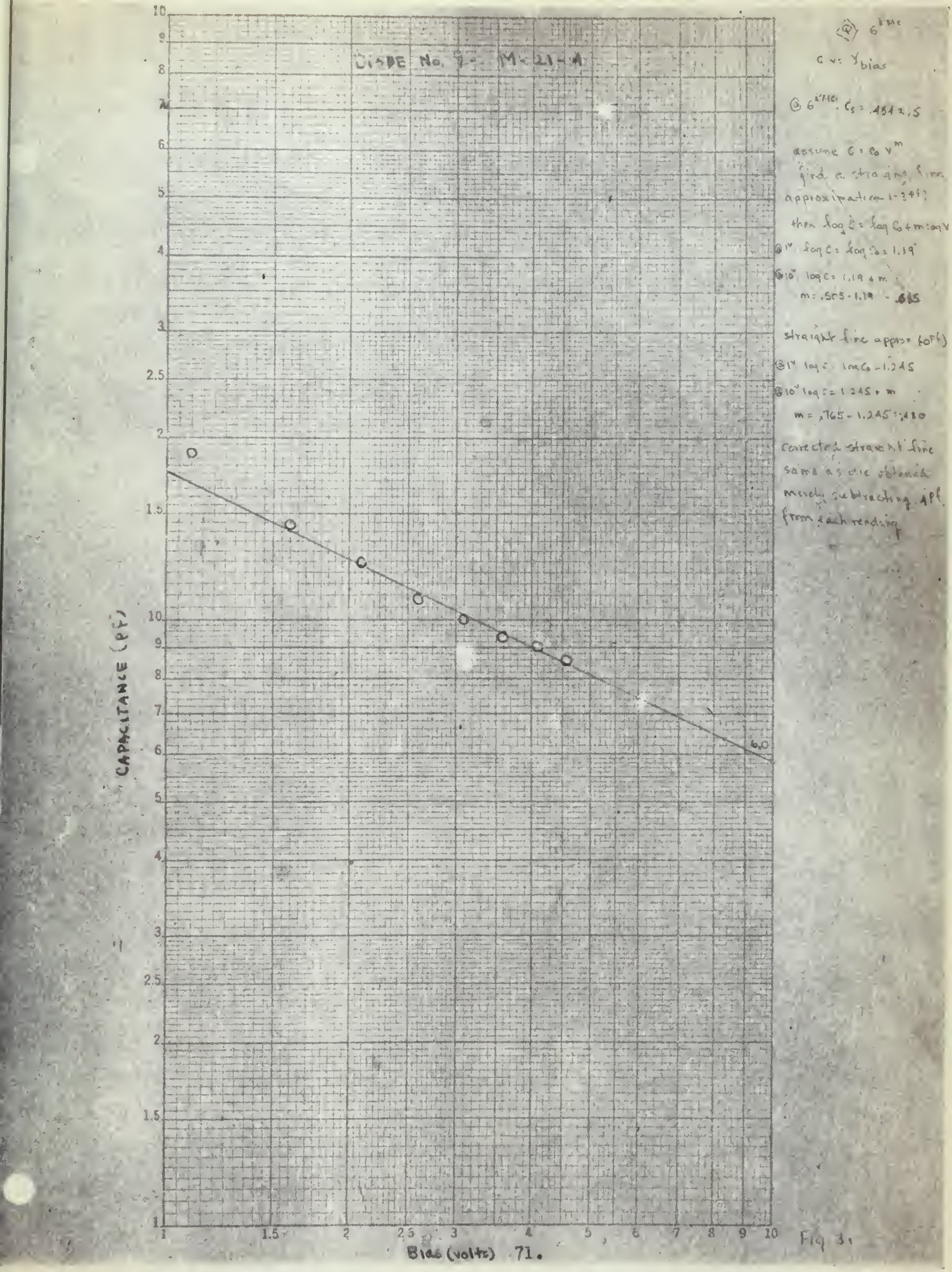

Fig 3.

71.

(Q) 6 [illegible]

C vs V_{bias}

@ 6 [illegible] C_s = .454 2.5

assume $C = C_0 V^m$

find a straight line approximation = 1.34pf

then $\log C = \log C_0 + m \log V$

@ 1V $\log C = \log C_0 = 1.19$

@ 10V $\log C = 1.19 + m$

$m = .505 - 1.19 = .685$

straight line approx for 4pf

@ 1V $\log C = \log C_0 = 1.245$

@ 10V $\log C = 1.245 + m$

$m = .765 - 1.245 = .480$

corrected straight line same as one obtained merely by subtracting 4pf from each reading

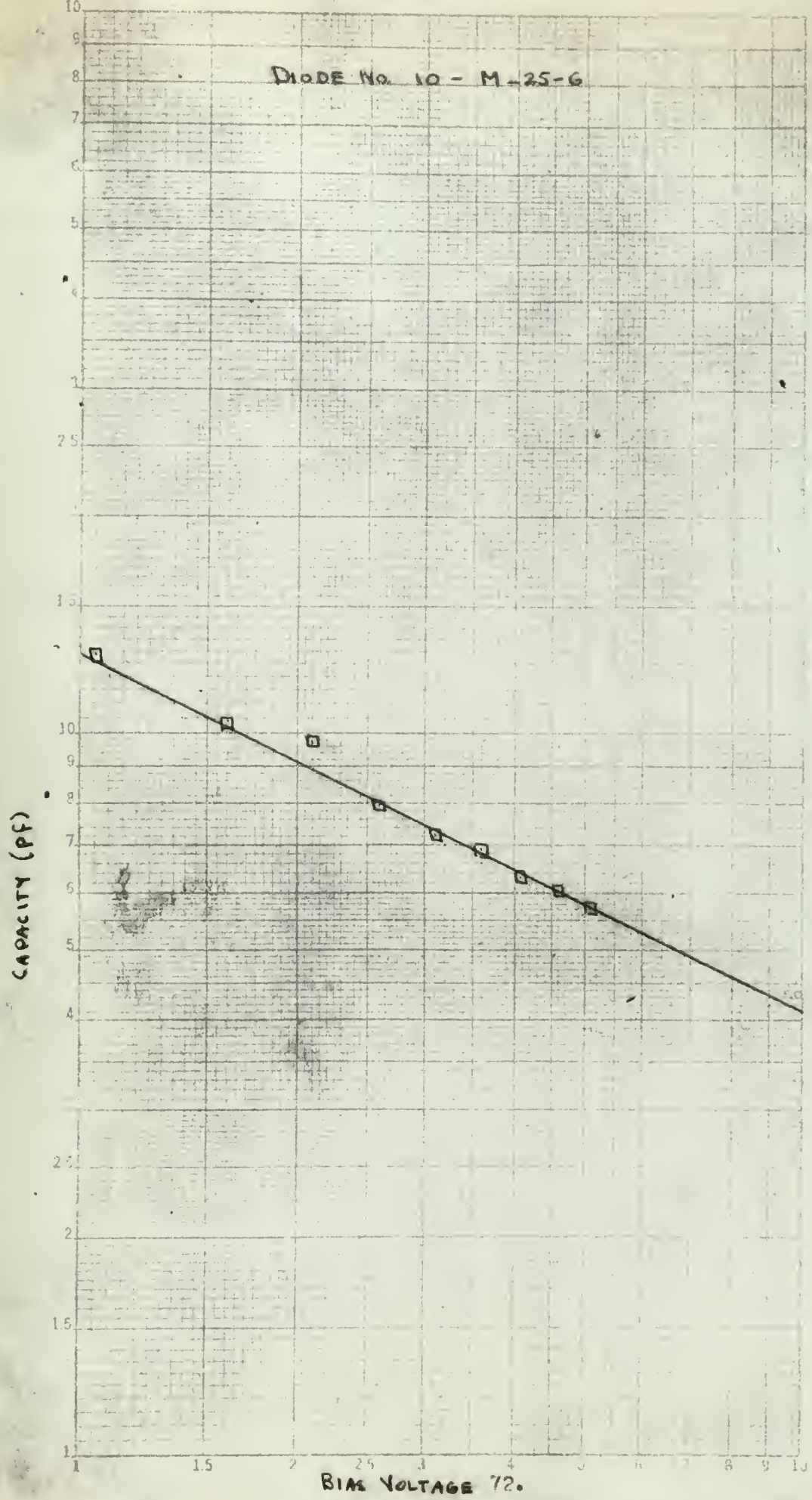

Fig 32

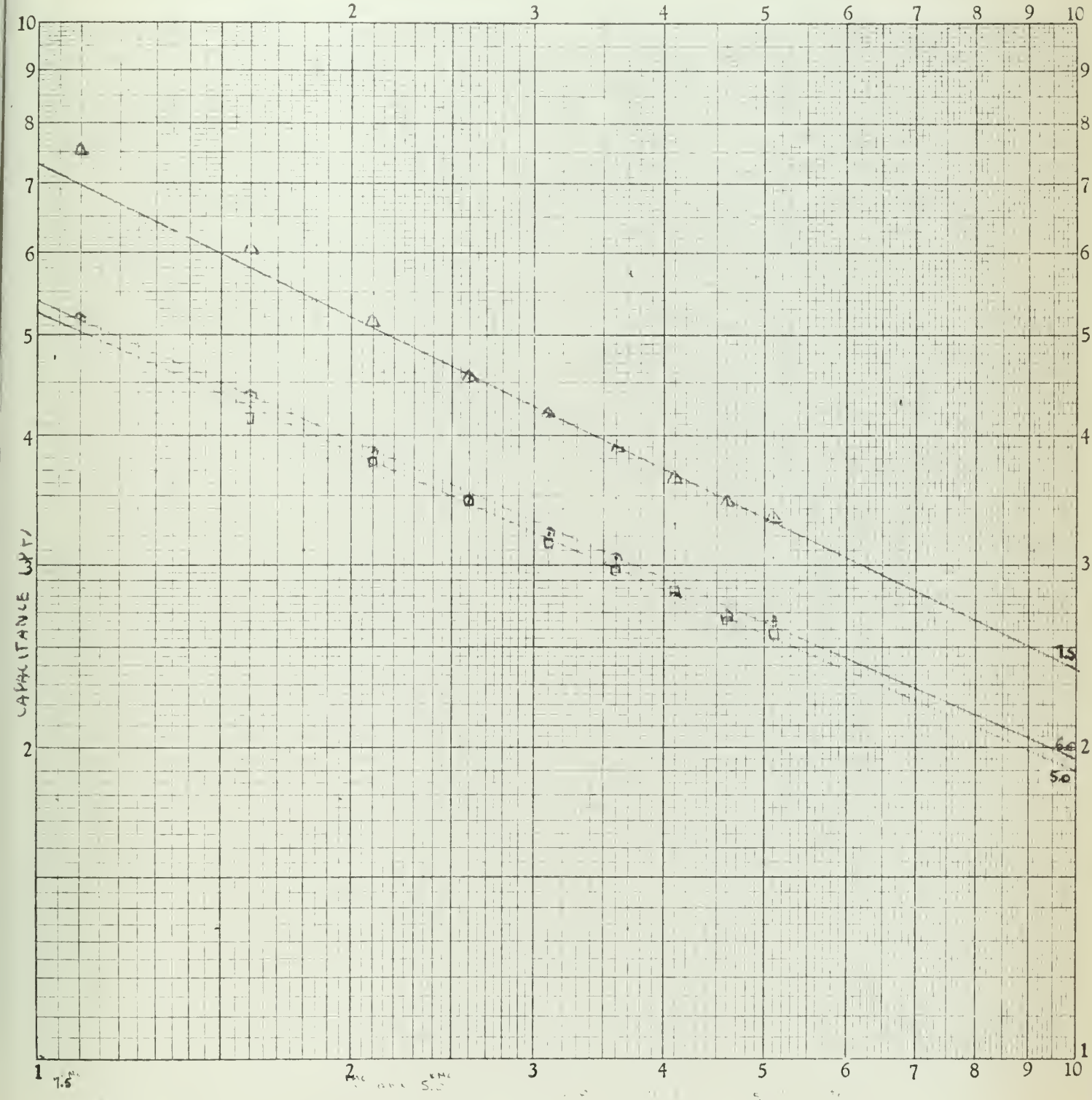
CAPACITANCE (PF)
BIAS VOLTAGE
7.5
6.0
5.0

LINDE No. 12 - M-22-23

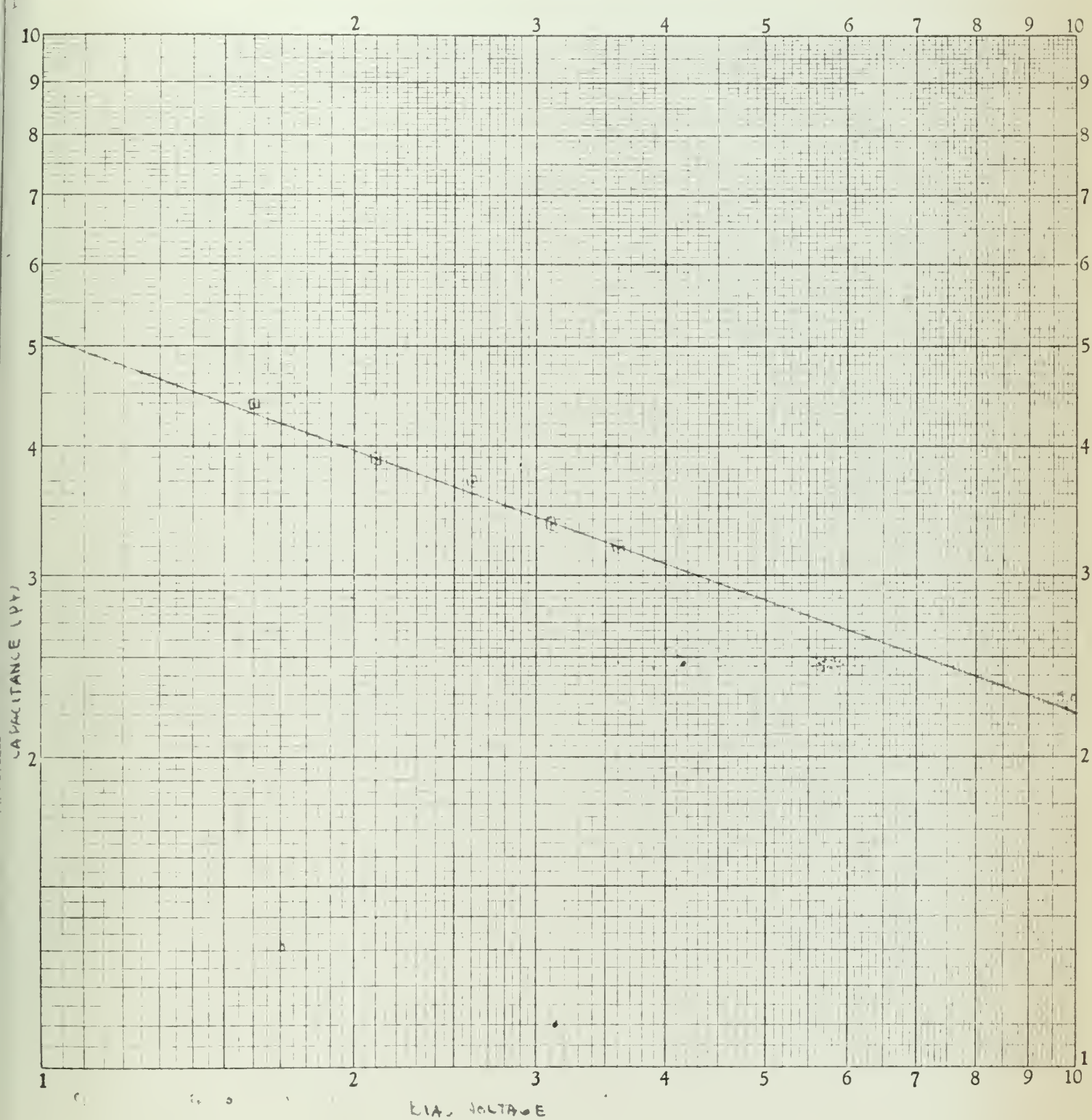

NAME	TITLE	DWG. NO.
WITH CHART FORM 828SPR (2-49)	DIODE No. 1 - M-27-21	DATE
	KAY ELECTRIC COMPANY, PINE BROOK, N.J. ©1949 PRINTED IN U.S.A.	

IMPEDANCE OR ADMITTANCE COORDINATES

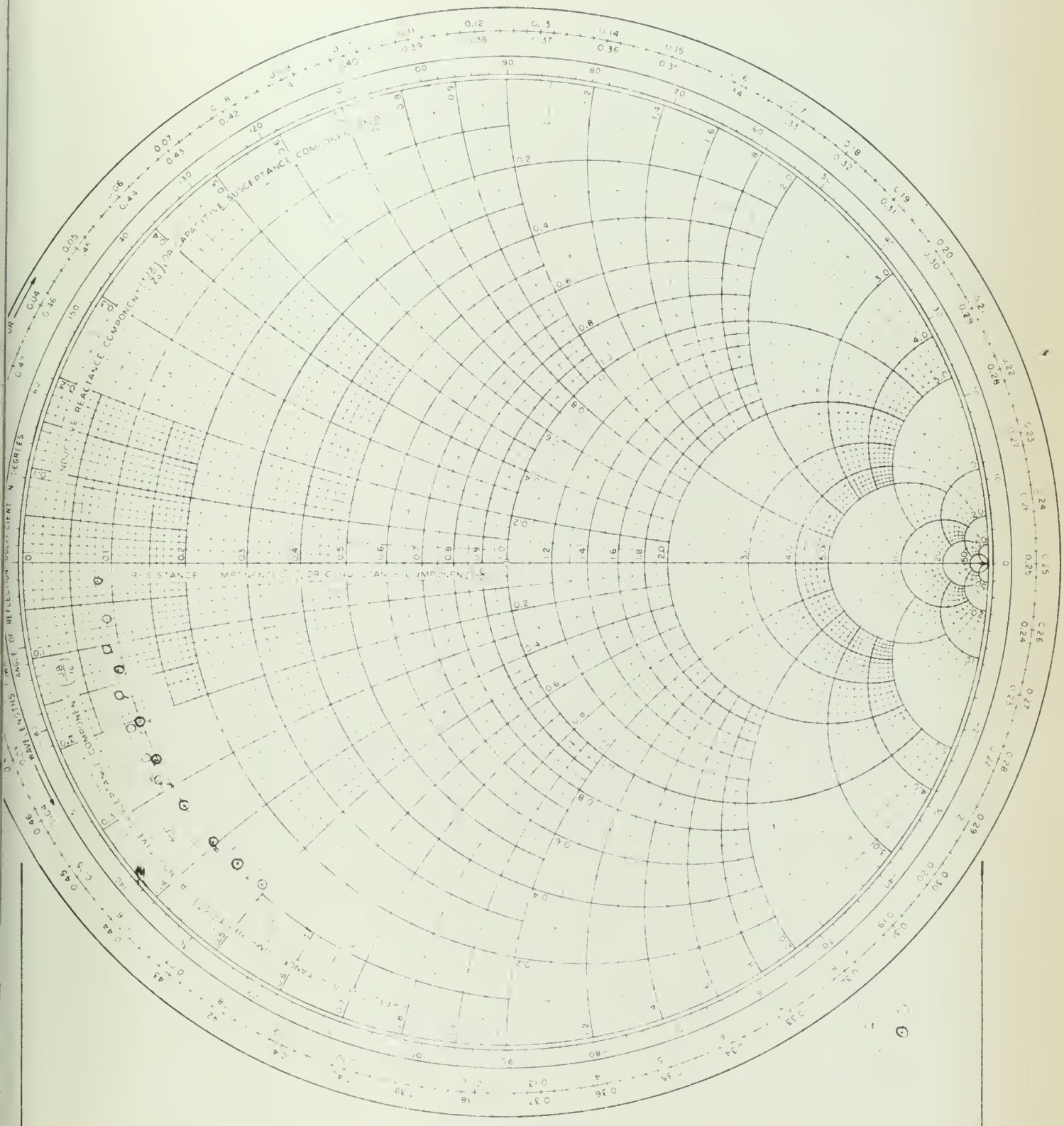
RESISTANCE COMPONENT (R/Z0) OR CONDUCTANCE COMPONENT (G/Y0)
INDUCTIVE REACTANCE COMPONENT (X/Z0) OR CAPACITIVE SUSCEPTANCE COMPONENT (B/Y0)
WAVELENGTHS TOWARD GENERATOR
ANGLE OF REFLECTION COEFFICIENT IN DEGREES
CONFORMAL MAPPING OF CONSTANT RESISTANCE AND REACTANCE CIRCLES

RADIALLY SCALED PARAMETERS

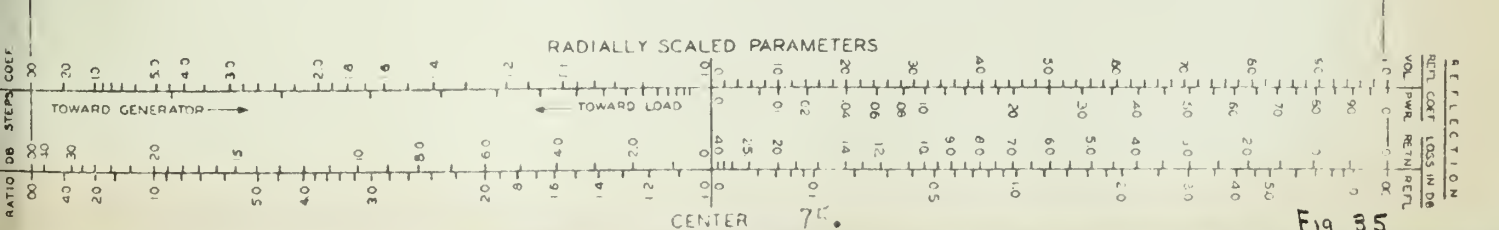

CENTER 75.

Fig 35

Electronics VOL. 17, NO. 1, PP. 130-133, 318-325, JAN. 1944

ME	TITLE	DWG. NO.
	DIODE No 2 - M-17-20	DATE
ITH CHART FORM 82BSPR (2-49)	KAY ELECTRIC COMPANY, PINE BROOK, N.J. ©1949 PRINTED IN U.S.A.	

IMPEDANCE OR ADMITTANCE COORDINATES

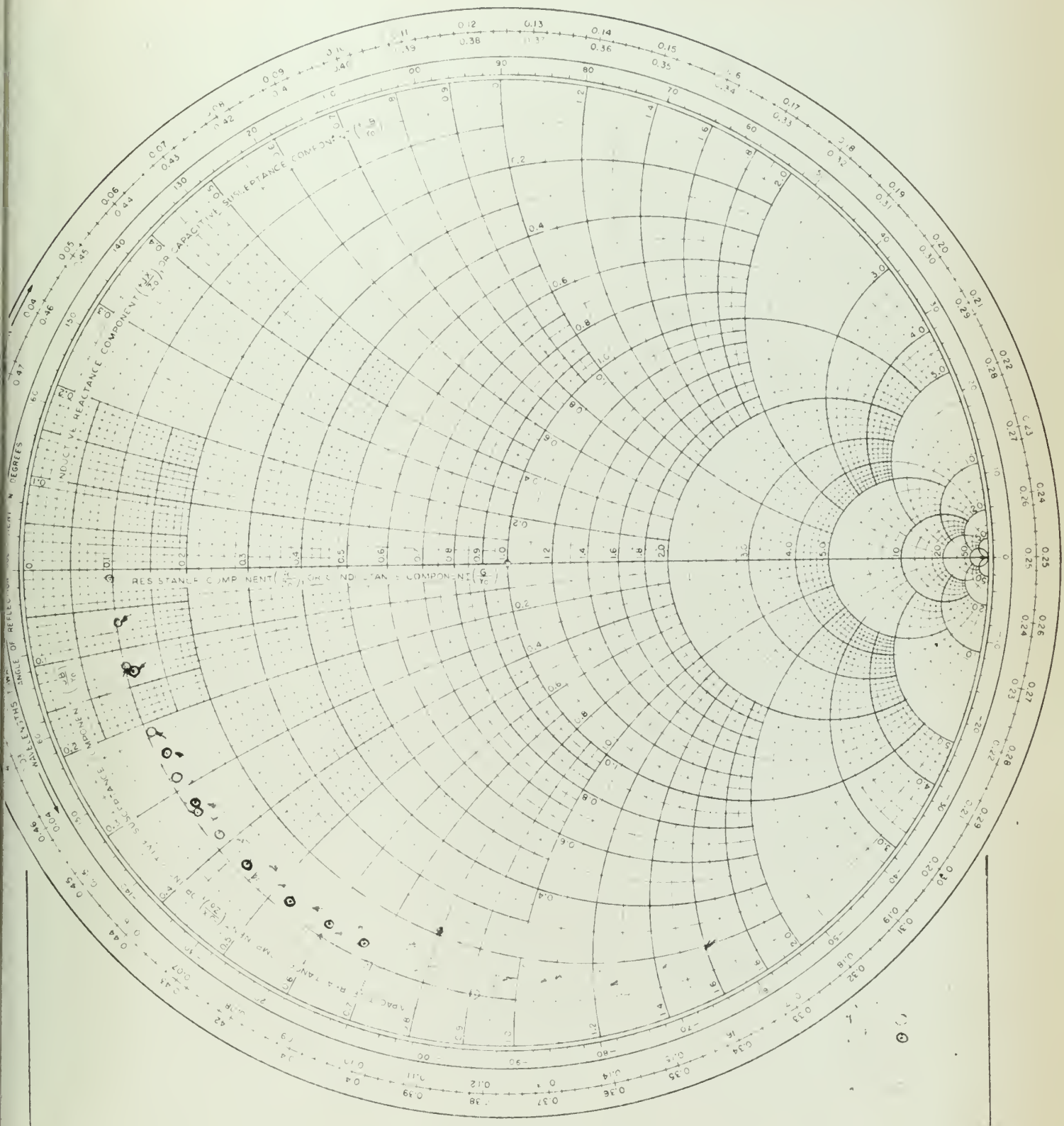
RESISTANCE COMPONENT OR CONDUCTANCE COMPONENT
INDUCTIVE REACTANCE COMPONENT OR CAPACITIVE SUSCEPTANCE COMPONENT
ANGLE OF REFLECTION IN DEGREES
WAVELENGTHS TOWARD GENERATOR
WAVELENGTHS TOWARD LOAD

RADIALLY SCALED PARAMETERS

TOWARD GENERATOR → ← TOWARD LOAD

CENTER

REFLECTION: REFL. COEF | VOL. PWR. REFL | LOSS IN DB | VOL. RATIO DB STEPS | VOL. IN DB

76.

Fig 36

Electronics VOL 17 NO 1 PP 130-133, 318-325, JAN 1944

A MF A-CHART

WE	TITLE Diode No 2 - M-17-20	DWG. NO.
ITH CHART FORM 82BSPR (2-49)	KAY ELECTRIC COMPANY, PINE BROOK, N.J. ©1949 PRINTED IN U.S.A.	DATE

IMPEDANCE OR ADMITTANCE COORDINATES

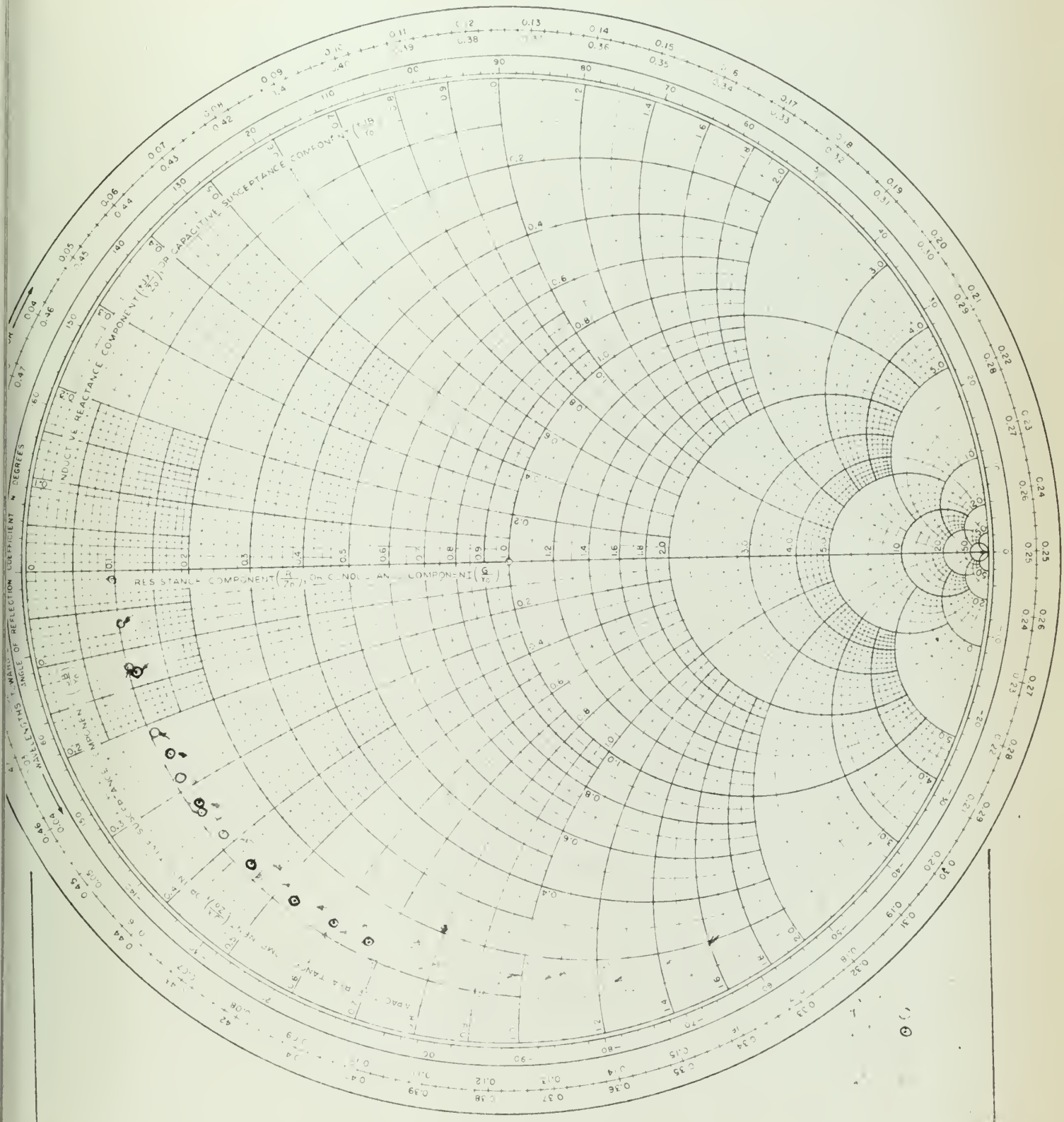
RESISTANCE COMPONENT (R/Z0) OR CONDUCTANCE COMPONENT (G/Y0)
INDUCTIVE REACTANCE COMPONENT (+jX/Z0) OR CAPACITIVE SUSCEPTANCE COMPONENT (+jB/Y0)
ANGLE OF REFLECTION COEFFICIENT IN DEGREES
RADIALLY SCALED PARAMETERS
TOWARD GENERATOR
TOWARD LOAD
CENTER

Fig 36

Electronics - VOL. 17 NO. 1, PP. 130-133, 318-329, JAN. 1944

NAME	TITLE	DWG. NO.
	DIODE No. 3 - M-17-19	
SMITH CHART FORM 82BSPR (2-49)	KAY ELECTRIC COMPANY, PINE BROOK, N.J. ©1949 PRINTED IN U.S.A.	DATE

IMPEDANCE OR ADMITTANCE COORDINATES

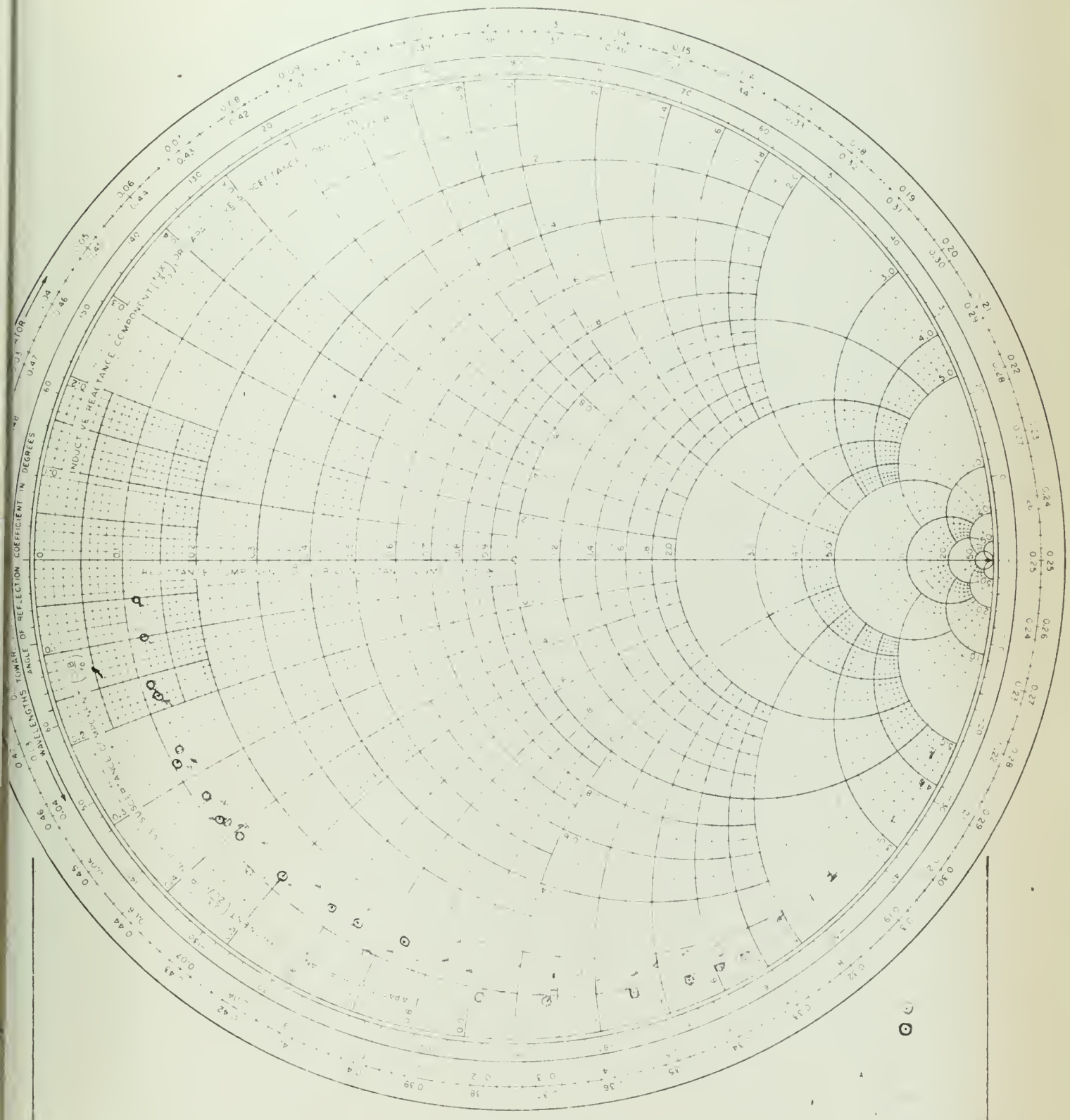

RADIALLY SCALED PARAMETERS

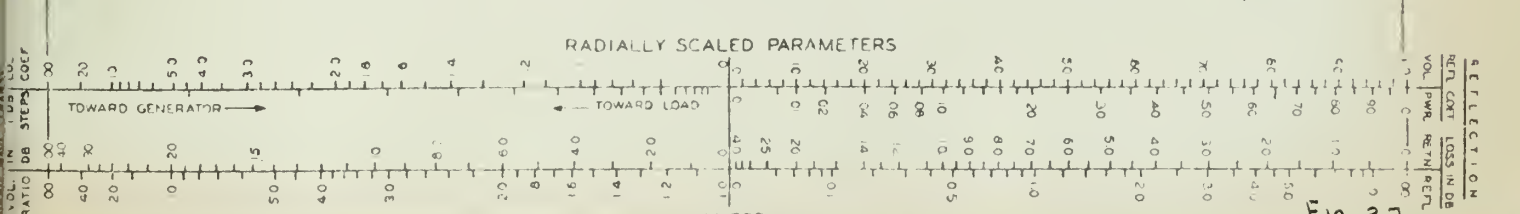

Fig 37

Electronics VOL. 17, NO. P...

NAME	TITLE	DWG. NO.
	DIODE No 9 - M-17-21	
SMITH CHART FORM 82BSPR (2-49)	KAY ELECTRIC COMPANY, PINE BROOK, N.J. ©1949 PRINTED IN U.S.A.	DATE

IMPEDANCE OR ADMITTANCE COORDINATES

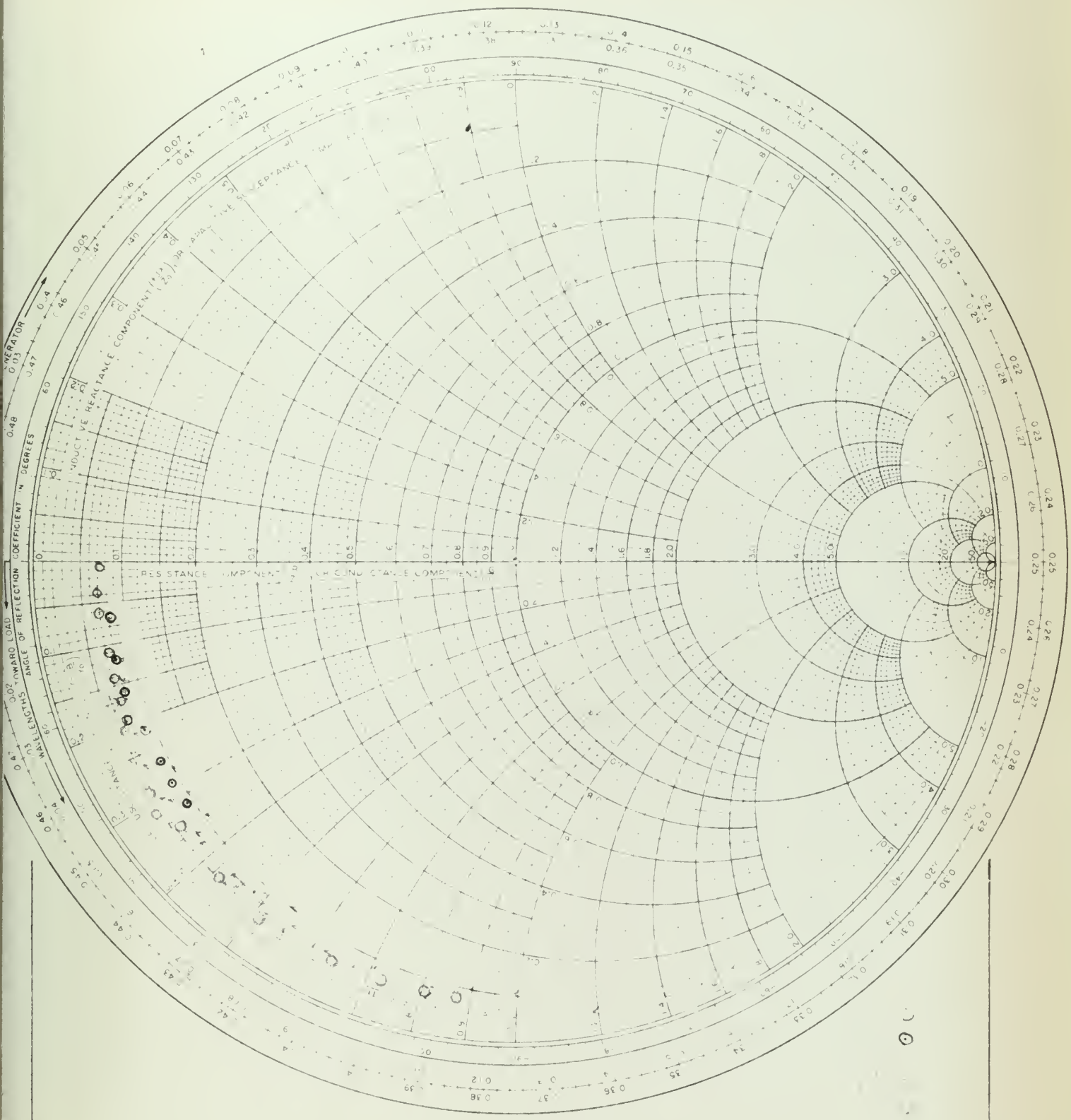
RESISTANCE COMPONENT
INDUCTIVE REACTANCE COMPONENT (+jX/Z0) OR SUSCEPTANCE
CAPACITIVE REACTANCE COMPONENT (-jX/Z0) OR SUSCEPTANCE
ANGLE OF REFLECTION COEFFICIENT IN DEGREES
WAVELENGTHS TOWARD LOAD
WAVELENGTHS TOWARD GENERATOR

RADIALLY SCALED PARAMETERS

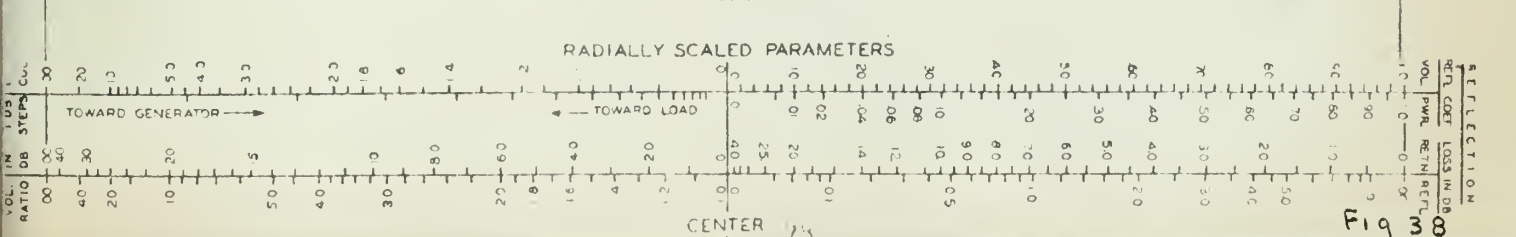

Fig 38

Electronics VOL. 17, NO 1, PP 130-133, 316-329, JAN 1944

AME	TITLE	DWG. NO.
	Diode No. 5-M-17-18	DATE
MITH CHART FORM 82BSPR (2-49)	KAY ELECTRIC COMPANY, PINE BROOK, N.J. ©1949 PRINTED IN U.S.A.	

IMPEDANCE OR ADMITTANCE COORDINATES

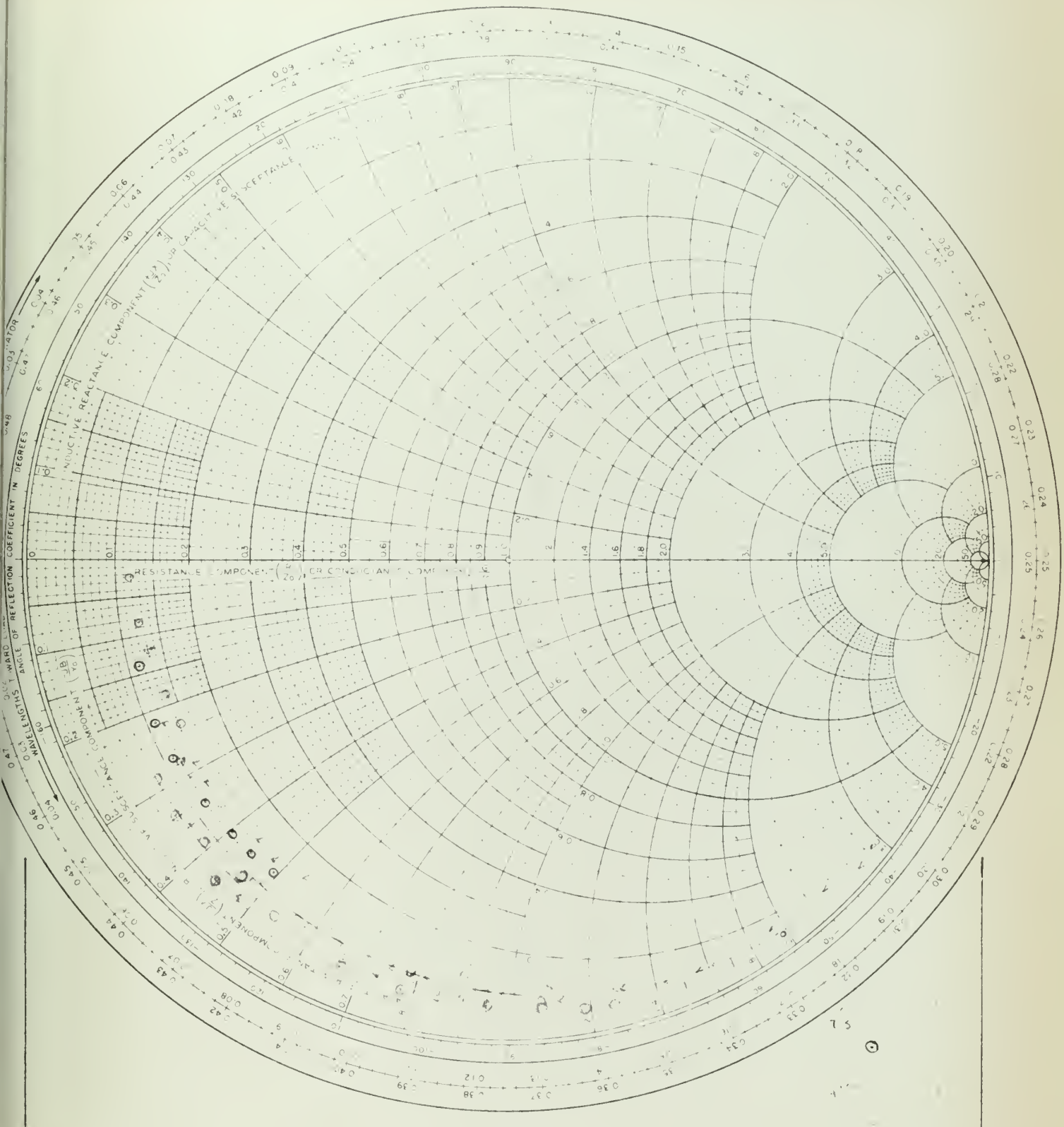

RADIALLY SCALED PARAMETERS

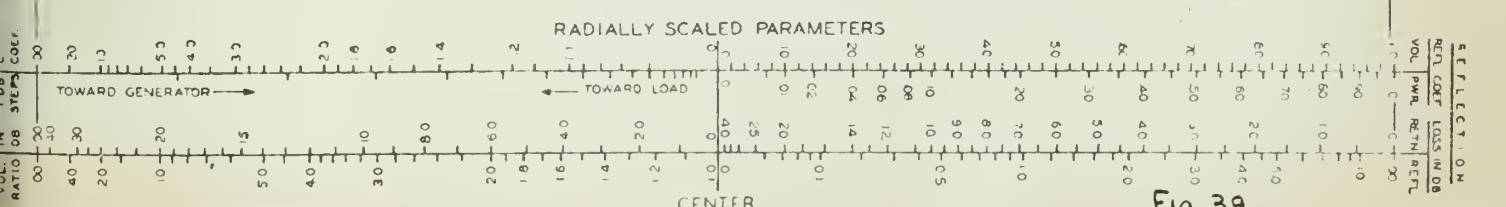

Fig 39

Electronics - VOL 17, NO 1, PP 130-133, 318-325, JAN 1944

NAME	TITLE Diode M-28-19 - No. 6	DWG. NO. (C)
SMITH CHART FORM 82BSPR (2-49)	KAY ELECTRIC COMPANY, PINE BROOK, N.J. ©1949 PRINTED IN U.S.A.	DATE

IMPEDANCE OR ADMITTANCE COORDINATES

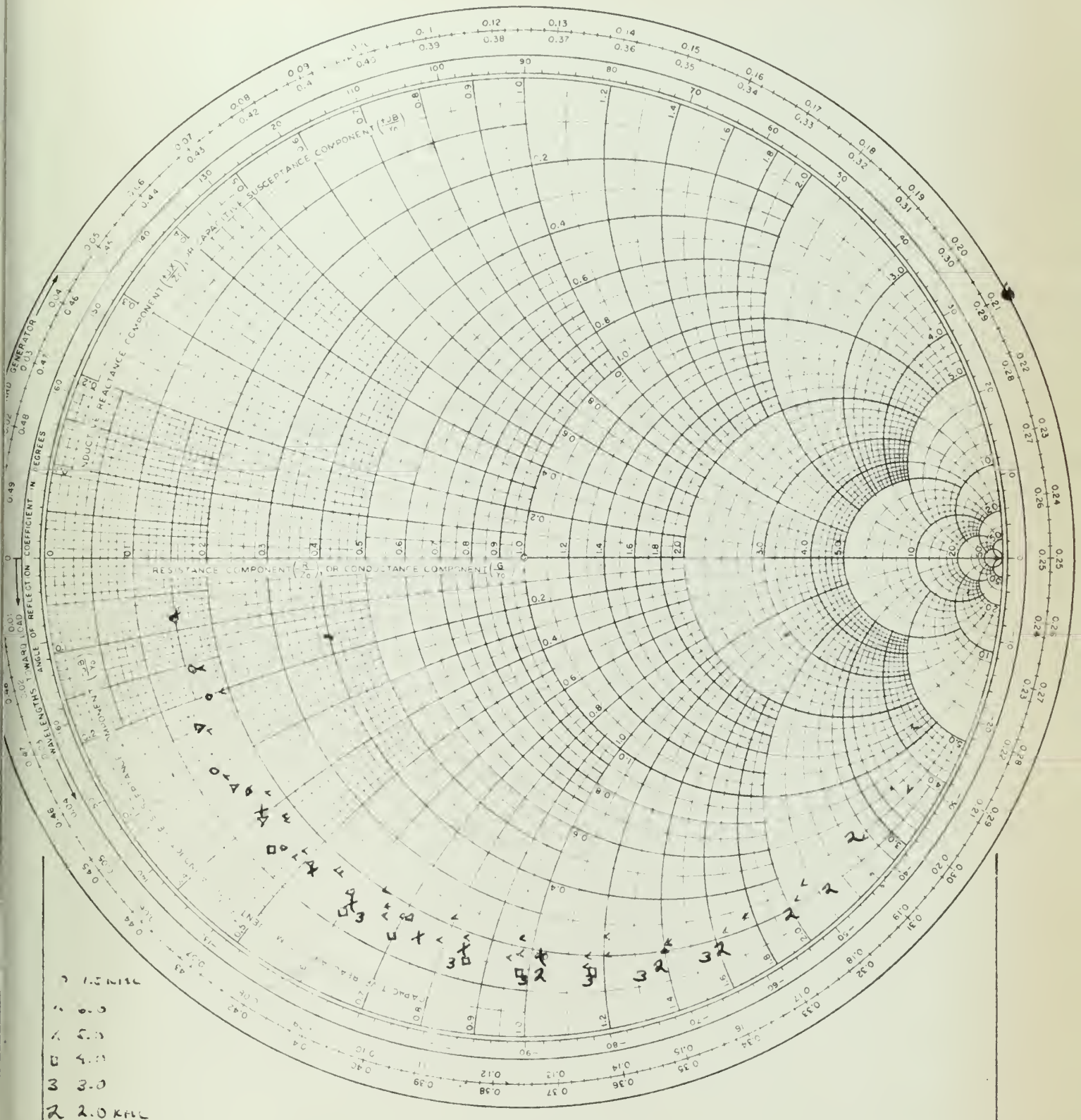

3 1.2 KMC
4 0.3
5 0.0
6 4.0
3 3.0
2 2.0 KMC

CENTER 80.

Fig 90

Electronics VOL. 17, NO 1, PP 130-133, 318-325, JAN 1944

A MEGA-CHART

NAME	TITLE	DWG. NO.
	Diode M-27-IN No 7	
SMITH CHART FORM 82BSPR (2-49)	KAY ELECTRIC COMPANY, PINE BROOK, N.J. ©1949 PRINTED IN U.S.A.	DATE

IMPEDANCE OR ADMITTANCE COORDINATES

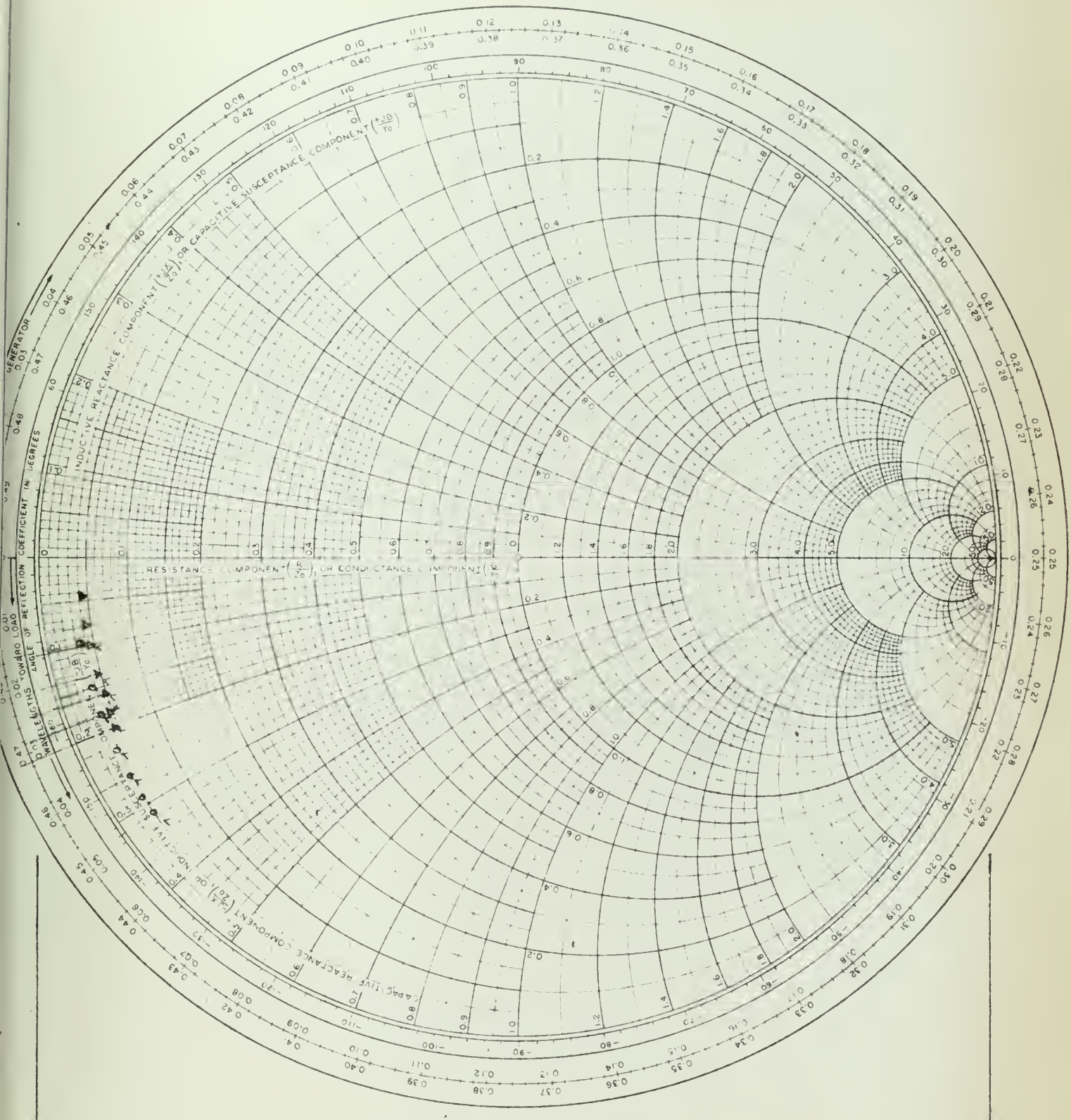
RESISTANCE COMPONENT $\left(\frac{R}{Z_0}\right)$, OR CONDUCTANCE COMPONENT $\left(\frac{G}{Y_0}\right)$
INDUCTIVE REACTANCE COMPONENT $\left(\frac{+jX}{Z_0}\right)$, OR CAPACITIVE SUSCEPTANCE COMPONENT $\left(\frac{+jB}{Y_0}\right)$
CAPACITIVE REACTANCE COMPONENT $\left(\frac{-jX}{Z_0}\right)$, OR INDUCTIVE SUSCEPTANCE COMPONENT $\left(\frac{-jB}{Y_0}\right)$
ANGLE OF REFLECTION COEFFICIENT IN DEGREES
DISTANCE IN WAVELENGTHS TOWARD LOAD
DISTANCE IN WAVELENGTHS TOWARD GENERATOR

RADIALLY SCALED PARAMETERS

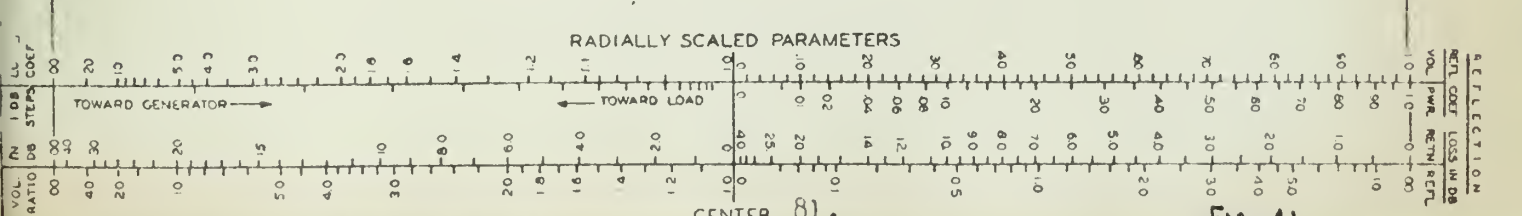

CENTER 81.

Fig 41

Electronics VOL 17 NO 1 PP 130-133 318-325 JAN 1944

A MEDA CHART

NAME	TITLE	DWG. NO.
	DIODE No 9	M-21-9
SMITH CHART FORM 82BSPR (2-49)	KAY ELECTRIC COMPANY, PINE BROOK, N.J. ©1949 PRINTED IN U.S.A.	DATE

IMPEDANCE OR ADMITTANCE COORDINATES

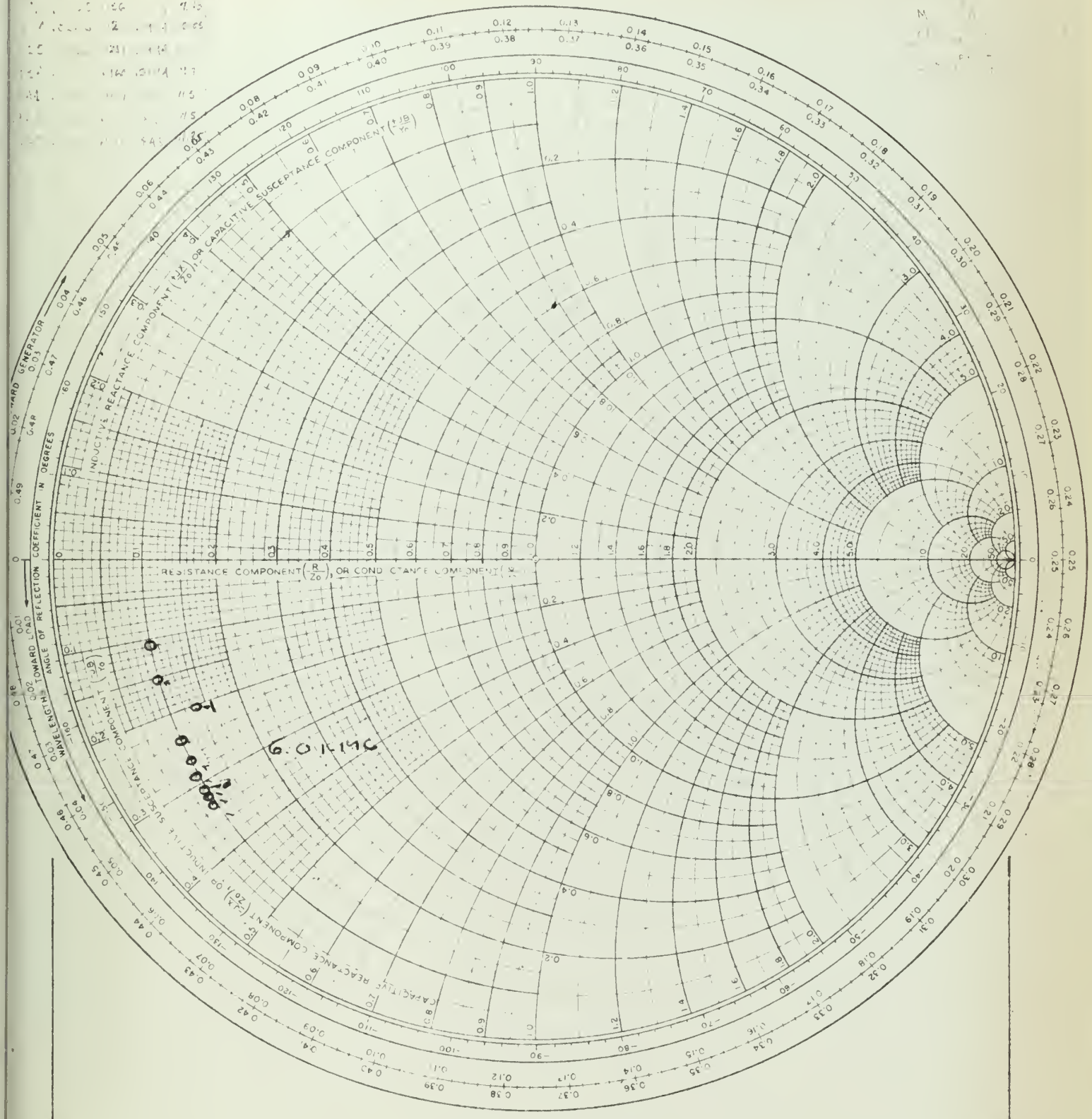
RESISTANCE COMPONENT $\left(\frac{R}{Z_0}\right)$, OR CONDUCTANCE COMPONENT $\left(\frac{G}{Y_0}\right)$
INDUCTIVE REACTANCE COMPONENT $\left(\frac{+jX}{Z_0}\right)$ OR CAPACITIVE SUSCEPTANCE COMPONENT $\left(\frac{+jB}{Y_0}\right)$
CAPACITIVE REACTANCE COMPONENT $\left(\frac{-jX}{Z_0}\right)$ OR INDUCTIVE SUSCEPTANCE COMPONENT $\left(\frac{-jB}{Y_0}\right)$
ANGLE OF REFLECTION COEFFICIENT IN DEGREES
TOWARD LOAD
TOWARD GENERATOR
WAVELENGTHS TOWARD GENERATOR
WAVELENGTHS TOWARD LOAD
6.01+j4C

RADIALLY SCALED PARAMETERS

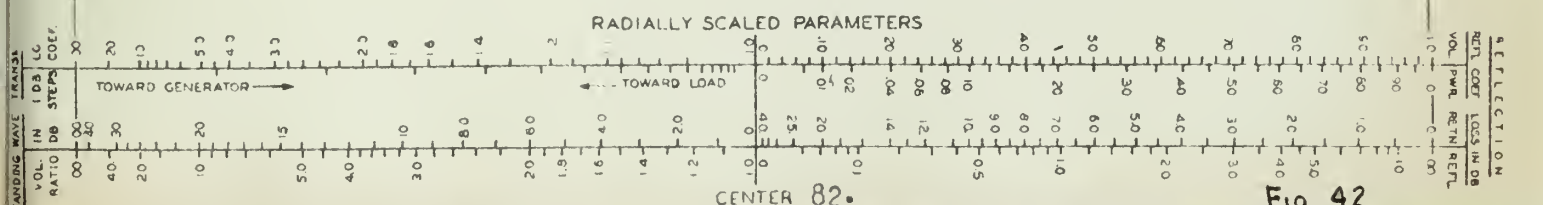

Fig 42
A MEGA CHART

Electronics VOL 17, NO 1, PP 130-133, 318-325, JAN 1944

NAME	TITLE	DWG. NO.
	DIODE No 10	19-25-6
SMITH CHART FORM 82BSPR (2-49)	KAY ELECTRIC COMPANY, PINE BROOK, N.J. ©1949 PRINTED IN U.S.A.	DATE

IMPEDANCE OR ADMITTANCE COORDINATES

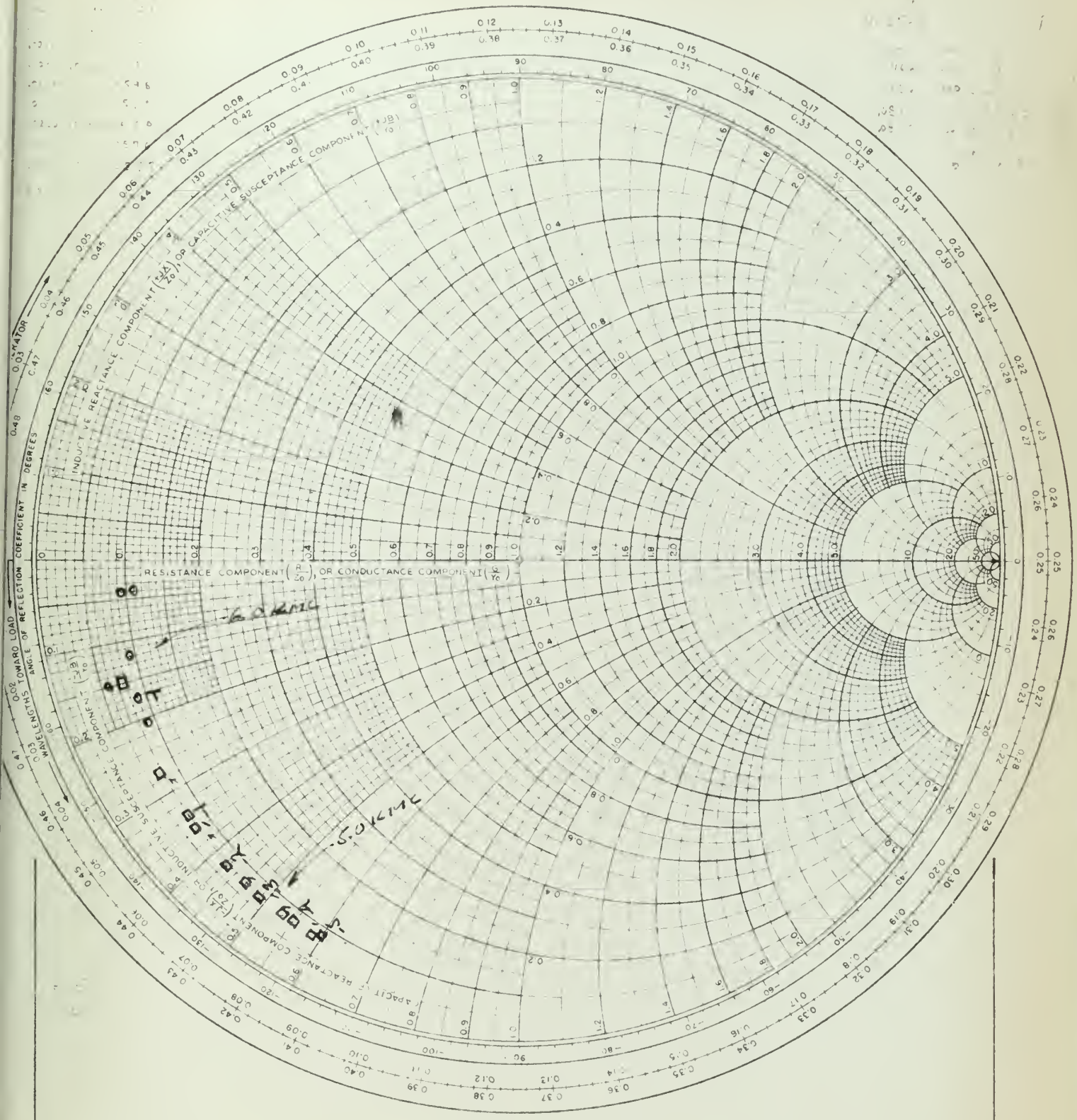
RESISTANCE COMPONENT $\left(\frac{R}{Z_0}\right)$, OR CONDUCTANCE COMPONENT $\left(\frac{G}{Y_0}\right)$
INDUCTIVE REACTANCE COMPONENT $\left(\frac{+jX}{Z_0}\right)$, OR CAPACITIVE SUSCEPTANCE COMPONENT $\left(\frac{+jB}{Y_0}\right)$
ANGLE OF REFLECTION COEFFICIENT IN DEGREES
WAVELENGTHS TOWARD LOAD
WAVELENGTHS TOWARD GENERATOR
CAPACITIVE REACTANCE COMPONENT $\left(\frac{-jX}{Z_0}\right)$, OR INDUCTIVE SUSCEPTANCE COMPONENT $\left(\frac{-jB}{Y_0}\right)$

RADIALLY SCALED PARAMETERS

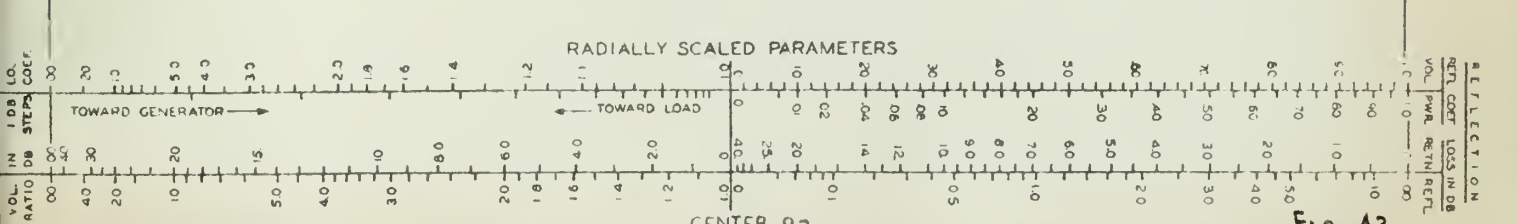

CENTER 83.

Fig 43

Electronics VOL. 17, NO. 1, PP. 130-133, 318-325, JAN. 1944

NAME	TITLE	DWG. NO.
	Diode No 11	M-22-10
SMITH CHART FORM 82BSPR (2-49)	KAY ELECTRIC COMPANY, PINE BROOK, N.J. ©1949 PRINTED IN U.S.A.	DATE

IMPEDANCE OR ADMITTANCE COORDINATES

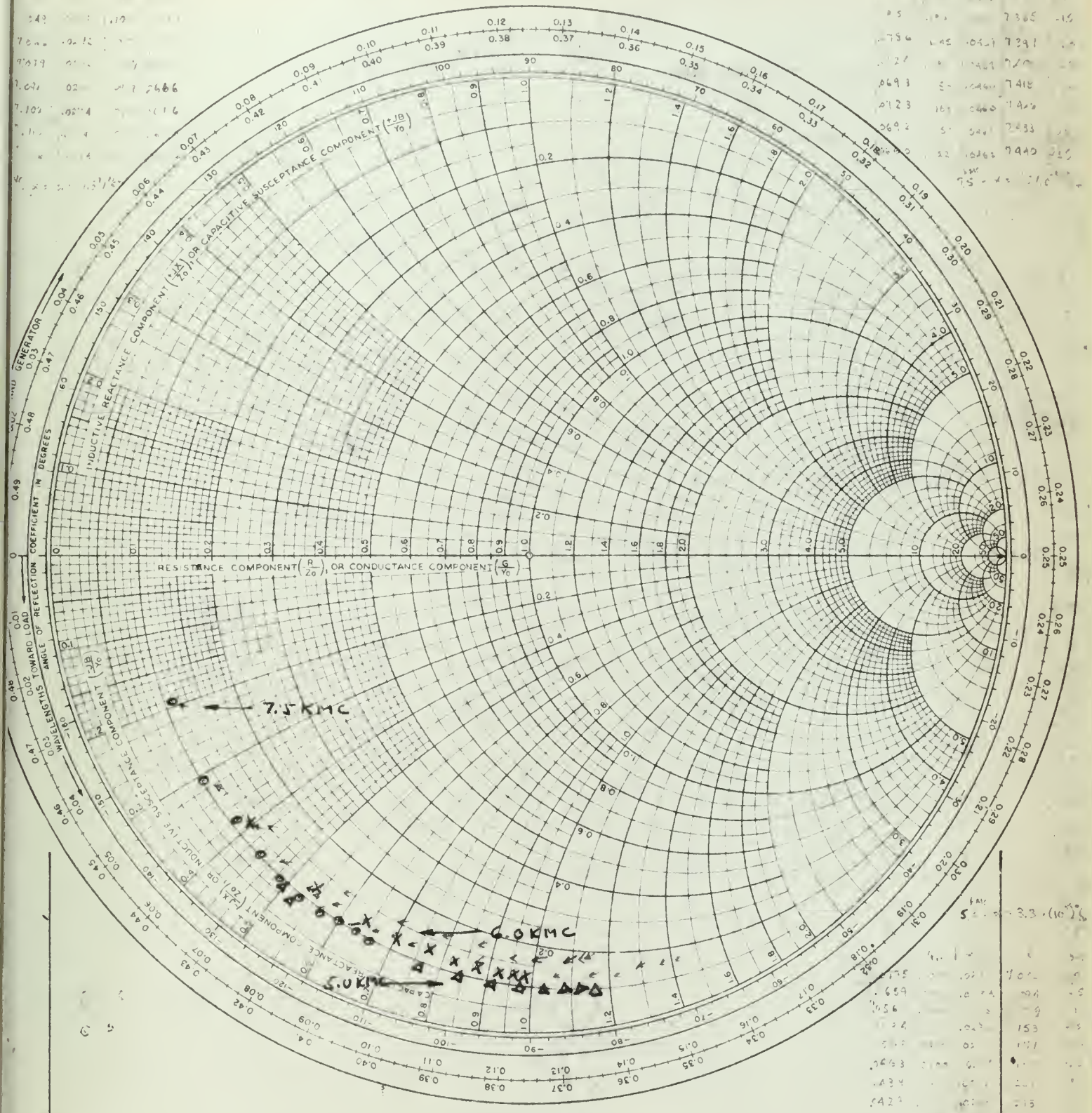
INDUCTIVE REACTANCE COMPONENT $\left(\frac{+jX}{Z_0}\right)$ OR CAPACITIVE SUSCEPTANCE COMPONENT $\left(\frac{+jB}{Y_0}\right)$
RESISTANCE COMPONENT $\left(\frac{R}{Z_0}\right)$ OR CONDUCTANCE COMPONENT $\left(\frac{G}{Y_0}\right)$
CAPACITIVE REACTANCE COMPONENT $\left(\frac{-jX}{Z_0}\right)$ OR INDUCTIVE SUSCEPTANCE COMPONENT $\left(\frac{-jB}{Y_0}\right)$
ANGLE OF REFLECTION COEFFICIENT IN DEGREES
WAVELENGTHS TOWARD LOAD
WAVELENGTHS TOWARD GENERATOR
7.5 KMC
6.0 KMC
5.0 KMC

RADIALLY SCALED PARAMETERS

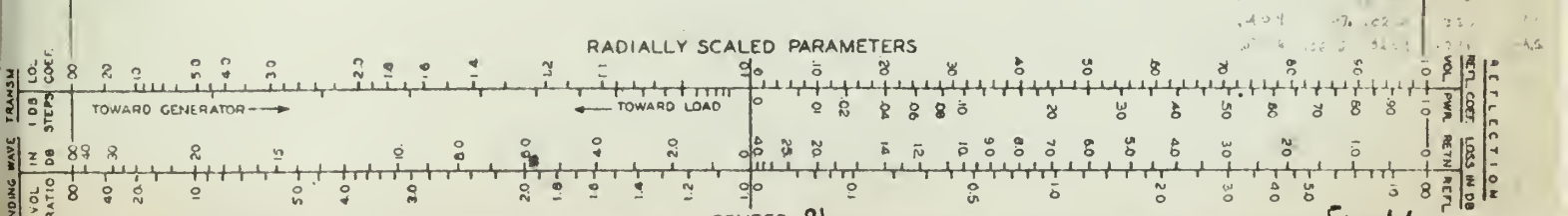

CENTER 84.

Fig 44

Electronics - VOL 17, NO 1, PP 130-133, 318-325, JAN 1944

A MEGA-CHART

NAME	TITLE	DWG. NO.
	Diode No 12- M-22-23	
SMITH CHART FORM 82BSPR (2-49)	KAY ELECTRIC COMPANY, PINE BROOK, N.J. ©1949 PRINTED IN U.S.A.	DATE

IMPEDANCE OR ADMITTANCE COORDINATES

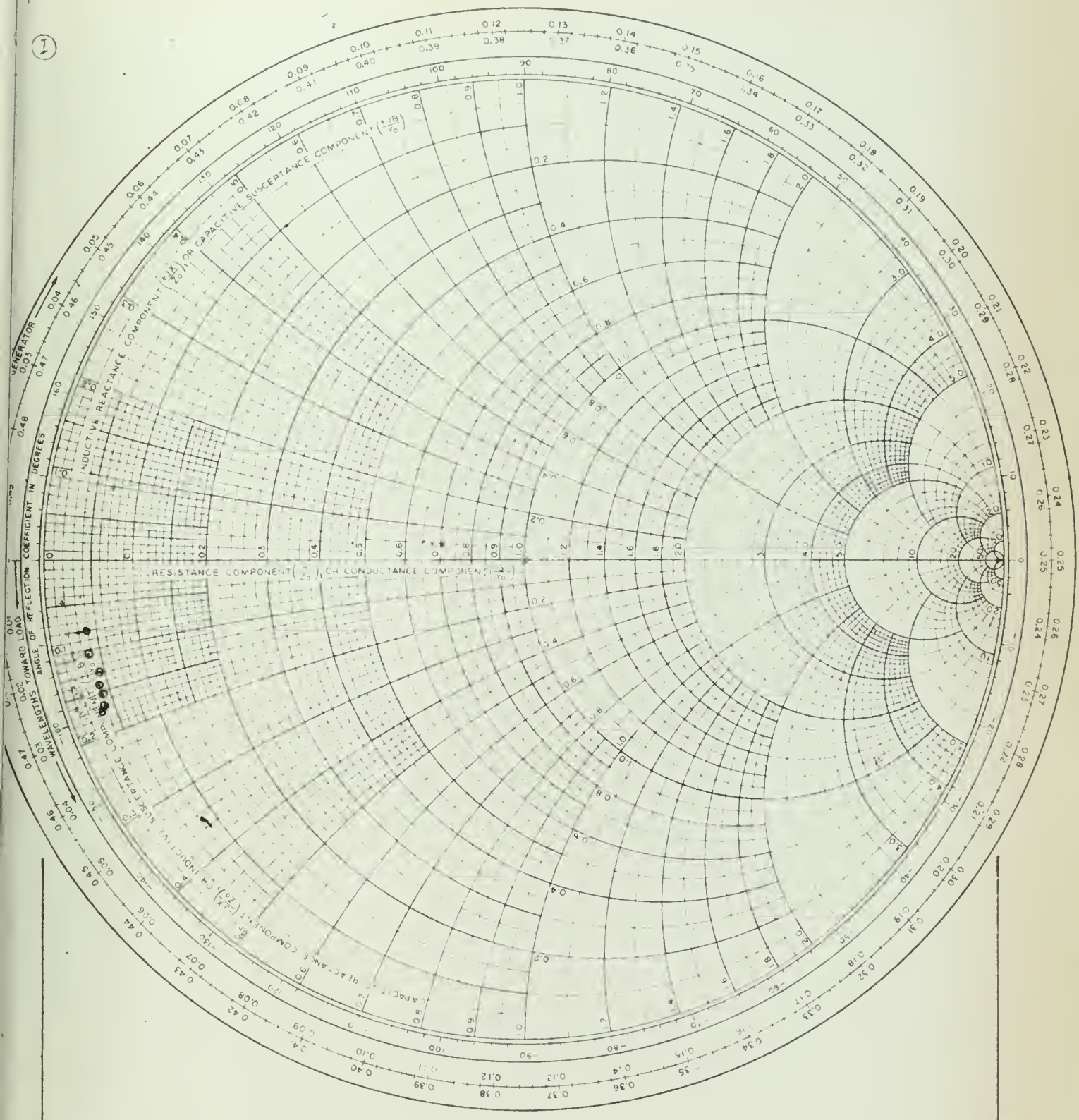
RESISTANCE COMPONENT (r/z0), OR CONDUCTANCE COMPONENT (g/y0)
INDUCTIVE REACTANCE COMPONENT (+jx/z0), OR CAPACITIVE SUSCEPTANCE COMPONENT (+jb/y0)
ANGLE OF REFLECTION COEFFICIENT IN DEGREES
WAVELENGTHS TOWARD LOAD
WAVELENGTHS TOWARD GENERATOR
CAPACITIVE REACTANCE COMPONENT (-jx/z0), OR INDUCTIVE SUSCEPTANCE COMPONENT (-jb/y0)

RADIALLY SCALED PARAMETERS

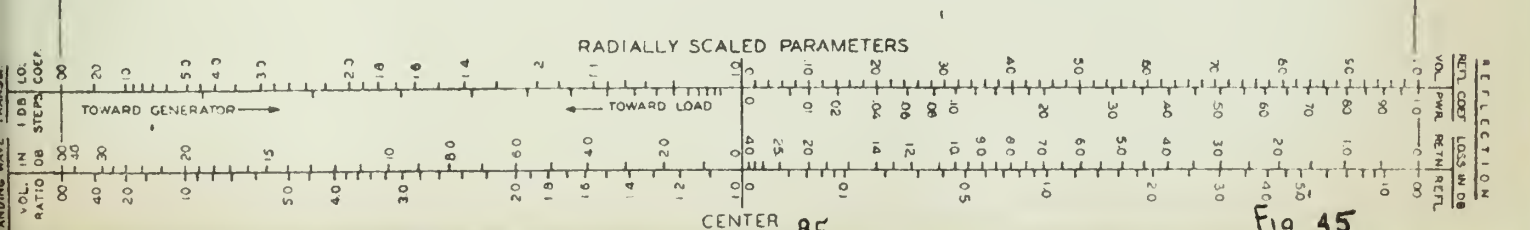

85.

Fig 45

A MEISA CHART

Electronics VOL. 17 NO. 1 PP. 130-133, 318-325, JAN. 1944

NAME	TITLE	DWG. NO.
	M-28-11	
SMITH CHART FORM 828SPR (2-49)	KAY ELECTRIC COMPANY, PINE BROOK, N J ©1949 PRINTED IN U.S.A.	DATE

IMPEDANCE OR ADMITTANCE COORDINATES

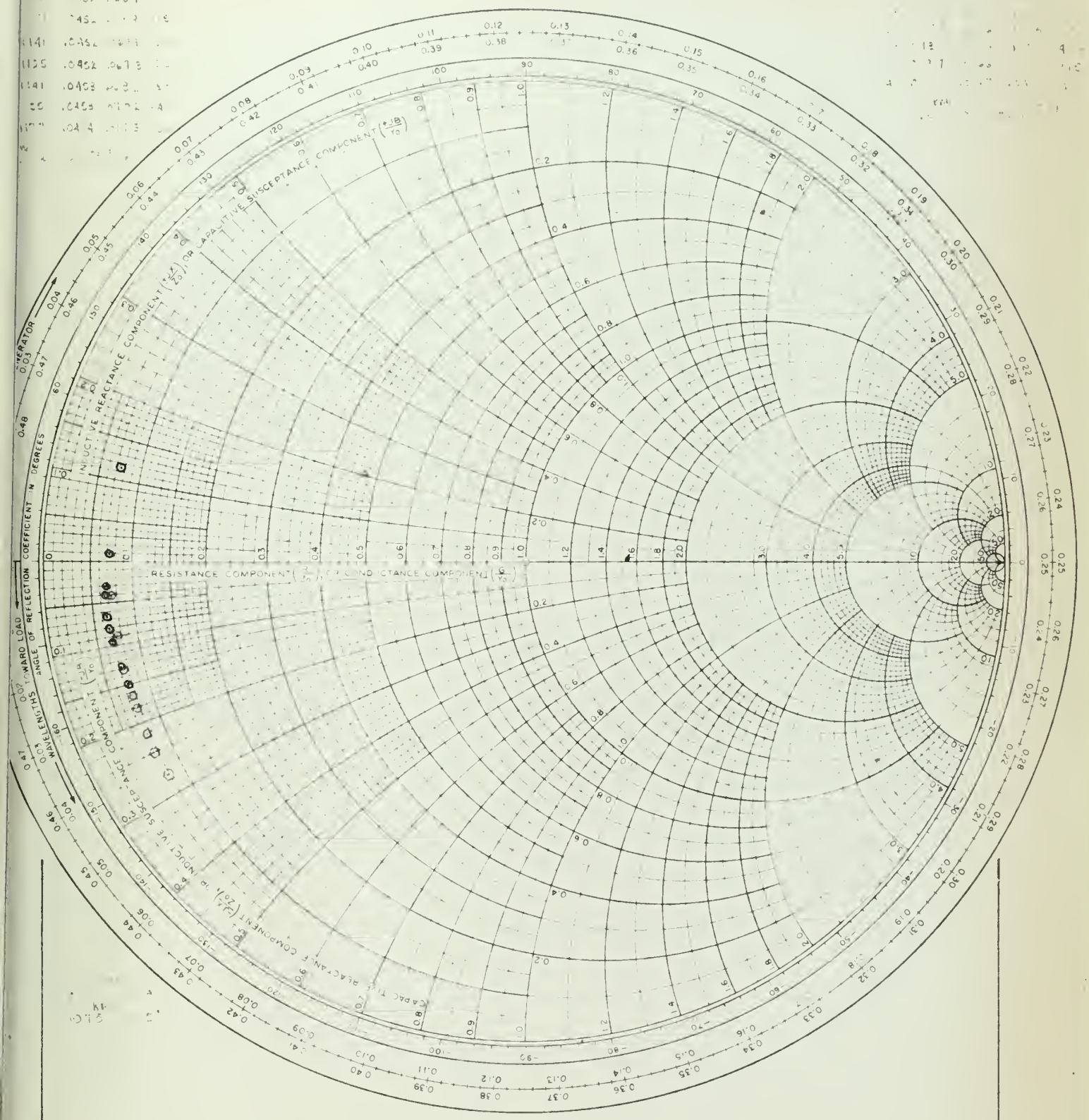
RESISTANCE COMPONENT (R/Z0) OR CONDUCTANCE COMPONENT (G/Y0)
INDUCTIVE REACTANCE COMPONENT (+jX/Z0) OR CAPACITIVE SUSCEPTANCE COMPONENT (+jB/Y0)
CAPACITIVE REACTANCE COMPONENT (-jX/Z0) OR INDUCTIVE SUSCEPTANCE COMPONENT (-jB/Y0)
ANGLE OF REFLECTION COEFFICIENT IN DEGREES
TOWARD LOAD
TOWARD GENERATOR
WAVELENGTHS

RADIALLY SCALED PARAMETERS

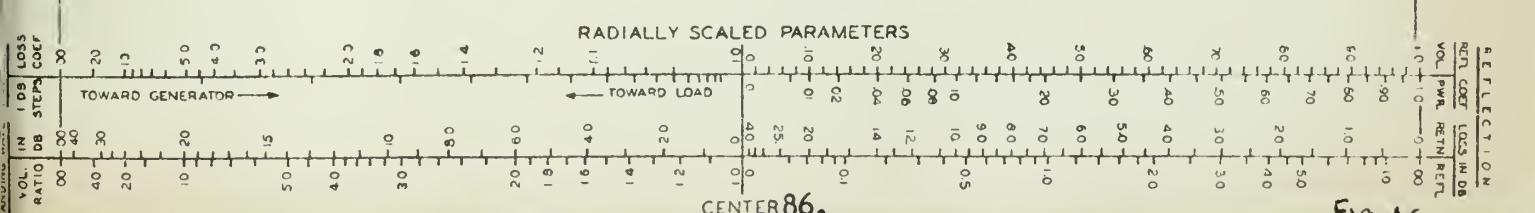

CENTER 86.

Fig 46

Electronics VOL 17 NO 1 PP 130-133 314-329 JAN 1944

NAME	TITLE M-25-13	DWG. NO.
SMITH CHART FORM 82BSPR (2-49)	KAY ELECTRIC COMPANY, PINE BROOK, N.J. ©1949 PRINTED IN U.S.A.	DATE

IMPEDANCE OR ADMITTANCE COORDINATES

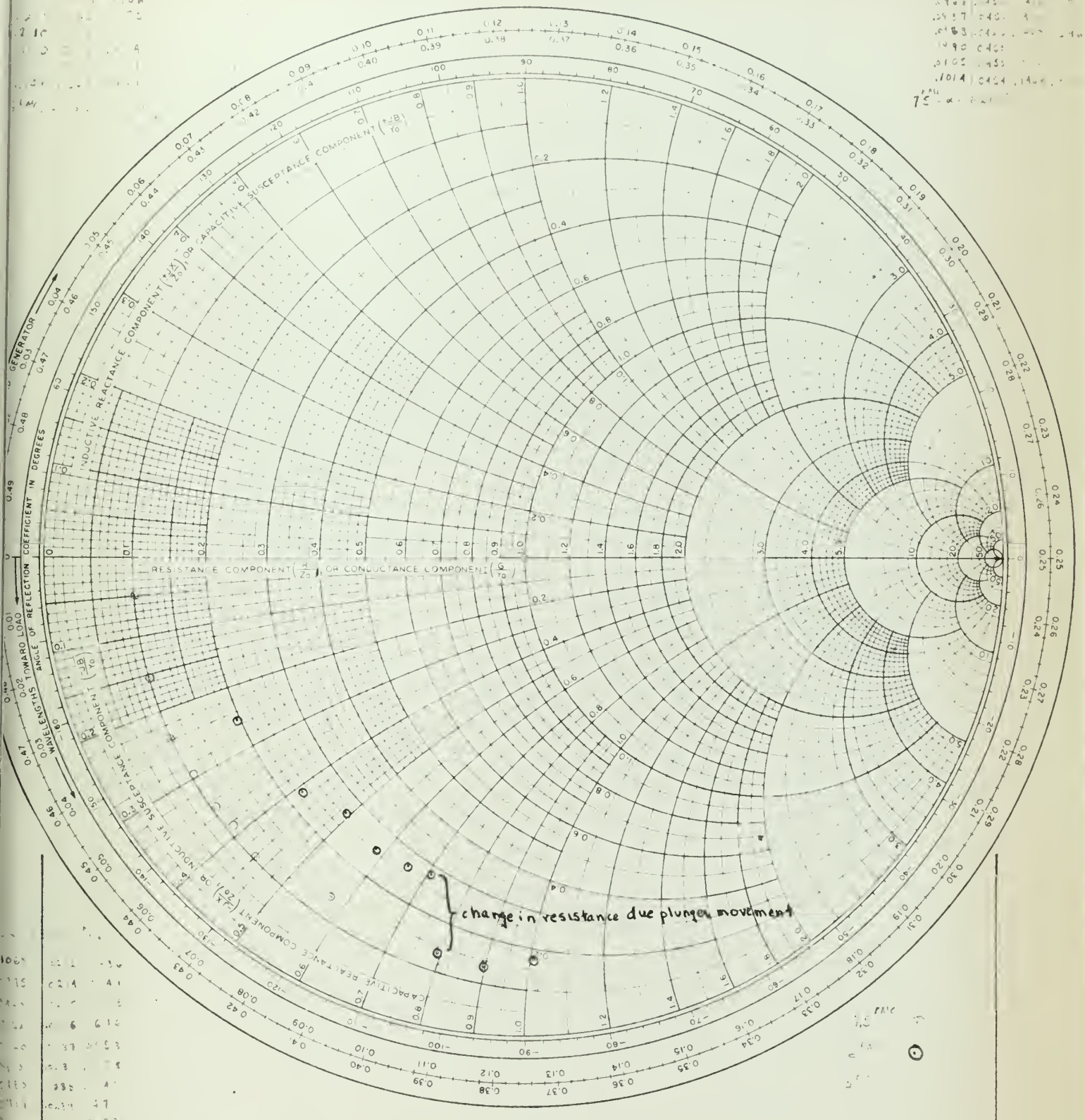
RESISTANCE COMPONENT $\left(\frac{R}{Z_0}\right)$ OR CONDUCTANCE COMPONENT $\left(\frac{G}{Y_0}\right)$
INDUCTIVE REACTANCE COMPONENT $\left(\frac{+jX}{Z_0}\right)$ OR CAPACITIVE SUSCEPTANCE COMPONENT $\left(\frac{+jB}{Y_0}\right)$
CAPACITIVE REACTANCE COMPONENT $\left(\frac{-jX}{Z_0}\right)$ OR INDUCTIVE SUSCEPTANCE COMPONENT $\left(\frac{-jB}{Y_0}\right)$
ANGLE OF REFLECTION COEFFICIENT IN DEGREES
WAVELENGTHS TOWARD LOAD
WAVELENGTHS TOWARD GENERATOR
change in resistance due plunger movement

RADIALLY SCALED PARAMETERS

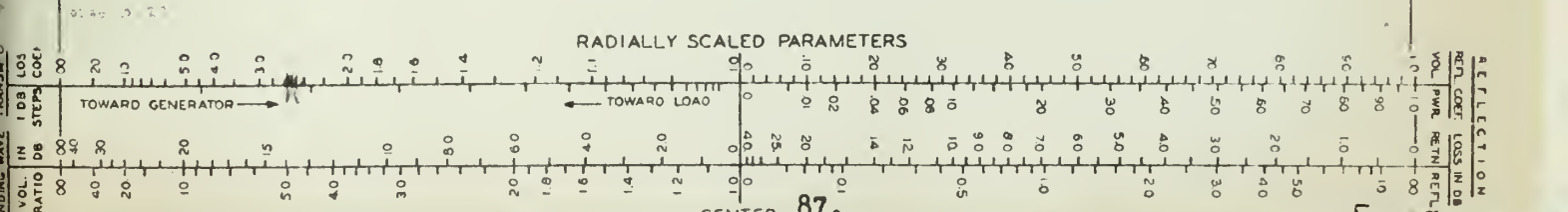

CENTER 87Ω

Fig 47

NAME	TITLE	DWG. NO.
SMITH CHART FORM 82BSPR (2-49)	KAY ELECTRIC COMPANY, PINE BROOK, N.J. ©1949 PRINTED IN U.S.A.	DATE

22-0-LG Mtp

E

IMPEDANCE OR ADMITTANCE COORDINATES

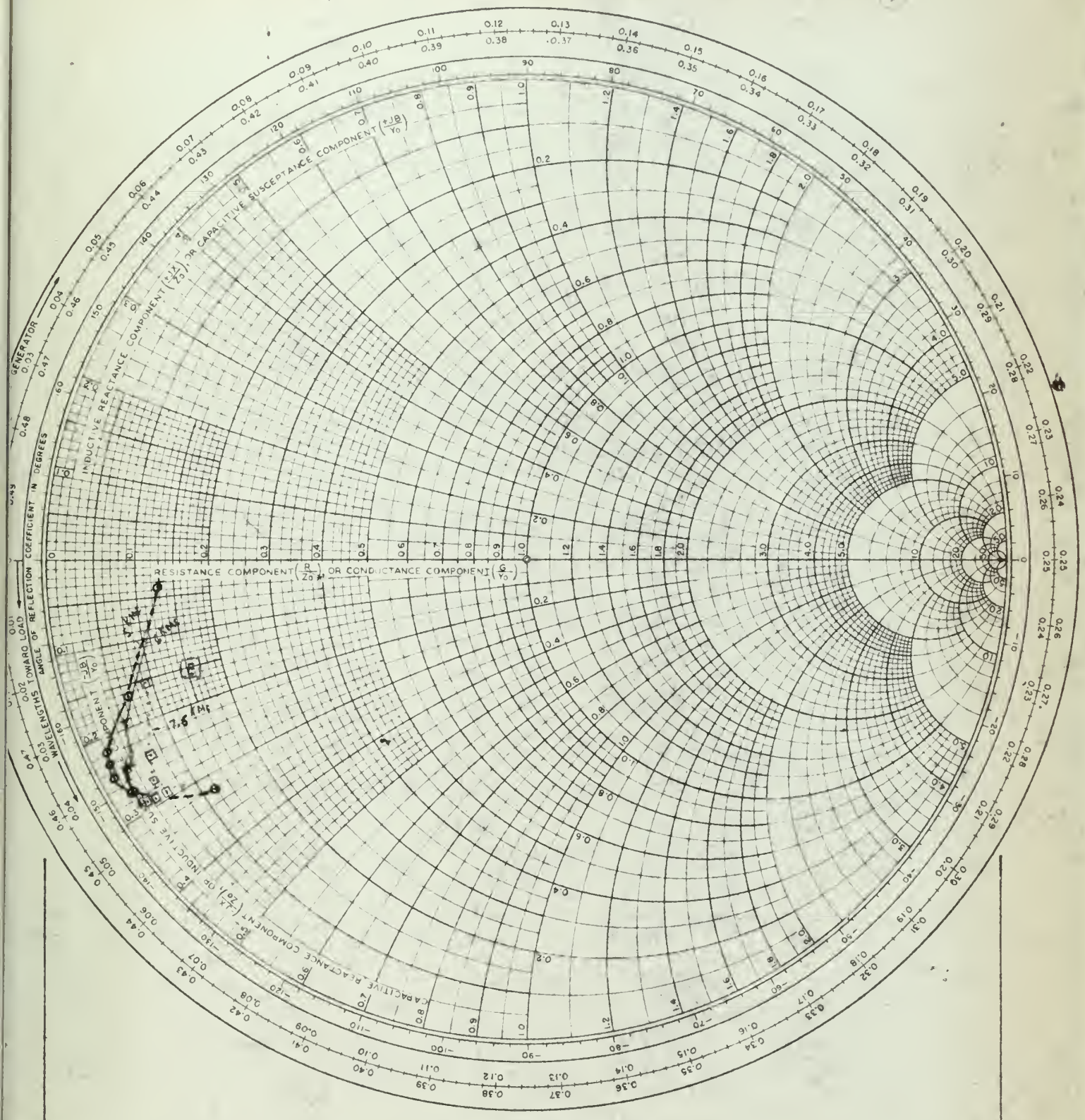
RESISTANCE COMPONENT $\left(\frac{R}{Z_0}\right)$ OR CONDUCTANCE COMPONENT $\left(\frac{G}{Y_0}\right)$
INDUCTIVE REACTANCE COMPONENT $\left(\frac{+jX}{Z_0}\right)$ OR CAPACITIVE SUSCEPTANCE COMPONENT $\left(\frac{+jB}{Y_0}\right)$
CAPACITIVE REACTANCE COMPONENT $\left(\frac{-jX}{Z_0}\right)$ OR INDUCTIVE SUSCEPTANCE COMPONENT $\left(\frac{-jB}{Y_0}\right)$
ANGLE OF REFLECTION COEFFICIENT IN DEGREES
WAVELENGTHS TOWARD LOAD
WAVELENGTHS TOWARD GENERATOR
- 7.6 IN.

RADIALLY SCALED PARAMETERS

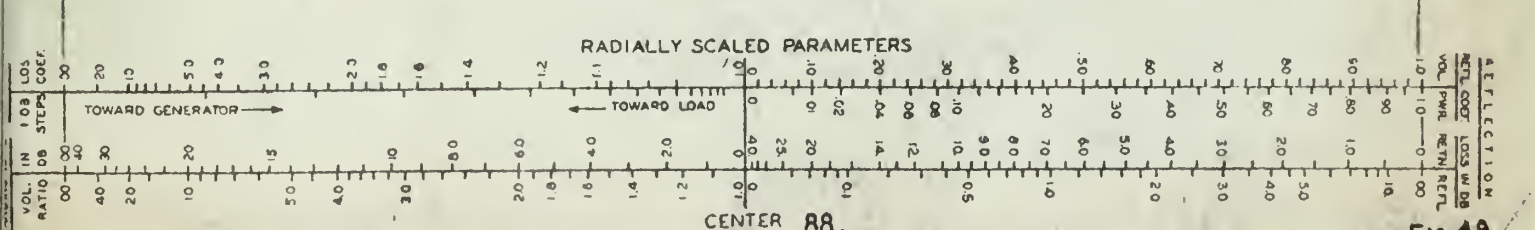

CENTER 88.

Electronics VOL 17 NO.1, PP 130-133, 318-325, JAN. 1944

A MEGA-CHART

Fig 18

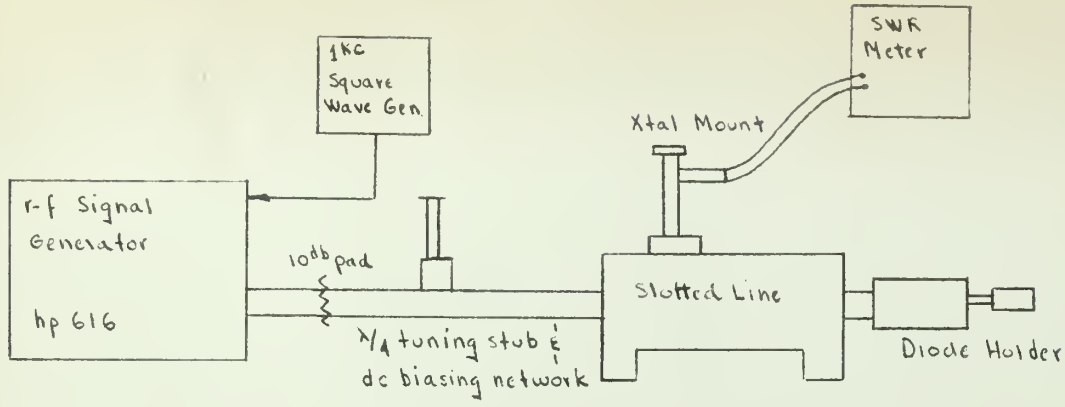

Fig I-1 Laboratory Set-up using 50 ohm line and original diode holder

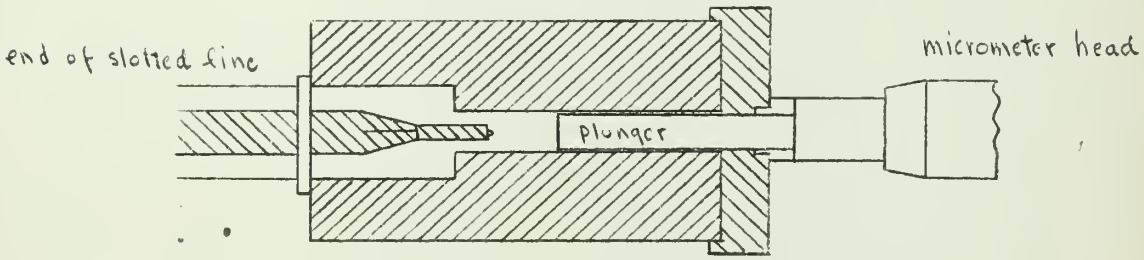

Fig I-2 Detail of original Diode Holder

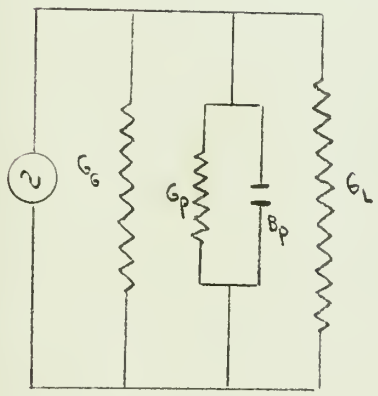

Fig I-3 An equivalent circuit representing the interaction between the generator, probe and the load admittances.

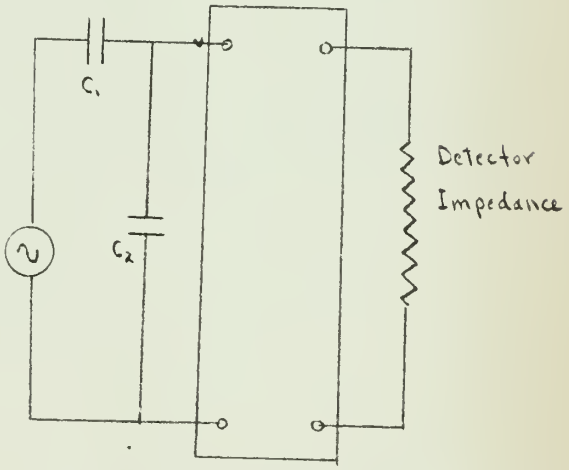

Fig I-4 Representation of the probe circuit and its equivalent circuit. C_1 = the coupling capacity, C_2 = the probe-to-slot capacity

(Both Fig I-3 and I-4 were adapted from Ginzton)

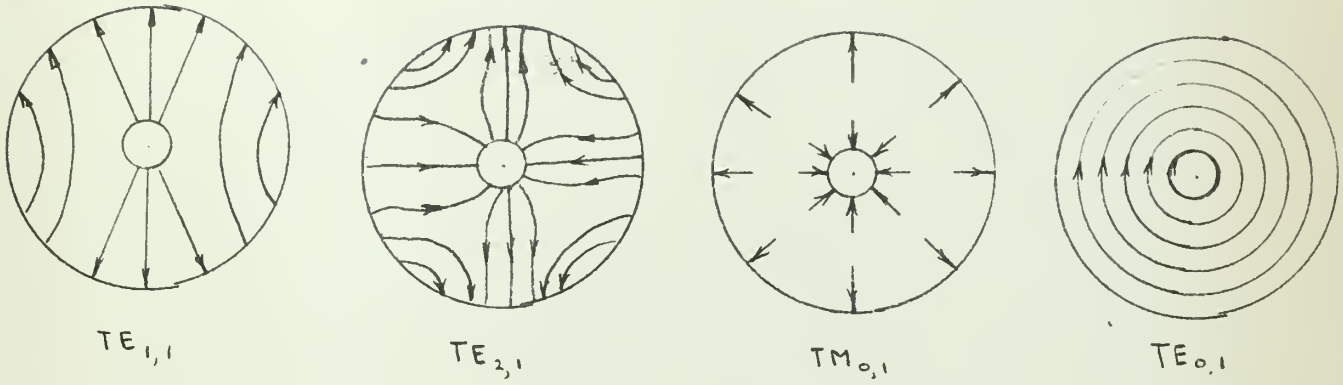

Fig I-5 Electric field of some higher modes in a coaxial line. (adapted from Moreno)

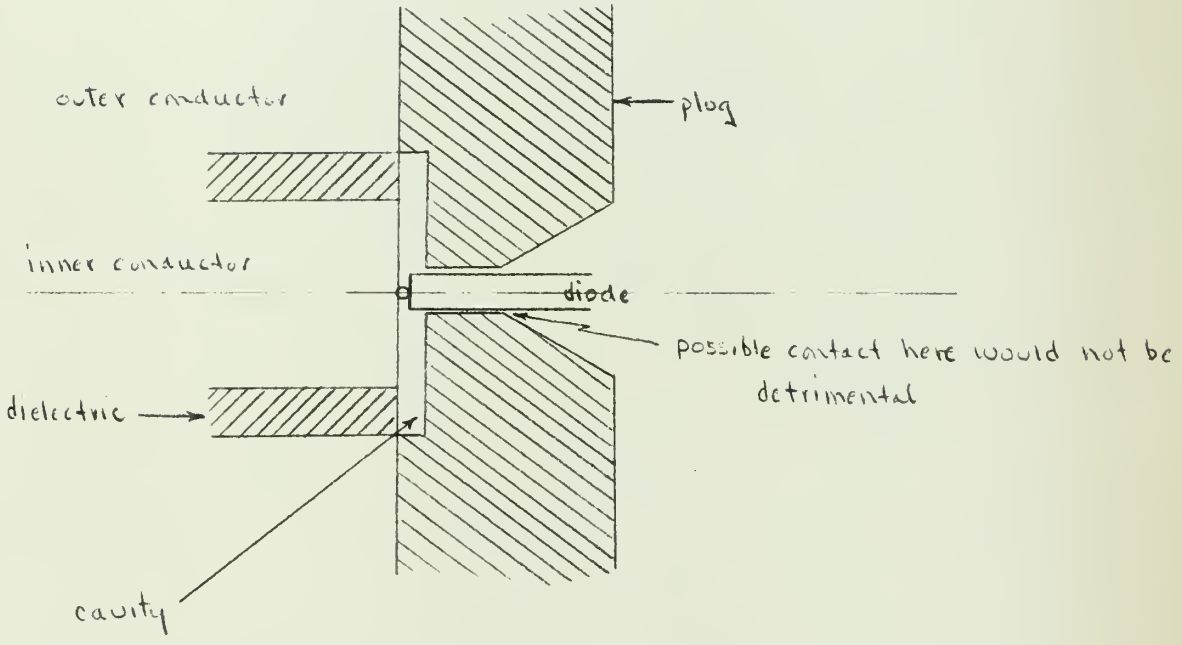

Fig I-6 Detail of the end of the slotted line with plug and diode in place.

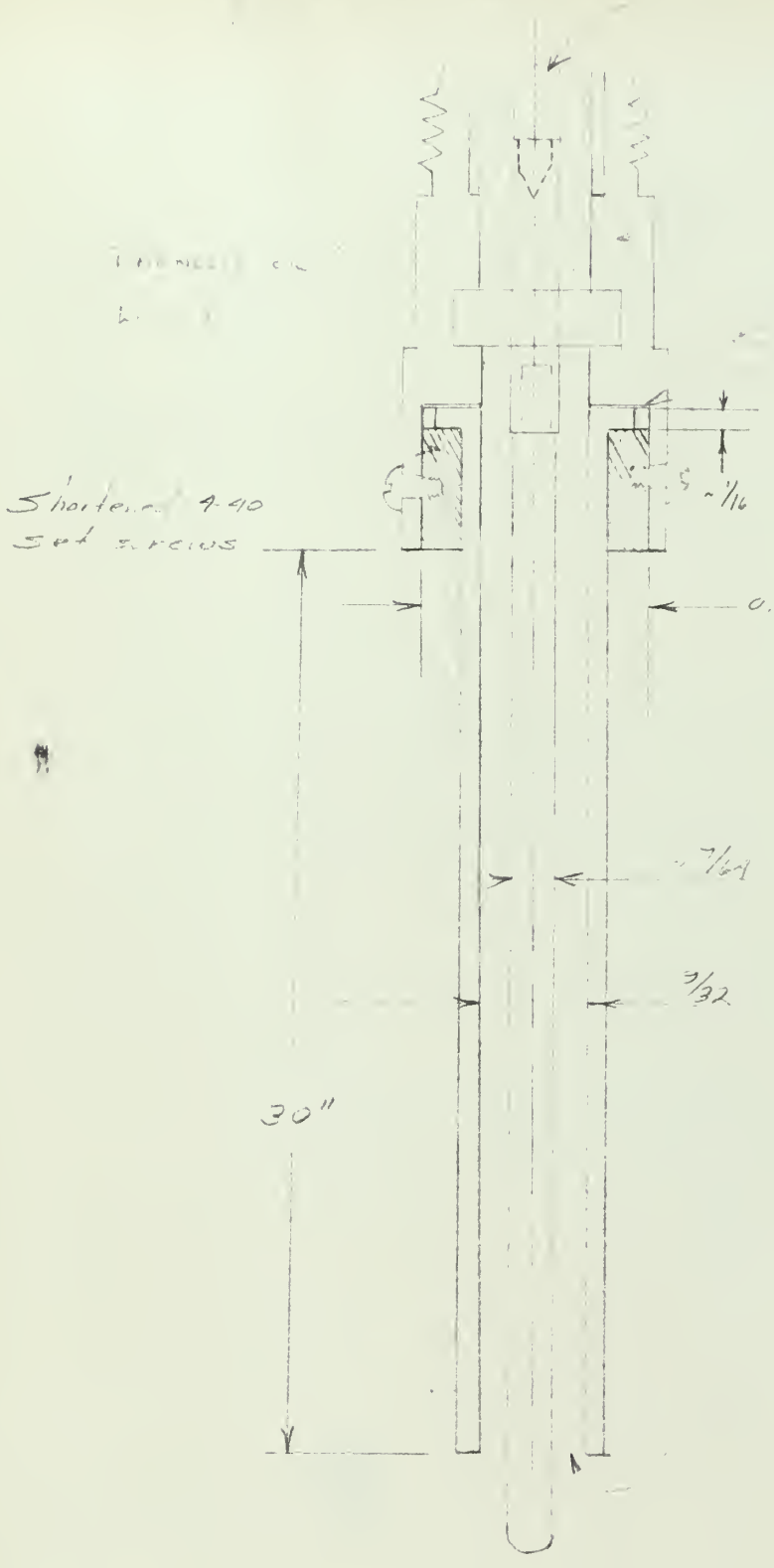

To fit shorting stub from PRD double-stub tuner

REVISIONS		TITLE Biasing Shoit	ENG. Smeltzaugh	DATE 11/10/58
		VARIAN associates ENGINEERING SKETCH	MAT'L. Brass / Plastic	MODEL
			FINISH	J. O. NO. 10034
			SCALE about 2:1	SK. NO.

COAXIAL SLOTTED LINE

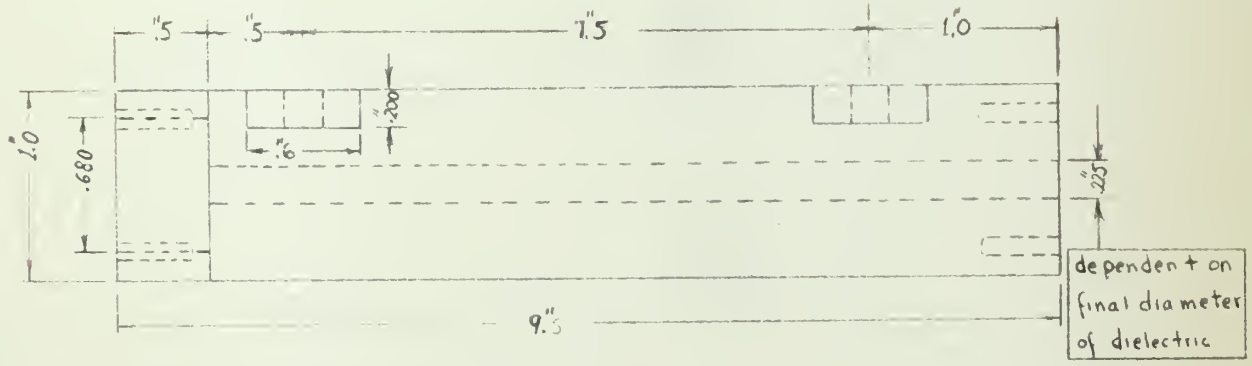

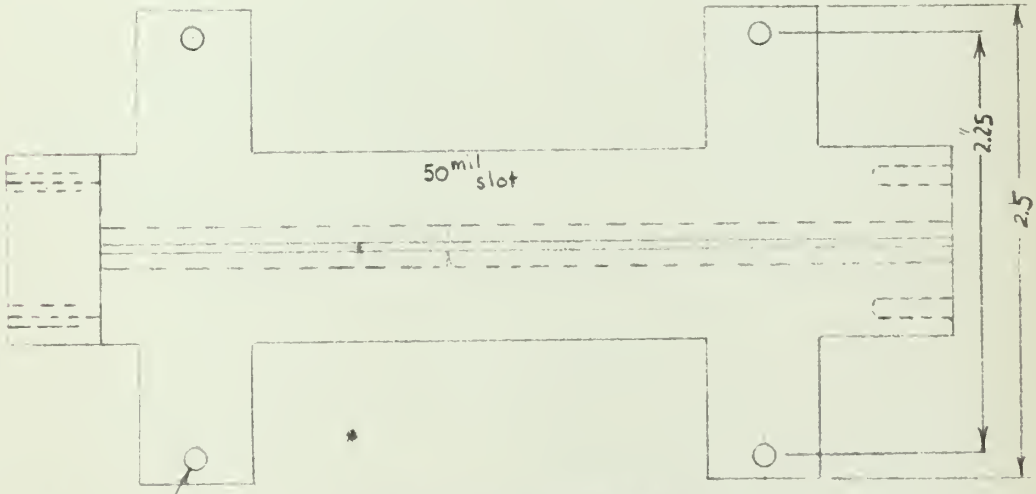

4 holes drilled # 18 and tapped 8-32 to match holes in hp 809 B slotted line carriage

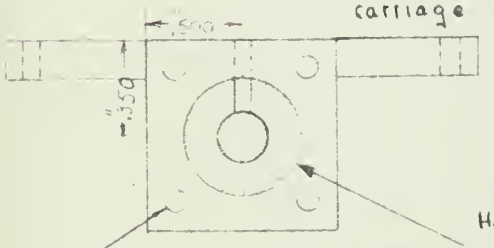

Hole for sliding fit with modified RG 22/U Connector

4 holes drilled #43 and tapped 4-40 to match holes in RG 22/U connector

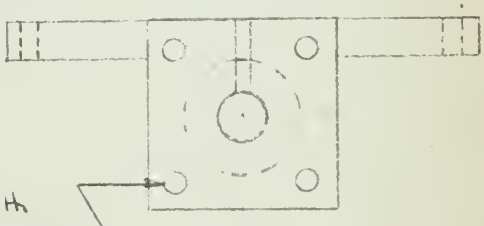

4 holes drilled #43 and tapped 4-40 to match holes in RG 22/U connector

REVISIONS		TITLE	ENG. W Potter	DATE 1/16/59
		VARIAN associates ENGINEERING SKETCH	MAT'L.	MODEL
			FINISH	J. O. NO.
			SCALE	SK. NO.

443-9-2 2MAY53

Modification of RG 22/U Connector

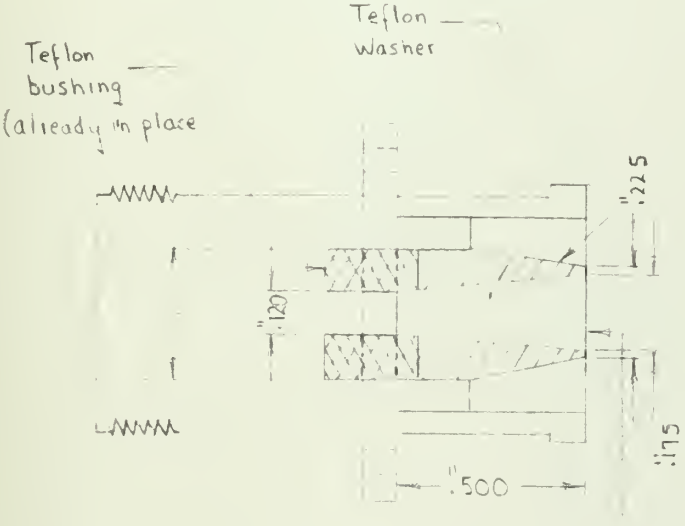

Inner conductor
Conic section

Center Cross-Section

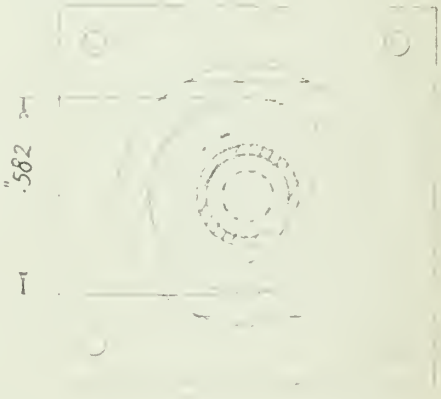

Teflon washer dimensions dependent on final diameter of slotted line dielectric

REVISIONS		TITLE	ENG. W. Fitch	DATE 1/6/53
		VARIAN associates ENGINEERING SKETCH	MAT'L.	MODEL
			FINISH	J. O. NO.
			SCALE	SK. NO.

REVISIONS	TITLE Diode Holder & Body	ENG. W Potter	DATE 11/16/5
	VARIAN associates ENGINEERING SKETCH	MAT'L.	MODEL
		FINISH	J. O. NO.
		SCALE	SK. NO.

BIBLIOGRAPHY

1. H. Heffner and G. Wade, "Gain, Bandwidth and Noise Characteristics of the Variable-Parameter Amplifier", Journal of Applied Physics, Vol. 29, No. 9, Sept. 1958, pp. 1321-31. The material for this entire section was taken from this excellent article.

2. R. S. Engelbrecht, A Low-Noise Non-linear Reactance Travelling Wave Amplifier, Proceedings of the IRE, Sept. 1958, p. 1655.

3. B. Salzberg and E. W. Sard, A Low-Noise Wide-Band Reactance Amplifier, Proceedings of the IRE, June 1958 correspondence, p. 1303.

4. A. Uhlir, Jr., The Potential of Semiconductor Diodes in High Frequency Communications, Proceedings of the IRE, June 1958, pp. 1099-1115.

5. Measurements at Higher Frequencies were not taken because of higher modes. See Attenuation Section and Appendix I.

6. Actual Z_o vs frequencies were: 2^{KMC} - 8.83 ohms 5^{KMC} - 8.80 ohms
3^{KMC} - 8.85 ohms 6^{KMC} - 8.82 ohms
4^{KMC} - 8.83 ohms 7.5 - 8.82 ohms

   A value of 9.05 ohms was obtained at 7^{KMC} but this frequency was not used for attenuation reasons.

7. E. L. Ginzton, Microwave Measurements, McGraw-Hill Publications, New York, 1957, p. 275.

8. Uhlir, op.cit.

9. Reference Data for Radio Engineers, 4th Edition, International Telephone and Telegraph Company, p. 62.

10. Ginzton, op.cit., pp. 240-41.

11. S. Ramo and J. R. Whinnay, Fields and Waves in Modern Radio, 2nd Edition, John Wiley and Sons, 1953, p. 460.

12. Ginzton, op. cit., pp. 244-247, An excellent analysis of the effect of the probe.

13. T. Moreno, Microwave Transmission Design Data, Dover Publications Inc., New York, p. 64.

14. Ginzton, op. cit., p. 254.

thesP749
Measurement of semi-conductor diodes at
3 2768 001 92353 5
DUDLEY KNOX LIBRARY